THE UNIVERSITY OF QUEENSLAND

AUSTRALIA

Thermochronology and stratigraphy of the Thomson Orogen, north-eastern Australia

Melanie Sophia Beckinsale

BSc (App Geo)

A thesis submitted for the degree of Master of Philosophy at

The University of Queensland in 2016

School of Earth Sciences

Abstract

The Tasmanides comprise the eastern third of the Australian continent and record the break-up of Rodinia and the subsequent formation and break-up of Gondwana. The Tasmanides are sub-divided into a number of basement terranes or orogens (the Delamerian, Lachlan, Mossman, Thomson, and New England Orogens), as well as an overlying Permo-Triassic basin system (the Bowen-Sydney-Gunnedah Basin). Due largely to lack of outcrop, the Thomson Orogen is the least understood of the various Tasmanides components, resulting in significant uncertainty about the age, lithology, thermal history, and internal stratigraphy of the Thomson Orogen. The present study combined field observations and $^{40}Ar/^{39}Ar$ geo- and thermo-chronology to address some of these uncertainties.

The first part of this thesis is focused on a previously undescribed succession of northern Thomson Orogen metasediments that are herein named the Mt. McLaren beds. These late Cambrian to Early Ordovician low-grade quartzites and metapelites are correlated both with other northern Thomson Orogen strata, as well with sandstones in the Centralian Superbasin. Findings from this project suggest that these eastern and central Australian sediments were deposited in the shallow Larapintine Sea, an epeiric seaway that may have spanned the entire continent in early Paleozoic time. The shallow marine environment responsible for the deposition of the Mt. McLaren beds and correlative northern Thomson Orogen strata differs from the deeper marine depositional environment of turbidites in the southern Thomson and Lachlan Orogens.

The second part of the thesis includes new $^{40}Ar/^{39}Ar$ results from the northern Thomson Orogen that constrain the timing of what seem to be distinct episodes of metamorphism and exhumation that span most of the Paleozoic Era. These results share similarities with previous data from both the Lachlan and New England Orogens, and they help develop a first-order thermal history of the northern Thomson Orogen. This history includes mid to late Cambrian metamorphism, as suggested by previous K-Ar data, which seems to have been at least broadly coincident with the Delamerian Orogeny in southern Australia. Many of the new $^{40}Ar/^{39}Ar$ ages from northern Thomson Orogen metasediments are Ordovician, as are previous results from the Lachlan Orogen, suggesting that many of the deformational episodes more clearly recognizable in the Lachlan Orogen can be traced northward into the Thomson Orogen. Cooling ages of ~310 to 400 Ma from both Thomson Orogen metasediments and Ordovician to Middle Devonian granites that intrude them point toward periods of extensional exhumation in the Late Devonian to mid Carboniferous, as well as in the late Carboniferous to early Permian. Both periods are marked by basin initiation, including the late

Carboniferous-early Permian development of the Bowen-Sydney-Gunnedah basin system. The youngest $^{40}Ar/^{39}Ar$ cooling age (~270 Ma) measured from the northern Thomson Orogen is similar to previous results from the New England Orogen and seems to marks the beginning of the Permo-Triassic Hunter-Bowen Orogeny.

Declaration by author

This thesis is composed of my original work, and contains no material previously published or written by another person except where due reference has been made in the text. I have clearly stated the contribution by others to jointly-authored works that I have included in my thesis.

I have clearly stated the contribution of others to my thesis as a whole, including statistical assistance, survey design, data analysis, significant technical procedures, professional editorial advice, and any other original research work used or reported in my thesis. The content of my thesis is the result of work I have carried out since the commencement of my research higher degree candidature and does not include a substantial part of work that has been submitted to qualify for the award of any other degree or diploma in any university or other tertiary institution. I have clearly stated which parts of my thesis, if any, have been submitted to qualify for another award.

I acknowledge that an electronic copy of my thesis must be lodged with the University Library and, subject to the policy and procedures of The University of Queensland, the thesis be made available for research and study in accordance with the Copyright Act 1968 unless a period of embargo has been approved by the Dean of the Graduate School.

I acknowledge that copyright of all material contained in my thesis resides with the copyright holder(s) of that material. Where appropriate I have obtained copyright permission from the copyright holder to reproduce material in this thesis.

Publications during candidature

Conference abstracts

Lee, M., Verdel, C., Welsh, K., and Oorloff, A. 2015. Stratigraphy of the Thomson Orogen – New Insights from Mount McLaren, North-east Australia. In PACRIM2015 Proceedings, (Carlton, Victoria: The Australasian Institute of Mining and Metallurgy), pp. 551–556.

Research Reports

Purdy, D.J., Carr, P.A., Brown, D.D., Cross, A.J., Bultitude, R.J., Lee, M.S. & Verdel, C., 2016: The Granite Springs Granite. *Queensland Geological Record* **2016/02**.

Publications included in this thesis

No publications included.

Contributions by others to the thesis

The following people contributed to this thesis:

- Access to drill core was arranged by Mr David Purdy of the Geological Survey of Queensland, from which a number of samples for the geochronology component of this thesis were taken,
- Prof Paulo Vasconcelos and Dr David Thiede completed early $^{40}Ar/^{39}Ar$ geochronology work,
- Dr Kevin Welsh provided critical revisions of Chapter 2,
- Dr Charles Verdel provided critical revisions of the entire thesis.

Statement of parts of the thesis submitted to qualify for the award of another degree

None.

Acknowledgements

There are many people I would like to thank for their support during this project, key amongst them is my principle advisor, Dr Charles Verdel. Thank you for always finding time to discuss my work, to read and comment on my drafts, and to patiently offer advice and encouragement. I would also like to thank my supervisor, Dr Kevin Welsh, for assistance with making sense of all things sedimentological, without which I would have been very much "out to sea". The advice of research committee members Professor Gregg Webb and Associate Professor Gideon Rosenbaum was also appreciated.

The assistance of Professor Paulo Vasconcelos and Dr David Thiede on technical aspects of Argon geochronology was extremely helpful, as were discussions with Argon lab research students Tracey Crossingham and Hevelyn Da Silva Monteiro which saved me a lot of time and unnecessary effort. There are many additional people from the School of Earth Sciences who are due thanks: Ashleigh Paroz for administrative support, Jacqueline Wong who assisted with SEM access and identification of some tricksy minerals, Gang Xia and Feliz Farrajota for their assistance in the Rock Lab, and my fellow postgraduate students who offered unwavering friendship and helped me navigate a new university.

The advice of Geology Survey of Queensland geologists Dave Purdy, Ian Withnall and Dominic Brown was very helpful in my fieldwork. Thanks are overdue to Dave for helping to organise access to samples and thin sections of drill core which were used in the geochronology part of my research. Dr Bob Henderson is thanked for the donation of a sample of the Halls Reward Metamorphics, obtained for me by Ian Withnall.

The Australian Institute of Geoscientists (AIG) provided a Postgraduate Bursary without which I would not have been able to present my research at the PACRIM2015 Congress in Hong Kong.

Friends and family suffered many discussions about rocks, and my husband Ben knows far more about geology than he probably ever wanted to know! His encouragement, support and unerring faith in my ability to complete this project is something for which I will always be grateful. My good friend and jiu-jitsu coach Dr David MacDonald mentored me through some rough patches. And lastly, but not least by any measure, I would like to thank my mother, Jenni Lee, for many things, but especially for refusing to allow "can't" into my vocabulary! Thank you.

Keywords

Thomson Orogen, eastern Australian tectonics, $^{40}Ar/^{39}Ar$ geochronology, thermochronology,

Australian and New Zealand Standard Research Classifications (ANZSRC)

ANZSRC code: 040303 Geochronology, 40%

ANZSRC code: 040313 Tectonics, 40%

ANZSRC code: 040310 Sedimentology, 20%

Fields of Research (FoR) Classification

FoR code: 0403, Geology, 100%

Table of Contents

List of Figures

Chapter 1

Chapter 2

Chapter 3

List of Tables

Chapter 3

List of Abbreviations used in the thesis

Abbreviations are explained in text.

Chapter 1: Introduction

The tectonic evolution of eastern Australia is defined by a number of orogenic events that can be temporally and spatially correlated, therefore assisting with tectonic models of supercontinent evolution. The east Australian Tasmanides, which consist of the Delamerian, Lachlan, New England, Mossman, and Thomson Orogens, as well as the Bowen-Gunnedah-Sydney Basin System, record the breakup of Rodinia and the subsequent formation of eastern Gondwana (Glen, 2005). Due largely to poor exposure, the Thomson Orogen is the least understood of the various components of the Tasmanides. Improved understanding of the Thomson Orogen will thus improve models of the tectonic evolution of eastern Australia, and will assist with temporal and spatial correlations of orogenic events that affected other parts of the Tasmanides.

Of the work that has been conducted on the Thomson Orogen, the vast majority has focussed on the main outcrops of the Anakie Inlier and Charters Towers Province (e.g., Withnall et al., 1995; Fergusson et al., 2001; Withnall and Henderson, 2012). As these areas represent only a small portion of the expansive Thomson Orogen, questions remain as to whether these outcrops are truly representative of the orogen as a whole. To help address this question, this project was undertaken to improve the understanding of the age and thermal history of the Thomson Orogen, as well as its stratigraphy. This was achieved via stratigraphic study of previously unnamed and undescribed outcrops of metasediments (chapter 2), as well as placing radiometric age constraints on metamorphism and exhumation through $^{40}Ar/^{39}Ar$ geochronology (chapter 3). I describe the depositional environment for the sediments of the north-easternmost Thomson Orogen, describe the thermal history of a number of intrusive magmatic rocks and metamorphosed sediments, and compare thermal events that have affected the Thomson Orogen to orogenies that have affected other portions of the Tasmanides.

1.2 The Tasmanides

Multiple episodes of deformation and metamorphism have affected the Tasmanides, in this thesis the tectonism of interest ranges from the late Neoproterozoic to the Permian. The late Neoproterozoic saw the deposition of the Centralian Superbasin from a large epicontinental sea that covered much of what is now central Australia (Walter et al., 1996; Maidment et al., 2007). The second super-sequence of the Centralian Superbasin is associated with the rifting of the supercontinent Rodinia (Li and Powell, 2001). The rifting of Rodinia is also associated with the deposition of sediments comprising the Adelaide Rift Complex of South Australia (Glen, 2005). In detail, Rodinia is believed to have undergone multiple phases of rifting (Direen and Crawford, 2003a; Direen and Crawford, 2003b; Glen, 2005; Fergusson and Henderson, 2015), from ~825 -

~740 Ma, though the first major episode of break up was at ~750 Ma (Li et al., 2008) and was associated with the development of the Palaeo-Pacific Ocean (Li and Powell, 2001). In Australia, the Tasman Line, which separates Palaeozoic eastern Australia from older crust to the west, is a key component in the history of Rodinia and Gondwana. The Tasman Line is believed to represent the boundary along which Rodinia broke apart, although some authors suggest this occurred much farther to the east (Direen and Crawford, 2003b).

Following the Neoproterozoic breakup of Rodinia, the Tasman Orogenic Belt developed. This belt, commonly referred to as the Tasmanides, formed as part of the Terra Australis Orogen of Gondwana (Cawood, 2005). A 600 - 580 Ma rifting event is associated with clastic sedimentation and igneous intrusions in eastern Australia (Direen and Crawford, 2003a; Direen and Crawford, 2003b). These sediments were sourced either locally (Fergusson and Henderson, 2015) or were washed north from Antarctica along the eastern margin of Gondwana (Veevers, 2004). The latter stages of the 600 – 580 Ma rifting event overlapped with the Petermann Orogeny of central Australia (650 - 580 Ma; Fergusson and Henderson, 2015).

By the middle to late Cambrian Gondwana had assembled (Li and Powell, 2001). East-west contraction during the Delamerian Orogeny occurred at ~514 - 490 Ma (Foden et al., 2006), with the effects felt as far north as the Anakie Inlier of the Thomson Orogen (Withnall et al., 1996). In the late Cambrian to Ordovician the shallow Larapintine Sea covered much of central Australia (Maidment et al., 2007), and quartz turbidites were deposited in the Lachlan Orogen and southern Thomson Orogen (Murray, 1986; Veevers, 2015). The cessation of the Delamerian Orogeny marks the end of the Delamerian Supercycle and the beginning of the Benambran Cycle of the Lachlan Supercycle, which itself concludes with the Benambran Orogeny (Glen, 2005). Turbidite deposition in the Lachlan Orogen is associate with the Benambran Cycle (~490 - 434 Ma; Glen, 2005), which has temporal links to the Mossman Orogenic event of north Queensland (Fergusson et al., 2013). The latter stages of contractional deformation during the Benambran Orogeny are associated with intrusions of the Lachlan Orogen in Victoria (Draper, 2006; Champion et al., 2009). The marine environment of the Cambro-Ordovician continued in the Silurian and early Devonian, though preserved sediments fall into two distinct types: clastic shoreline sediments that grade into deep marine environments, and those associated with an active volcanic margin (Li and Powell, 2001). Their significance, and their relationship to each other, is speculative, though southward movement along the eastern Gondwana margin might be the cause, potentially associated with late Silurian subduction under the north Queensland part of the Gondwana margin (Li and Powell, 2001).

The Tabberabberan Orogeny of the middle Devonian (~390 - 380 Ma) is associated with back-arc extension and emplacement of granitoids throughout the Lachlan Orogen. Evidence of the Tabberabberan Orogeny is also preserved in the New England Orogen and the far north of the Thomson Orogen (Glen, 2005).

The Kanimblan Orogeny of the late Devonian to Carboniferous (~340 Ma; Glen, 2005) involved rifting and sedimentation associated with a convergent margin that led into the Permian-Triassic Hunter Bowen Orogeny (~265 - 230 Ma; e.g., Kositcin et al., 2009). Widespread evidence of the Hunter Bowen Orogeny is observed in the New England Orogen and, to a lesser extent, the northernmost Thomson Orogen (Davis et al., 1998).

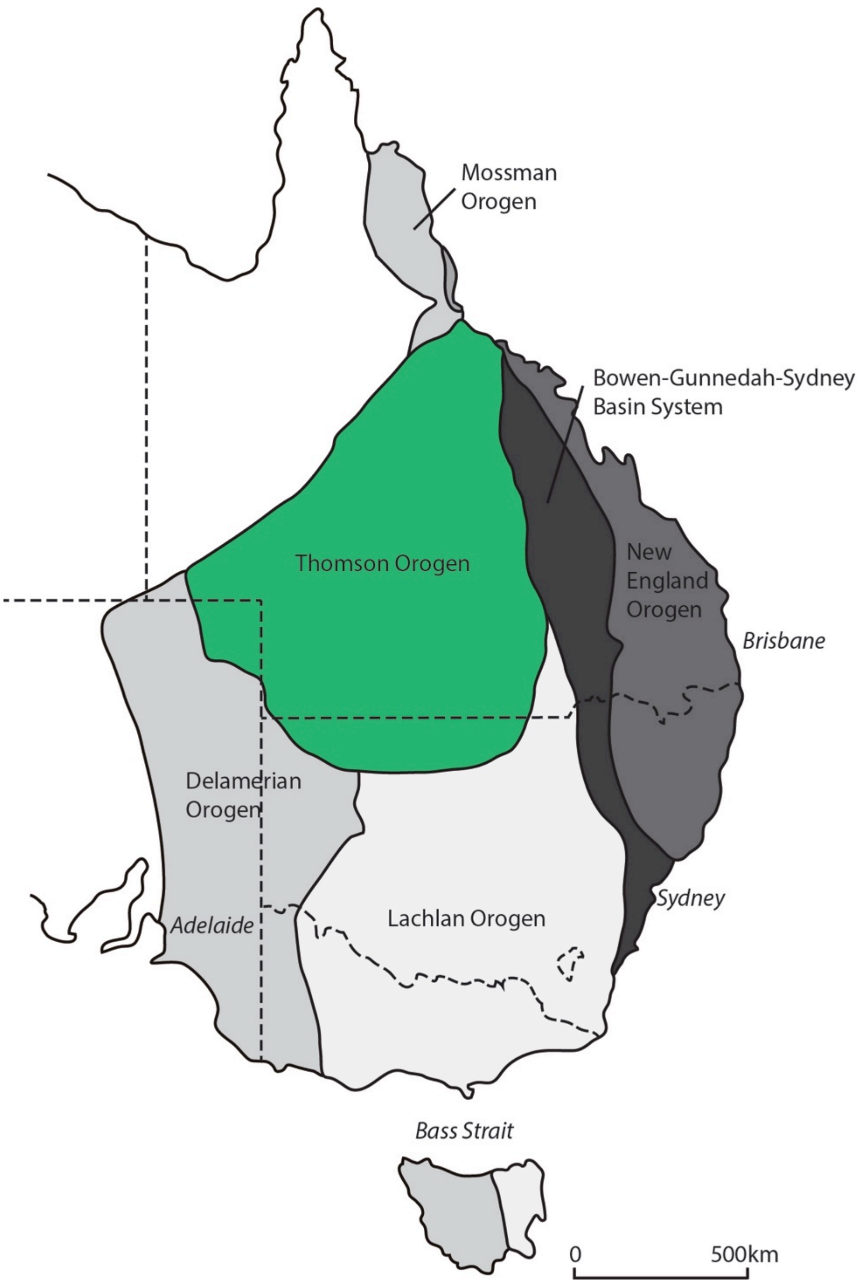

Figure 1.1: *The Tasmanides (after Glen, 2005).*

1.3 The Thomson Orogen

The name Thomson Orogen was coined by Murray and Kirkegaard (1978) as a way of distinguishing the northern Tasmanides, then referred to as the Tasman Orogenic Zone, from the Lachlan and Kanmantoo (now Delamerian) Orogens of the south. The great expanse, and the hidden nature, of the Thomson Orogen warranted study as an entity entirely of its own. Despite comprising a significant portion of Australia, the tectonic evolution of the Thomson Orogen is poorly understood and constrained. Previous work has focussed on the largest exposures of the Anakie Inlier and Charters Towers Province, also known as the Lolworth-Ravenswood Block (e.g., Withnall et al., 1995; Fergusson et al., 2001), with some work conducted on drillcore obtained from government sponsored extension of oil exploration wells into basement rocks (Webb and McDougall, 1968; Murray, 1994). These drillcore were dated with K-Ar geochronology in the 1960s (Harding, 1969), which provided some early, though somewhat unreliable, radiometric age constraints.

The oldest known rocks of the Thomson Orogen are the Neoproterozoic outcrops of the Anakie Inlier (Withnall et al., 1995; Fergusson et al., 2001). These rocks were deformed multiple times, likely during the Delamerian Orogeny as suggested by K-Ar dating (Withnall et al., 1996), and earlier K-Ar dating of basement drill core has provided somewhat unreliable Devonian ages for intrusions into the Thomson Orogen (Harding, 1969). Combined, these geochronological data provide a basis from which to build a more accurate thermal history of the Thomson Orogen.

1.4 Thesis overview

In chapter 2 a previously undescribed outcrop of Thomson Orogen sediments is described and named. The outcrop at Mount McLaren is compared to other units in the northern Anakie Inlier and Charters Towers Province, a number of which are found to be deposited in potentially similar environments, and are of comparable provenance and age.

Chapter 3 details the $^{40}Ar/^{39}Ar$ geochronology undertaken for this project. A number of drillcore and surface samples were obtained from the Geological Survey of Queensland's Exploration Data Centre, with further samples of metamorphic rocks from key areas of the north-eastern Thomson Orogen obtained during fieldwork undertaken for this project. Many samples were previously dated by the K-Ar method, thus new $^{40}Ar/^{39}Ar$ step-heating data test the accuracy of the previous K-Ar results.

In chapter 4 I summarise the main findings of my research, and propose possibilities for future work. Appendix A contains sample location information, including coordinates. Appendix B contains tables of the $^{40}Ar/^{39}Ar$ analytical results. Appendix C contains $^{40}Ar/^{39}Ar$ geochronology step-heating spectra, ideograms, and isochrons of data from the Thomson Orogen.

Chapter 2: Sedimentology and stratigraphy of the Mount McLaren beds, NE Queensland, and implications for Cambrian-Ordovician depositional environments of eastern Australia

Abstract

The Thomson Orogen comprises basement rocks of a large part of north-eastern Australia. Much of the Thomson Orogen is made up of metasediments, but the depositional environments of these rocks remain largely undescribed. Most previous studies of the northern Thomson Orogen have focused on relatively large exposures in the Anakie Inlier and Charters Towers Province, leaving some smaller exposures overlooked. One of these relatively small exposures is at Mount McLaren in east-central Queensland, where >2,000 m of previously undescribed strata of the northern Thomson Orogen are exposed. These metasediments are herein named the Mount McLaren beds. Based on lithological and geochronological similarities, we suggest that the Mount McLaren beds correlate with the Les Jumelles beds and the Puddler Creek Fm. We propose that the late Cambrian-Early Ordovician relatively shallow-marine environment of the Mount McLaren beds was a precursor to the Ordovician deep marine environment of much of the Lachlan and southern Thomson Orogens.

2.1 Introduction

The Thomson Orogen is one of a number of east Australian crustal domains (collectively referred to as the Tasmanides) that record evidence of Rodinia breakup and the subsequent formation of the eastern margin of Gondwana (Glen, 2005). The Tasmanides include the Thomson, Delamerian, Lachlan, New England and Mossman Orogens, as well as the overlying Permo-Triassic Bowen, Gunnedah and Sydney Basin system (Figure 2.1).

The Neoproterozoic to early Paleozoic Thomson Orogen, which consists, primarily, of meta-sandstone, pelites, and granite, underlies much of Queensland and northern New South Wales (e.g., Draper, 2006; Purdy et al., 2013). The primary exposures of the Thomson Orogen are within the Anakie Inlier and in the Charters Towers Province of NE Queensland (Purdy and Brown, 2011; Withnall and Henderson, 2012; Purdy et al., 2013; Figure 2.1), both of which have been the focus of significant previous research (see summaries in Withnall et al. (1995) and Fergusson and Henderson (2013). In the Anakie Inlier, Thomson Orogen rocks are collectively referred to as the "Anakie Metamorphic Group", a succession of Neoproterozoic to Cambrian sediments that have undergone greenschist- to amphibolite-facies metamorphism (Withnall et al., 1995; Withnall et al., 1996; Fergusson et al., 2001; Fergusson et al., 2007a).

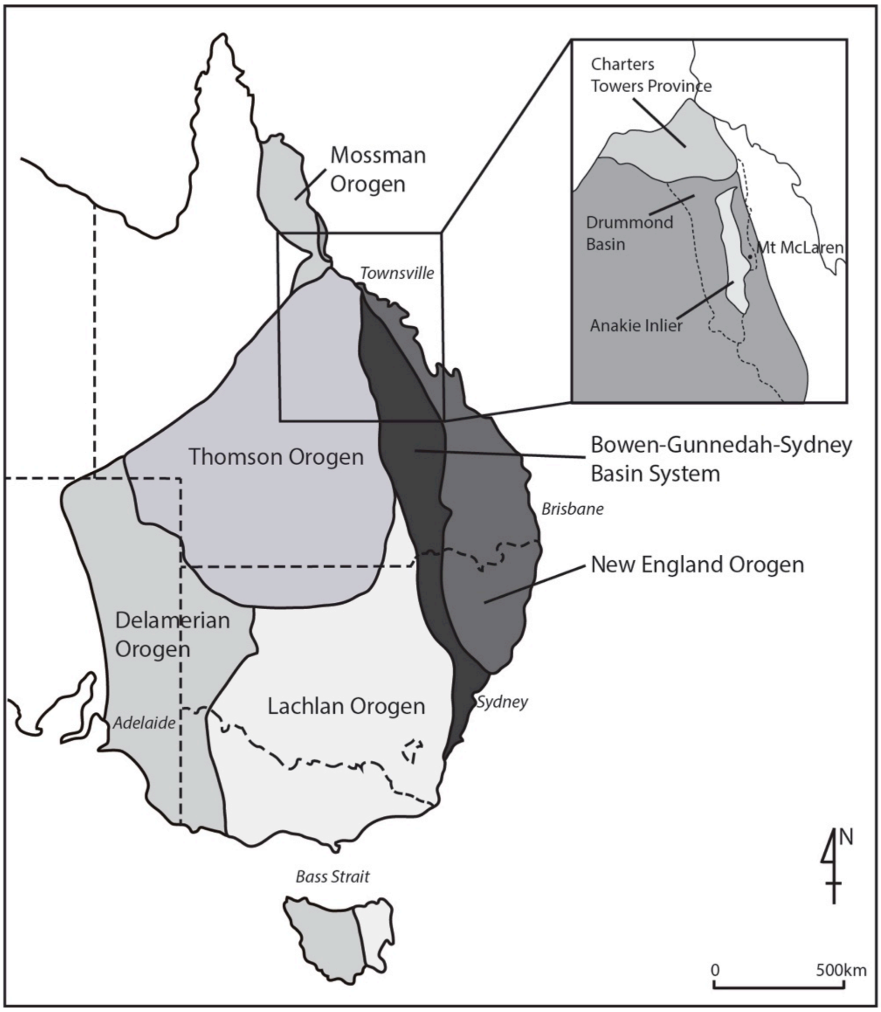

Figure 2.1: *Geologic and tectonic divisions of the Tasmanides, eastern Australia (after Glen 2005), with inset showing major divisions of the northern Thomson Orogen (after Purdy et. al., 2013; Fergusson and Henderson, 2013).*

The Anakie Metamorphic Group and correlative strata continue at depth below younger basins such as the Drummond, Bowen, Galilee, Adavale and Eromanga Basins (Withnall et al., 1995). The Charters Towers Province is composed of Neoproterozoic to early Palaeozoic metasediments (Purdy et al., 2013; Fergusson et al., 2007).

Smaller exposures of the Thomson Orogen also provide insight into its depositional environment. Mount McLaren in east-central Queensland is one such exposure of coherent basement stratigraphy. In this contribution we describe the basic sedimentology of the newly named Mount McLaren beds, evaluate potential correlative units in the northern Thomson Orogen, and discuss implications for proposed models of extensive Cambrian to Ordovician sandstone and turbidite deposition in eastern Australia.

2.2 Mount McLaren and the Mount McLaren beds

Mount McLaren is located 40 km north-east of Clermont in central Queensland, to the east of the Anakie Inlier and to the west of the Permian-Triassic Bowen Basin, one of the major sedimentary basins that overlie the Thomson Orogen. Mount McLaren is a circular basement outcrop, with a diameter of ~5000 m, of moderate relief compared to the surrounding central highlands. The basement stratigraphy at Mount McLaren is well exposed along a number of shallow streambeds that run roughly perpendicular to strike. In places, along-strike exposures are also quite extensive. The Mount McLaren basement rocks were mapped in the 1990s as "Neoproterozoic to Cambrian undivided phyllite, cleaved sandstone, labile meta-arenite and quartzite" (Withnall et al., 1995), but the extent of the Mount McLaren exposure warrants more detailed description.

The majority of Mount McLaren is made up of a succession of tilted quartzites that we have named the Mount McLaren beds. In general, these beds consist of west-dipping, greenschist-facies meta-sandstones and lesser meta-siltstones. Field relationships and detrital zircon U-Pb data bracket the age of the Mount McLaren beds to between the late Cambrian and Late Devonian (Oorloff, 2014), but, as described below, likely correlation with other northern Thomson stratigraphic sequences narrow this range to late Cambrian to Early Ordovician. On the western side of Mount McLaren, the Mount McLaren beds are structurally overlain by Devonian volcanic rocks that are temporally correlative with the Silver Hills Volcanics of the Drummond Basin (Oorloff, 2014). On the eastern side of Mount McLaren, the Mount McLaren beds are structurally overlain by an east-dipping conglomeratic unit containing clasts of both the Mount McLaren beds and Devonian volcanic rocks (Oorloff, 2014; Figure 2.2).

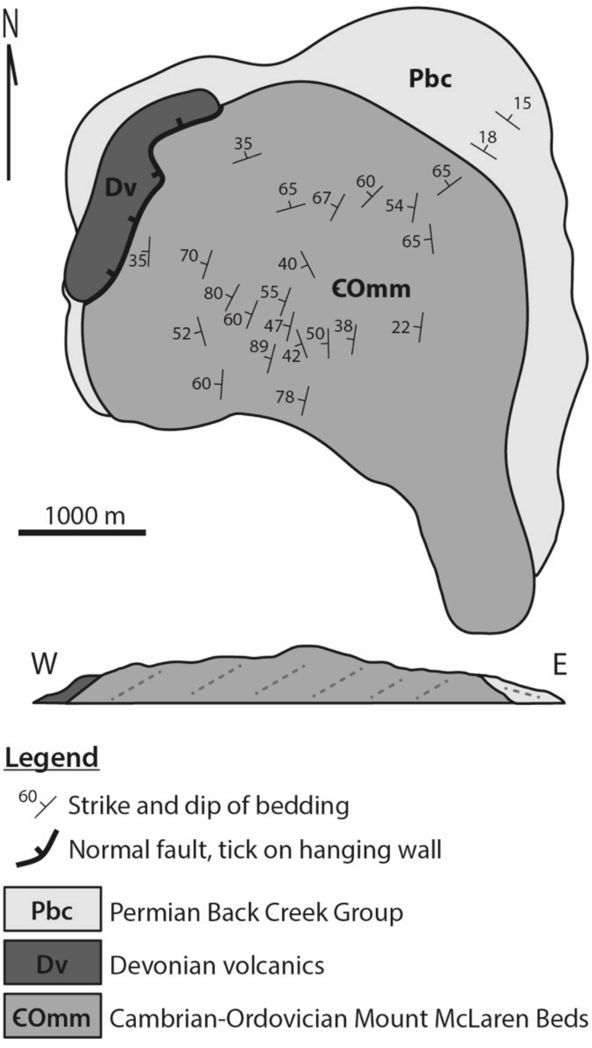

Figure 2.2: *Simplified geology of Mt. McLaren (-22.35° latitude, 147.78° longitude) and geologic cross-section.*

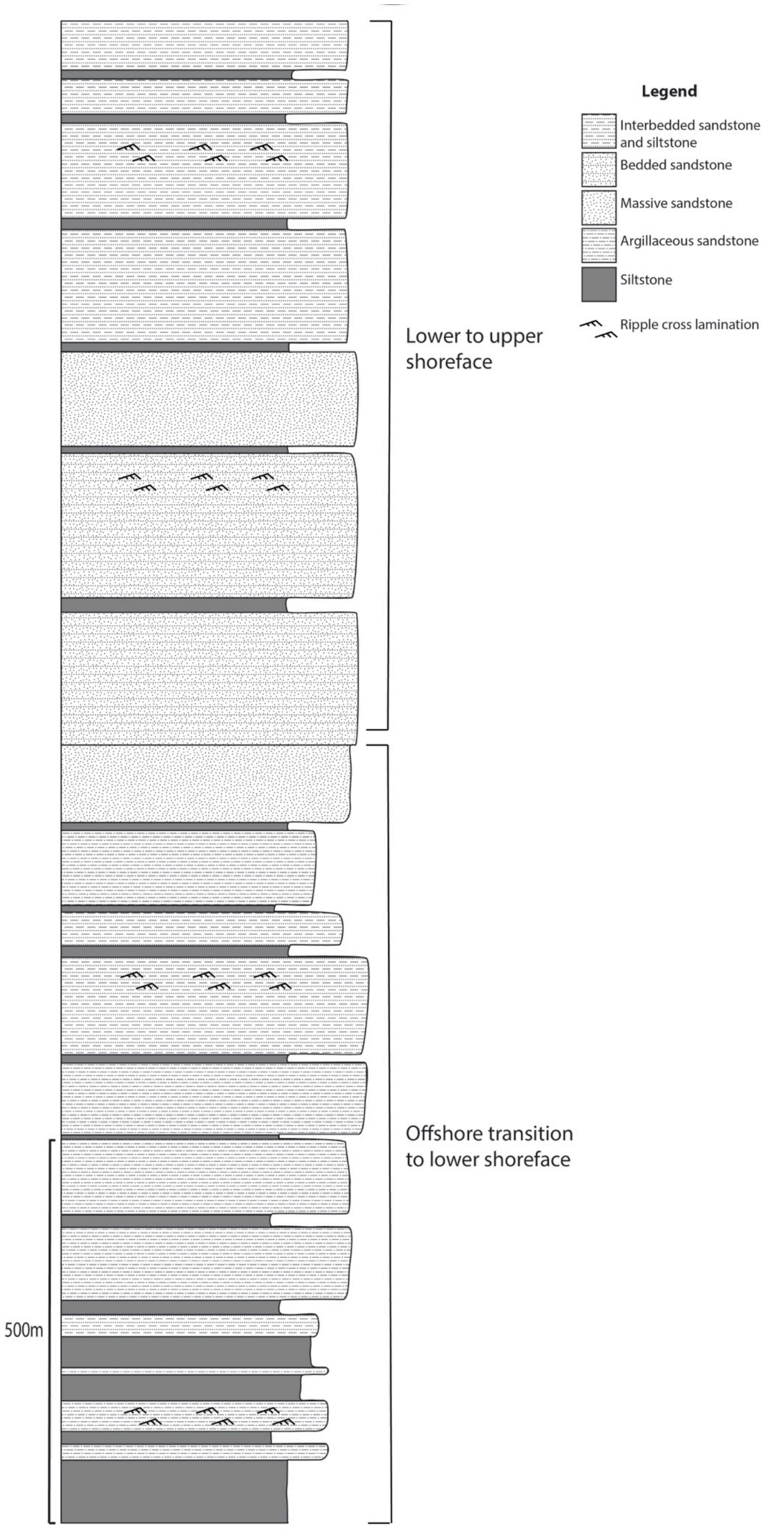

Figure 2.3: *Stratigraphic column of the Mt. McLaren Fm. with interpretation of depositional environments.*

2.3 Sedimentology and stratigraphy of the Mount McLaren beds

The exposed portion of the Mount McLaren beds at their type locality is ~2,200 m-thick, although this is a minimum thickness estimate because both the upper and lower contacts are faults. The Mount McLaren beds have undergone greenschist-facies metamorphism, which has obscured sedimentary structures, but sufficient sedimentary detail is preserved to broadly describe the sedimentology of the formation.

Figure 2.4: *Sedimentary structures in the Mt. McLaren beds. Clockwise from top-left: (a) Bedding in sandstone, (b) planar- and cross-stratification, (c) hummocky cross-stratification, (d) graded bedding.*

We subdivide the Mount McLaren beds into upper and lower successions that are defined by broad lithological and textural differences (Figure 2.3). The lower succession is 950 m-thick and is dominated by medium- to fine-grained, quartz-rich sandstones that have been metamorphosed to quartzite. The sandstones are up to 200 m-thick with sharp, erosive bases, separated by thinner (generally <20 m-thick) siltstone units (Figure 2.4a) that occur near the base of the beds. The siltstones (which are now metapelities) are finely laminated but otherwise have few observable sedimentary structures. The sandstone beds vary in thickness between 0.5 and 10 m, although they are generally between 2 and 4 m-thick. The sandstones are planar bedded (Figure 2.4a), often massive but also displaying normal grading in places and are locally cross-bedded (Figure 2.4b). Examples of hummocky cross-stratification (HCS, Figure 2.4c) are present toward the top of the lower succession.

The upper succession is of similar lithology to the lower succession, but there is broad-scale coarsening of grain size up-section, including very coarse and subangular quartz clasts within the base of some beds in the upper succession. Sandstone units of the upper succession are up to 200 m-thick, and although they are interbedded with minor sandy siltstones (as in the lower succession), the siltstones of the upper succession are fewer and thinner, such that overall silt content is reduced in the upper 1,200 m of the exposed section. In general, few sedimentary structures are present in the upper succession, though toward the top of the section repeated units of interbedded sands and silts were observed, as were graded beds >10 cm-thick that have coarse bases and possible contorted bedding (Figure 2.4d).

Petrographic analysis of sandstone samples from both the upper and lower successions revealed little compositional variation. The samples are dominated by quartz and secondary micas. Moderately to well sorted, sub-rounded quartz grains have syntaxial overgrowths and undulose extinction, with primary grain shape preserved in many cases. These observations indicate that the sandy units were deposited as sub-rounded and moderately to well sorted, quartz-rich sand, with some minor clays. One sample contains alternating layers of recrystallised quartz and actinolite.
The amphiboles in this sample form a bladed, intergrown mass of crystals that overprint the original quartz grains, and are therefore the result of a later event likely unrelated to the deposition of the beds.

2.4 Discussion

2.4.1 Depositional environment of the Mount McLaren beds

The general sedimentology of the Mount McLaren beds is coarse- to medium-grained, massive sands with occasionally observable <1 m-scale planar cross-bedding, alternating with silty clays. The lower succession consists of massive and cross-bedded, fine-grained sandy units that alternate with silty clays with poorly preserved but convincing HCS is observed in the middle of the beds, which suggests shallow-marine deposition (Johnson and Baldwin, 1996; Myrow and Southard, 1996; Dumas and Arnott, 2006). We therefore propose that the depositional environment of the Mount McLaren beds was similar to a storm-dominated clastic shelf containing elements of the offshore transition and the lower to upper shore face. A potential alternate interpretation is a deep water, fan-type deposit, though the lack of more recognizable Bouma-sequence deposits or channels in thicker sandstone units usually observed in submarine fan deposits (e.g., Mutti and Ricci Lucchi, 1972) and the presence of HCS in at least some areas of the succession argues against this. Although it is difficult to identify small-scale regressive and transgressive cycles within the beds, silt content decreases, and sand units are generally coarser, up-section. This observation suggests an overall shoaling from the base to the middle of the upper succession, above which cm-scale interbedded sands and silts, in association with possible contorted bedding near the top of the upper succession, may indicate a change to a deeper water facies (e.g. Bourgeois, 1980). Stratigraphic sequences such as the Mount McLaren beds that consist of thousands of meters of sandy, shallow marine deposits are somewhat unusual but are not without precedent (e.g. Levell, 1980; Lindsey and Gaylord, 1992; Higgs, 1996).

2.4.2 Cambrian-Ordovician stratigraphic correlations in eastern Australia

Similarities in lithology and detrital zircon U-Pb ages suggest that the Mount McLaren beds correlate with the Les Jumelles beds and Puddler Creek Fm. of the nearby northern Anakie Inlier and Charters Towers Province, respectively (Oorloff, 2014; Lee et al., 2015; Figure 2.5). Similarities in detrial zircon U-Pb ages were determined by visual matching of histogram peaks, as well as comaprisons of maximum depositional ages. The Les Jumelles beds, which are located in the northernmost part of the Anakie Inlier, consist of very fine- to medium-grained quartzose to feldspathic sandstones and mudstones (Blewett et al., 1998; Blake et al., 2012). Detrital zircon U-Pb data constrain the maximum depositional age of the Les Jumelles beds to 528 ± 9 Ma (middle Cambrian; Cross et al., 2015), and they are intruded by the Early to Middle Ordovician Coquelicot Tonalite (Blake et al., 2012). These age constraints therefore permit temporal correlation with the ≥505 Ma Mount McLaren beds, determined by the youngest detrital zircon (Oorloff, 2014).

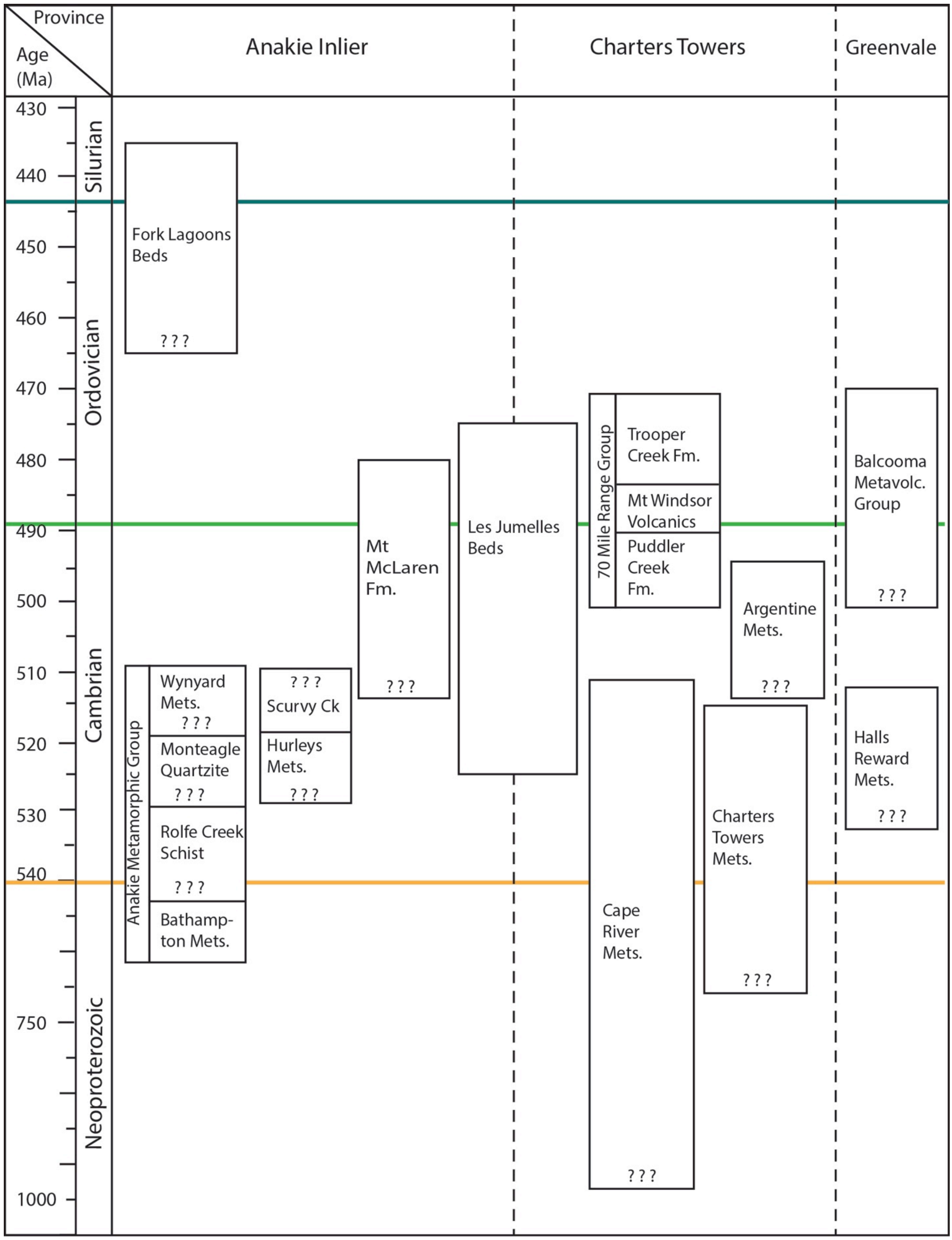

Figure 2.5: *Proposed stratigraphic relationships between the siliciclastic rocks of the Thomson Orogen. Age constraints for Fork Lagoons beds from Palmieri (1978) and Fergusson et al. (2007a); Mt. McLaren Fm. from Oorloof et al. (in review); Scurvy Creek Meta-arenite, Hurleys Metamorphics, and the Anakie Metamorphic Group from Withnall et al. (1996) and Fergusson et al. (2001); Les Jumelles beds from Fergusson and Henderson (2013) and* Purdy et al. (2013)*; Cape River Metamorphics from Fergusson et al. (2007a), and Hutton (1997) in Fergusson and Henderson (2013); Charters Towers Metamorphics from Hutton and Crouch (1993), and Fanning (1995) in Fergusson and Henderson (2013); Seventy Mile Range Group from Henderson (1986), Fergusson et al. (2007a), and Cross et al. (2015); Argentine Metamorphics from Fergusson et al. (2007a); Balcooma Metavolcanics from Withnall et al. (1991); and Halls Reward Metamorphics from Nishiya et al. (2003).*

The Puddler Creek Fm., which is the oldest stratigraphic unit of the Charters Towers Province, likely correlates with the Les Jumelles beds (Fergusson and Henderson, 2013; Purdy et al., 2013; Cross et al., 2015). A recent geochronology report published by the Geological Survey of Queensland (Cross et al., 2015) provides a maximum depositional age of ~499 Ma for the Puddler Creek Fm. based on unpublished detrital zircon U-Pb data. A minimum depositional age is provided by the overlying Early Ordovician Mount Windsor Volcanics, which have been dated at 479 ± 5 Ma. The Puddler Creek Fm. consists of graded, fine- to medium-grained sandstone beds of 5 cm to 2.5 m thickness, interspersed with siltstones that are up to 4 m-thick (Henderson, 1986; Berry et al., 1992), similar to both the Les Jumelles beds and Mount McLaren beds.

Importantly, the Mount McLaren beds seem to be roughly the same age as the youngest part of the Anakie Metamorphic Group, the Wynyard Metamorphics, which have a maximum depositional age of ~510 Ma and are made up of fine- to medium-grained meta-quartzite and medium-grained mica schist (Fergusson et al., 2001; Offler et al., 2011; Purdy et al., 2013). In summary, lithological and detrital zircon U-Pb data, in conjunction with radiometric dating of the Coquelicot Tonalite and Mount Windsor Volcanics, suggest that the Mount McLaren beds, Les Jumelles beds, Puddler Creek Fm., and Wynyard Metamorphics are correlative and were deposited in the late Cambrian to Early Ordovician (Figure 2.5).

2.4.3 Implications for Cambrian-Ordovician sandstone deposition in eastern and central Australia

In addition to the east Australian correlations described above, there are also likely correlations between the Thomson Orogen and strata of the Neoproterozoic to Paleozoic Centralian Superbasin (Walter et al., 1992; Maidment et al., 2007). Specifically, the Mount McLaren beds correlate with the shallow marine, Early Ordovician Pacoota Sandstone of the Amadeus Basin in central Australia on the basis of similarities in detrital zircon ages, with the main histogram peak at ~500 Ma (Maidment et al., 2007; Oorloff, 2014). The widespread Cambrian-Ordovician sandstones of eastern and central Australia are depositional remnants of the Larapintine Sea, an early Paleozoic shallow, epi-continental sea that covered much of central and eastern Australia (Li and Powell, 2001; Haines and Wingate, 2007; Maidment et al., 2007; Figure 2.6). The early Paleozoic deposits of the Larapintine Sea are linked by detrital zircons that have both Pacific-Gondwanan (~700 to 500 Ma)

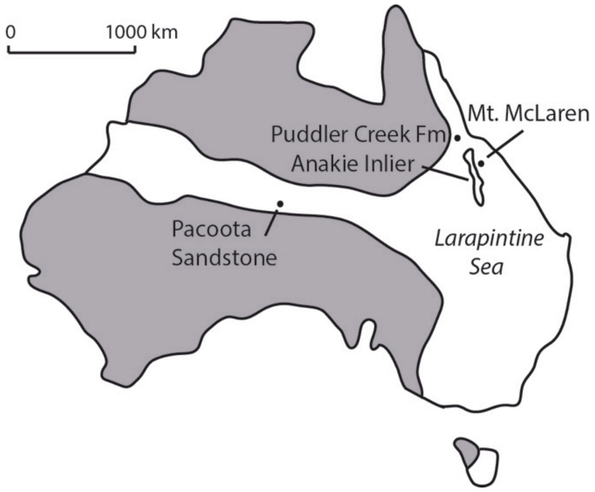

Figure 2.6: *Extent of the Cambrian-Orodovician Larapintine Sea showing the location of Mt. McLaren (after Squire et. al. 2006).*

and Grenville-Gondwanan (~1300 to 1000 Ma) age populations, attributes that are useful for tracing sediment provenance (Fergusson et al., 2001; Squire et al., 2006; Maidment et al., 2007; Fergusson et al., 2007c). A number of studies have suggested that the Ross Orogen of eastern Antarctica was the source of both these Australian Cambrian-Ordovician sediments (Cawood, 2005; Maidment et al., 2007), as well as the somewhat younger Ordovician turbidites of the Lachlan Orogen (Fergusson et al., 2013), which are discussed in more detail below. The older, Grenville-Gondwanan aged sediments are likely derived from the Musgrave Province in Central Australia, although a more distal source is also likely (Maidment et al., 2007). This interpretation implies that sediment was transported north from the Ross and Delamerian Orogens, reworked along the margin of eastern Gondwana, and eventually deposited in the offshore to shoreface transition of the Larapintine Sea (Cook, 1972; Maidment et al., 2007), a process not unlike the modern-day transportation of beach sands from south-eastern Australia to the coast of Queensland (Boyd et al., 2008).

2.4.4 Comparison with Ordovician turbidites in the Lachlan Orogen

In the southern part of the Thomson Orogen, turbidites logged in basement drill core (Murray, 1994) may be correlative with some Ordovician turbidites of the Lachlan Orogen, e.g.: those of the Sunbury Group of Victoria (Glen et al., 2009). One prominent model for the source of these sediments is the so-called "Trans-Gondwanan Supermountain" (TGSM), which is proposed to have developed in Neoproterozoic to Cambrian time during the collision of East and West Gondwana (Squire et al. 2006). Erosion of the TGSM may have resulted in a "super-fan" that was similar to, though much larger than, the present-day Bengal fan (Squire et al., 2006; Veevers, 2015). The most northerly extent of this super-fan is regarded by Veevers (2015) as the Argentine and Wynyard Metamorphics of the northern Thomson Orogen, as well as the Ordovician Fork Lagoons beds of the Anakie Inlier. However, we draw a different conclusion on the basis of depositional facies and temporal correlations. Our interpretation of the depositional environment of the Mount McLaren beds, in conjunction with our proposed correlations for the Cambrian-Ordovician rocks of the northern Thomson Orogen, argues against a super-fan interpretation, because we view the northern Thomson Orogen metasediments as shallow marine deposits unrelated to a deep-water fan. Moreover, based on the radiometric ages from the northern Thomson Orogen, the Mount McLaren beds, Wynyard Metamorphics, Les Jumelles beds, and Puddler Creek Fm. all seem to be older than Ordovician turbidites of the Lachlan Orogen, and most of the metasediments of the northern Thomson Orogen, including the Argentine Metamorphics, are older still (e.g., Fergusson et al., 2001). Additionally, although some studies have interpreted a deep water depositional environment for the Fork Lagoons beds (e.g. Fergusson and Henderson, 2013) there is considerable evidence, such as the presence of carbonates, for shallow water deposition of these sediments (see Withnall et al., 1995). We suggest, therefore, that the Ordovician turbidites of the Lachlan Orogen differ, both in terms of age and depositional environment, from the more shallow marine Cambrian-Ordovician sandstones of the Mount McLaren beds and their northern Thomson Orogen correlatives. This conclusion implies that (1) the northern Thomson Orogen metasediments were not deposited at the northern extent of a super-fan system emanating from the TGSM; and (2) there was a change in relative sea level during the intervening 20 to 60 My period between deposition of the late Cambrian-Early Ordovician Mount McLaren beds in offshore to shoreface transition conditions in the northern Thomson Orogen, and Ordovician deep marine deposition of turbidites in the Lachlan and southern Thomson Orogens. The apparent change in depositional environment recorded by the uppermost portion of the Mount McLaren beds may be a harbinger of this transition.

2.5 Conclusions

The newly-named Mount McLaren beds are a ~2,200 m-thick, late Cambrian to Early Ordovician accumulation of northern Thomson Orogen metasediments deposited in a shallow, clastic sea that covered a large portion of north-eastern and central Australia. Based on lithological similarities and detrital zircon U-Pb data, the Mount McLaren beds seem to correlate with other stratigraphic units in the northern Thomson Orogen, including the Les Jumelles beds in the northern Anakie Inlier and the Puddler Creek Fm. of the Seventy Mile Range Group of the Charters Towers Province (Oorloff, 2014; Lee et al., 2015). The most probable source of the sediment comprising these stratigraphic units is the Ross-Delamerian Orogen, with transport occurring along the eastern margin of Gondwana (e.g., Maidment et al., 2007; Fergusson and Henderson, 2015). The Mount McLaren beds and their stratigraphic correlatives were part of a large, shallow sea that was the precursor to a deep marine environment in which Ordovician turbidites of the Lachlan Orogen were subsequently deposited.

Chapter 3: $^{40}Ar/^{39}Ar$ thermochronology of the Thomson Orogen

Abstract

The Thomson Orogen is part of the east Australian Tasmanides, a province of deformed rocks that records the breakup of Rodinia and subsequent formation and break-up of Gondwana. The least understood of the Tasmanides, being covered by younger sedimentary basins in many places, the Thomson Orogen comprises the majority of Queensland and extends into northern New South Wales. In comparison, the Lachlan and New England Orogens, which lie to the south and east of the Thomson Orogen, respectively, are relatively well-studied, but the lack of geochronological data from the Thomson Orogen precludes detailed comparisons. Understanding the age and thermal history of the Thomson Orogen is key to placing it in context with the remainder of the Tasmanides. This chapter provides an overview of K-Ar and $^{40}Ar/^{39}Ar$ geo- and thermo-chronology undertaken on rocks of the Thomson Orogen, adds new $^{40}Ar/^{39}Ar$ data, and places these results within the context of eastern Australian tectonism.

The Thomson Orogen preserves evidence of having undergone temporally similar tectonic events to those reported in the New England and Lachlan Orogens, and, to a lesser degree, the Delamerian Orogen. The results from this study show that metamorphic rocks of the Thomson Orogen are dominantly Ordovician to Silurian, likely recording events which have been attributed to Benambran, Tabberabberan and/or Kanimblan orogenic events in the Lachlan Orogen. The sole evidence for Delamerian ages in this study are from the Anakie Inlier. In the east of the Thomson Orogen, evidence for deformation during the early Hunter-Bowen Orogeny (HBO) was found, though lack of these ages <100km to the west suggest the effects of the HBO were not widespread in the Thomson Orogen. $^{40}Ar/^{39}Ar$ ages from igneous rocks are interpreted as cooling ages, and are similar to ages recorded in the Lachlan Orogen which have been attributed to the Tabberabberan Cycle of the Lachlan Supercycle. This synthesis should prove useful to the development of future tectonic models of the Thomson Orogen.

3.1 Introduction

The Tasmanides of eastern Australia (Figure 3.1; e.g., Glen, 2005) have been divided into a number of orogens, the development of which are related to convergent-margin tectonism over a wide timeframe that spans most of the Phanerozoic. This long history has been most thoroughly examined in easternmost Australia, where the New England Orogen contains most of the important features (e.g., magmatic arc, accretionary prism, forearc basin) of a convergent margin (e.g., Leitch, 1978; Coney et al., 1990; Li et al., 2012), and in southern Australia, where the Lachlan and

Delamerian Orogens preserve evidence for a multitude of events including accretion, arc magmatism, and continental extension (Glen, 2013). Much of our understanding of the timing of these events comes from $^{40}Ar/^{39}Ar$ studies of basement rocks in the Lachlan, Delamerian, and New England Orogens (e.g., Foster et al., 1999; VandenBerg, 1999; Shaanan et al., 2014).

Owing partially to poor outcrop, the tectonic history of the northern part of the Tasmanides is considerably less understood than the southern and eastern counterparts. Nevertheless, some previous studies have suggested that the overall tectonic development of the northern Tasmanides shares strong similarities with the Delamerian (Withnall et al., 1996; Nishiya et al., 2003; Wood, 2006; Wood and Lister, 2013; Spampinato et al., 2015b) and Lachlan Orogens (Fergusson et al., 2001; Burton, 2010), thereby implying periods of deformation that were coincident along the entire length of the east Australian margin (e.g., Fergusson et al., 2007b; Fergusson and Henderson,

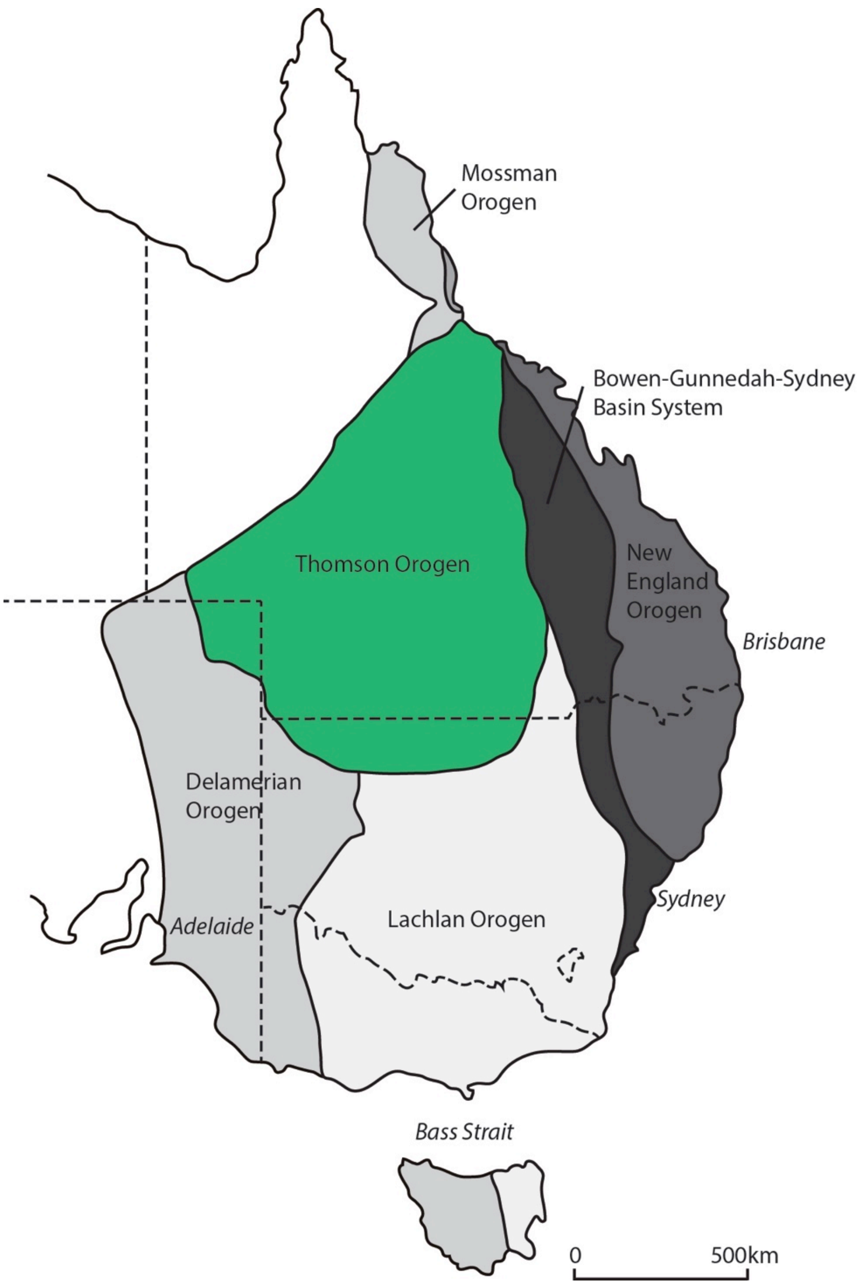

Figure 3.1: *The Tasmanides, with the Thomson Orogen highlighted (after Glen, 2005).*

2015). In order to test this idea, this project aims to expand and evaluate the $^{40}Ar/^{39}Ar$ record of a large component of the northern Tasmanides (the Thomson Orogen), in a manner similar to studies previously conducted in the Lachlan, Delamerian, and New England Orogens. Two specific questions of particular interest that can potentially be answered with the results from this project are (1) are periods of Paleozoic deformation recognized in the Lachlan Orogen also manifest in the Thomson Orogen? and (2) were basement rocks of the Thomson Orogen affected by a period of Permian-Triassic deformation (the Hunter-Bowen Orogeny) that is clearly evident in both the New England Orogen and in basins that overlie the Thomson Orogen, for instance the Bowen Basin? Insight into the first question has implications for the continuity of deformation along convergent margins, while an answer to the second question sheds light on whether the Hunter-Bowen Orogeny was fundamentally thin- or thick-skinned.

3.1.1 Background

Much of the Thomson Orogen is composed of metamorphosed pelitic sediments that are intruded by granites. The $^{40}Ar/^{39}Ar$ method is useful for rocks of this type, in particular granites, as they typically contain multiple K-bearing minerals that are suitable for $^{40}Ar/^{39}Ar$ geo- and thermo-chronology. Dating of multiple minerals from a single sample facilitates an understanding of thermal histories, which are particularly important for understanding complex deformation histories.

Previous geochronology of the Thomson Orogen is limited to surface exposures, drill core from mineral exploration, and drill core obtained from a 1960s government program to obtain basement intervals from oil wells. An initial program to date these rocks via the K-Ar method was undertaken in the 1960s, and it ultimately determined Late Devonian to Carboniferous ages for intrusive rocks from basement drill core of what is now the central and southern Thomson Orogen (Harding, 1969). Further K-Ar geochronology of Carboniferous and Devonian igneous rocks of the Anakie High (now the Anakie Inlier) was undertaken by Webb and McDougall (1968). They found that that ages decreased toward the east, in what is now the New England Orogen. More recent work by Withnall et al. (1996) and Nishiya et al. (2003) used K-Ar ages to suggest that the Delamerian Orogeny of south-eastern Australia also affected areas as far north as the Anakie Inlier and the Charters Towers Province, and Henderson et al. (1998) used K-Ar dating to constrain the age of the Silver Hills Volcanics (Anakie Inlier region) to the early Carboniferous.

The $^{40}Ar/^{39}Ar$ method builds on the K-Ar method with less potential for error, greater understanding of thermal events due to step-heating, and the potential to determine whether excess or low Ar in a sample is artificially altering the apparent age. The $^{40}Ar/^{39}Ar$ method has been used in a limited number of studies of Thomson Orogen rocks (e.g.: Wood and Lister, 2004, 2013; Fergusson et al., 2005; Wood, 2006). Adding to the work by Withnall et al. (1996), Wood and Lister (2013) concluded that ductile deformation in the Clermont region of the Anakie Inlier occurred at ~510 to 483 Ma, and Wood (2006) demonstrated that metamorphic grade increases while $^{40}Ar/^{39}Ar$ ages decrease from NE to SW across the Anakie Inlier, in a similar manner to that reported by Webb and McDougall (1968).

The studies mentioned above notwithstanding, modern $^{40}Ar/^{39}Ar$ geochronology studies of the Thomson Orogen have been limited. This study aims to provide a better understanding of the age and thermal history of the Thomson Orogen through a comparative study of previous K-Ar and $^{40}Ar/^{39}Ar$ results, as well as by adding new $^{40}Ar/^{39}Ar$ ages from key areas. Where other geochronological methods add to these data, i.e., where U-Pb dating of zircons has been conducted from the same unit, these previous results are also referenced.

3.2 Methods

Sixteen samples from the Thomson Orogen, including surface samples and basement drill core, were dated using $^{40}Ar/^{39}Ar$ geochronology (Figure 3.2). Samples were selected based on geographical location, as well as previous geochronology studies such as U-Pb dating of both detrital and primary zircons and previous K-Ar dating. The addition of $^{40}Ar/^{39}Ar$ data to this existing database reveals a previously unknown thermal history.

Both drill core and surface samples were obtained from the Geological Survey of Queensland (GSQ) Exploration Data Centre (EDC) at Zillmere, Queensland, as well as from field work. An additional surface sample (NQ37) of the Halls Reward Metamorphics was donated by Dr. Bob Henderson via Mr. Ian Withnall. Nine of the 16 samples were from drill core, the remainder were surface samples. From these 16 samples, a total of 21 sub-samples were prepared for $^{40}Ar/^{39}Ar$ geochronology. Petrographic analysis was undertaken to confirm that the samples contained minerals suitable for dating, and further SEM analysis was completed to confirm mineralogy prior to irradiation. The minerals dated in this study include muscovite, biotite, hornblende, potassium feldspar and plagioclase feldspar. Where possible, multiple single minerals were selected, however some samples were too fine-grained, and, in these cases, whole rock geochronology was more suitable.

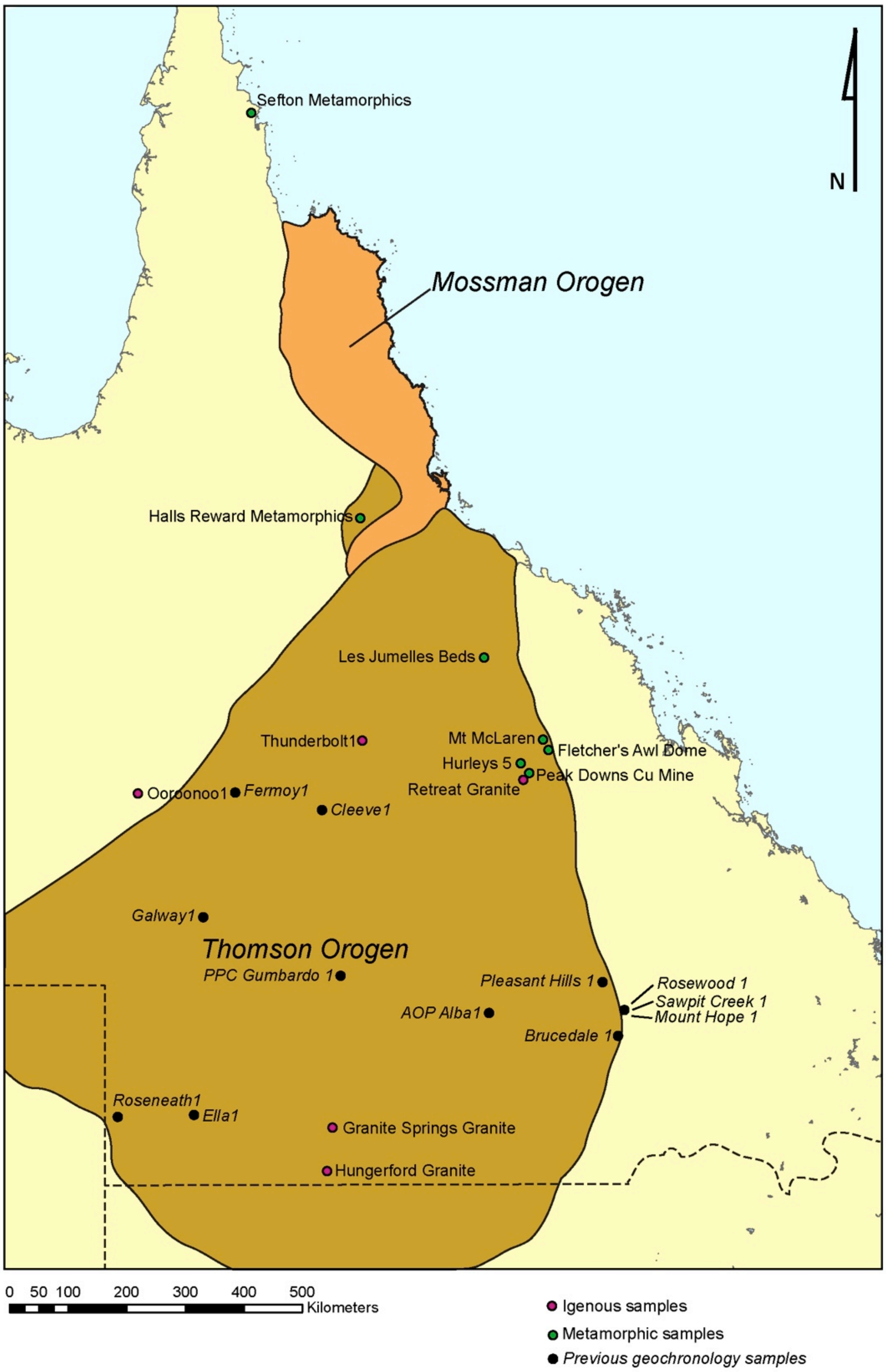

Figure 3.2: *$^{40}Ar/^{39}Ar$ geochronology sample locations, and locations of previous K-Ar geochronology samples from the Thomson Orogen.*

Micro-samples of around 1 cm^3 were taken from samples 2122054, 2122055, 2130084, 2152164, 2152166, AOM03 and MLRG01, which were then hand crushed in a percussion mill to pieces of 0.5 - 3 mm in size. These samples were then cleaned in an ultrasonic bath with distilled water for a total of thirty minutes, followed by ethanol for an additional ten minutes, after which they were given a final rinse with acetone and allowed to dry. Similarly, micro samples were taken from samples NQ37, MLHR02, MLLJ06, MLPD01, MLPD02, MLH501, MLH502, MLH503, and

MLH505, which were then hand crushed in a percussion mill to pieces <0.5 mm in size. Due to the presence of carbonate, these samples were acid treated by the following method: they were initially cleaned in a ultrasonic bath with water for a total of thirty minutes, acid-treated with 3.5N HCl for 60 minutes, rinsed with distilled water, acid-treated with 1N nitric acid for a further 60 minutes, then sequentially rinsed with distilled water, acetone, and ethanol. After a final rinse with acetone, the samples were allowed to dry, and then hand-picked under a binocular microscope with selection for irradiation based on size, freshness, and equant habit. Depending on the mineral being used for geochronology, sizes ranged from 0.5 - 3 mm, with the larger sizes for biotite and the smaller for K-feldspar. The grains were loaded into a 21-pit aluminum disk with the neutron fluency monitor Fish Canyon sanidine (age 28.201 ± 0.04 Ma, Kuiper et al., 2008), and GA1550 (98.5 ± 0.5 Ma (McDougall and Wellman, 2011) following the geometry illustrated in Vasconcelos et al., (2002).

Biotite crystals from samples 2122054, 2122055, and 2152164, plagioclase crystals from samples 2122054, 2122055, 2130084, and 2152164, K-feldspar crystals from sample MLRG01, and amphibole crystals from 2152166 were irradiated in October 2014 for 14 hours at Oregon State University, USA in a TRIGA-type reactor in a Cd-lined CLCIT facility. A second disk, containing whole rock grains from samples AOM03, MLLJ06, MLPD01, MLPD02, MLH501, MLH502, MLH503, and MLH505, muscovite crystals from samples NQ37 and MLHR02, and biotite crystals from MLHR02, was irradiated in June 2015 for 16 hours at Oregon State University, USA in a TRIGA-type reactor in a Cd-lined CLCIT facility. After a 6 month decay period samples were heated using a defocused continuous-wave argon-ion laser beam and the gas fractions were analysed in a MAP215-50 mass spectrometer at the University of Queensland Argon Geochronology in Earth Sciences Laboratory (UQ-AGES) following the procedures outlined in Vasconcelos et al., (2002). Full system blanks and air pipettes were analysed before and after each sample.

Individual sample analyses were corrected for mass discrimination, nucleonic interferences, and atmospheric contamination, adopting a $^{40}Ar/^{39}Ar$ value for atmospheric argon of 298.56 ± 0.31 (Lee et al., 2006). Analyses of individual sanidine crystals from the neutron fluency monitor Fish Canyon and GA1550 were used to calculate the J irradiation factor, and were within error of previously reported primary and refined ages (Spell and McDougall, 2003; McDougall and Wellman, 2011).

3.3 Results

Forty-two step-heating experiments were conducted on 16 samples: 26 step-heating experiments

Sample No.	***Sample Name***	***Lab No.***	***Material***	***No. of steps***	***Plateau age ± 2σ (Ma)[a]***	***Steps & % in plateau***	***Integrated age ± 2σ(Ma)***	***Ideogram age ± 2σ(Ma)[b]***	***Isochron age ± 2σ (Ma)[c]***	***$^{40}Ar/^{39}Ar$ intercept***
2122054a (1)	Granite Springs Granite	8646-01	biotite	1	397.3 ± 3.8	A-H (96%)	396.3 ± 4.3	397.2 ± 1.2 (n = 11)	398.8 ± 4.4 (n = 12)	244 ± 62
2122054a (2)	Granite Springs Granite	8646-02	biotite	1	406.0 ± 2.8	A-L (100%)	405.7 ± 3.8	406.00 ± 0.75 (n=12)	N/A	N/A
2122054b (1)	Granite Springs Granite	8635-01	plag	10	350.7 ± 2.5	C-J (99.5%)	352.7 ± 3.4	350.73 ± 0.77 (n = 9)	347.9 ± 6.0 (n = 9)	560 ± 410
2122054b (2)	Granite Springs Granite	8635-02	plag	10	N/A	N/A	379.9 ± 3.5	348.64 ± 0.93 (n = 5)	N/A	N/A
2122055a (1)	Hungerford Granite	8642-01	biotite	12	361.4 ± 2.6	A-J (95.1%)	361.3 ± 3.3	361.40 ± 0.68 (n = 12)	362.7 ± 3.0 (n = 12)	140 ± 82
2122055a (2)	Hungerford Granite	8642-02	biotite	12	365.5 ± 2.8	E-L (83.3%)	364.5 ± 3.3	365.49 ± 0.73 (n = 9)	N/A	N/A
2122055b (1)	Hungerford Granite	8634-01	plag	10	332.6 ± 5.7	C-G (58%)	337.8 ± 6.2	332.1 ± 1.7 (n = 6)	324 ± 10 (n = 10)	335 ± 30
2122055b (2)	Hungerford Granite	8634-02	plag	10	321.6 ± 2.9	C-H (56.9%)	332.1 ± 3.2	325.75 ± 0.77 (n = 5)	312 ± 11 (n = 8)	750 ± 370
MLRG01 (1)	Retreat Granite	8643-01	k-spar	11	355.9 ± 3.7	B-F (78%)	354.9 ± 3.5	356.41 ± 0.79 (n = 10)	357.7 ± 4.0 (n = 11)	260 ± 42
MLRG01 (2)	Retreat Granite	8643-02	k-spar	15	344.1 ± 2.6	D-O (89.7%)	343.5 ± 3.7	344.16 ± 0.68 (n = 14)	346.4 ± 2.8 (n = 15)	269 ± 14
2130084 (1)	Thunderbolt	8632-01	plag	18	349.5 ± 2.8	H-P (70.1%)	349.4 ± 3.3	348.86 ± 0.65 (n = 13)	347.4 ± 6.6 (n = 18)	370 ± 150
2130084 (2)	Thunderbolt	8632-02	plag	15	N/A	N/A	371.7 ± 7.6	380.8 ± 2.2 (n = 10)	390 ± 18 (n = 15)	264 ± 35
2152166 (1)	Sefton	8641-01	amph	10	397.6 ± 3.3	E-J (65.7%)	388.3 ± 3.8	396.19 ± 0.93 (n = 7)	N/A	N/A
2152166 (2)	Sefton	8641-02	amph	10	335.1 ± 3.6	C-F (75.5%)	325.2 ± 3.1	334.88 ± 0.86 (n = 5)	N/A	N/A

Sample No.	*Sample Name*	*Lab No.*	*Material*	*No. of steps*	*Plateau age ± 2σ (Ma)*[a]	*Steps & % in plateau*	*Integrated age ± 2σ(Ma)*	*Ideogram age ± 2σ(Ma)*[b]	*Isochron age ± 2σ (Ma)*[c]	*$^{40}Ar/^{39}Ar$ intercept*
2152164a (1)	Ooroonoo	8631-01	biotite	13	N/A	N/A	599.4 ± 5.6	600.1 ± 2.0 (n = 5)	598 ± 33 (n = 13)	280 ± 160
2152164a (2)	Ooroonoo	8631-02	biotite	11	N/A	N/A	644.5 ± 7.5	613.2 ± 3.0 (n = 4)	N/A	N/A
2152164b (1)	Ooroonoo	8644-01	plag	10	585 ± 12	C-E (50.5%)	427.9 ± 4.2	585.0 ± 2.9 (n = 3)	640 ± 16 (n = 10)	680 ± 270
2152164b (2)	Ooroonoo	8644-02	plag	10	N/A	N/A	759.8 ± 10.0	426.7 ± 1.9 (n = 4)	N/A	N/A
2152164c (1)	Ooroonoo	8645-01	plag	11	N/A	N/A	603 ± 14	391.9 ± 6.7 (n = 3)	N/A	N/A
2152164c (2)	Ooroonoo	8645-02	plag	11	N/A	N/A	481.1 ± 9.3	408.5 ± 5.0 (n = 3)	320 ± 120 (n = 10)	1030 ± 800
MLHR02a (1)	Halls Reward	8764-01	musc	10	441.5 ± 2.0	A-J (100%)	441.3 ± 2.3	441.48 ± 0.63 (n = 10)	N/A	N/A
MLHR02a (2)	Halls Reward	8764-02	musc	10	480.3 ± 4.2	E-G (52.4%)	490.4 ± 2.7	480.3 ± 1.1 (n = 3)	N/A	N/A
MLHR02b (1)	Halls Reward	8771-01	biotite	11	446.6 ± 2.4	E-K (77.7%)	431.4 ± 2.4	446.57 ± 0.78 (n = 7)	N/A	N/A
MLHR02b (2)	Halls Reward	8771-02	biotite	11	448.1 ± 3.0	C-I (72.9%)	426.5 ± 2.8	448.1 ± 1.1 (n = 7)	N/A	N/A
NQ37 (1)	Halls Reward	8770-01	musc	9	447.8 ± 2.0	B-I (97.8%)	447.3 ± 2.2	447.81 ± 0.67 (n = 8)	448.0 ± 2.5 (n = 9)	230 ± 140
NQ37 (2)	Halls Reward	8770-02	musc	8	447.4 ± 1.7	C-H (96.1%)	444.8 ± 2.0	447.61 ± 0.43 (n = 7)	N/A	N/A
MLLJ06 (2)	Les Jumelles	8763-02	WR	10	N/A	N/A	452.0 ± 2.2	451.81 ± 0.62 (n = 10)	N/A	N/A
AOM03 (1)	Mt McLaren	8769-01	WR	10	312.8 ± 1.8	B-E (64.8%)	307.1 ± 1.6	312.79 ± 0.58 (n = 5)	307.8 ± 6.2 (n = 10)	160 ± 120
AOM03 (2)	Mt McLaren	8769-02	WR	9	315.3 ± 1.9	B-D (66.0%)	308.0 ± 1.4	315.25 ± 0.44 (n = 3)	N/A	N/A

Sample No.	Sample Name	Lab No.	Material	No. of steps	Plateau age ± 2σ (Ma)[a]	Steps & % in plateau	Integrated age ± 2σ(Ma)	Ideogram age ± 2σ(Ma)[b]	Isochron age ± 2σ (Ma)[c]	$^{40}Ar/^{39}Ar$ intercept
MLH501 (1)	Anakie	8777-01	WR	11	N/A	N/A	485.0 ± 2.4	499.4 ± 1.0 (n = 3)	N/A	N/A
MLH501 (2)	Anakie	8777-02	WR	11	N/A	N/A	479.8 ± 2.4	491.1 ± 1.1 (n = 5)	N/A	N/A
MLH502 (1)	Anakie	8776-01	WR	11	489.7 ± 3.5	E-H (52%)	480.2 ± 2.5	491.80 ± 0.88 (n = 5)	N/A	N/A
MLH502 (2)	Anakie	8776-02	WR	11	N/A	N/A	502.3 ± 2.5	491.4 ±1.1 (n = 4)	N/A	N/A
MLH503 (1)	Anakie	8775-01	WR	11	496.3 ± 3.2	E-H (53.4%)	481.4 ± 2.3	496.25 ± 0.80 (n = 6)	N/A	N/A
MLH503 (2)	Anakie	8775-02	WR	11	496.9 ± 3.0	E-H (51.7%)	483.1 ± 2.5	498.65 ± 0.807 (n = 6)	N/A	N/A
MLH505 (1)	Anakie	8774-01	WR	12	N/A	N/A	479.5 ± 2.3	488.6 ± 1.1 (n = 3)	N/A	N/A
MLH505 (2)	Anakie	8774-02	WR	12	N/A	N/A	479.8 ± 2.3	492.37 ± 0.92 (n = 3)	N/A	N/A
MLPD01 (1)	Anakie	8767-01	WR	11	469.7 ± 1.8	D-J (91%)	468.2 ± 2.1	470.37 ± 0.46 (n = 8)	470.5 ± 2.6 (n = 10)	270 ± 210
MLPD01 (2)	Anakie	8767-02	WR	10	469.5 ± 2.2	E-I (82.5%)	464.9 ± 2.1	470.27 ± 0.51 (n = 7)	N/A	N/A
MLPD02 (1)	Anakie	8766-01	WR	9	468.8 ± 1.8	D-I (82.9%)	465.0 ± 2.1	468.79 ± 0.54 (n = 7)	N/A	N/A
MLPD02 (2)	Anakie	8766-02	WR	10	469.1 ± 1.9	E-G (58.4%)	466.7 ± 2.0	468.41 ± 0.56 (n = 4)	N/A	N/A

Table 3.1: *$^{40}Ar/^{39}Ar$ geochronology results summary.*

(a) A plateau age is defined as 3 or more consecutive steps which comprises of at least 50% of the total ^{39}Ar released and the age values overlap within a 95% confidence interval (Fleck et al., 1977). Errors, including errors in irradiation corrections factors and errors in J, are reported at the 95% confidence level and is calculated based on the mean weight by inverse variance. All plateau definitions use error-overlap (2σ). (b) The Ideogram is an age-probability plot, where the age is given by the weight mean of both grains and error based on the standard error of that mean, which is given to (2σ). (c) Isochron age errors include the errors in J and irradiation correction factors but not the uncertainty in the potassium decay constant. Isochron ages are measured to the 95% confidence level (2σ).

were conducted on mineral separates, and the remaining 16 were on whole-rock samples. The results are in Table 3.1. Incremental heating of two separate aliquots for each sample was undertaken, shown as run 01 and run 02, except for sample MLLJ06, where only one run was completed. Where multiple minerals per sample were analysed, the sample number suffix “a”, “b”, etc. was used. Plateaus were defined as three or more continuous steps on the step-heating spectra that achieve ≥50% of the total ^{39}Ar released, and with an age overlap of steps at the 95% confidence interval. All $^{40}Ar/^{39}Ar$ results have been corrected for mass discrimination and interfering isotopes. Apparent ages obtained from all steps during the step-heating process are reported as integrated ages, which should correspond with previous K-Ar ages if the sample experienced no ^{39}Ar loss by recoil. Please refer to McDougall and Harrison (1999) for further details on the $^{40}Ar/^{39}Ar$ method.

3.3.1 Igneous rocks

Plagioclase and biotite mineral separates were obtained from a surface sample of the Granite Springs Granite and Hungerford Granite, and a drill core sample of granodioirite from the Ooroonoo 1 drill core. Both biotite and plagioclase were separated from samples of the Granite Springs Granite (2122054) and Hungerford Granite (2122055), and biotite and two phases of plagioclase were separated from granite in the basement drill core of well Ooroonoo1 (2152164). Additional samples of igneous rocks come from the Retreat Granite (MLRG01), from which potassium feldspar was separated, and rhyolitic ignimbrite obtained from the Thunderbolt 1 drill core (2130084), from which plagioclase was separated.

3.3.1.1 Granite Springs Granite

Two minerals from sample 2122054 (Granite Springs Granite) were analysed: biotite and plagioclase, referred to as 2122054a and 2122054b, respectively. The biotite produced flat step-heating spectra, with plateau ages of 397.3 ± 3.8 Ma (MSWD 1.59) for run 01 steps A through H, dominated by the lower temperature steps, and 406.0 ± 2.8 Ma (MSWD 1.16) for run 02 steps A through L. The integrated age for biotite run 01 was 396.3 ± 4.3 Ma, and 405.7 ± 3.8 Ma for run 02, within error of their respective plateau ages. The ideogram age for run 01 is 397.2 ± 1.2 Ma (MSWD 1.35, n = 11) and for run 02 it is 406.00 ± 0.75 Ma (MSWD 1.16, n 12). The ideogram age of the plateau steps of both runs is 405.09 ± 0.69 Ma (MSWD 1.34, n 21). An isochron age of 398.8 ± 4.4 Ma was achieved for run 01, which is within error of the plateau, integrated, and ideogram ages. An isochron was not achieved for run 02 due to data clustering. Of the two runs, run 02 is considered more reliable, as it contains significantly more gas than run 01. On this basis, the preferred age for biotite in the Granite Springs Granite is 406.0 ± 2.8 Ma.

Plagioclase from the same sample of Granite Springs Granite yielded a plateau age from step C through step J for run 01 of 350.7 ± 2.5 Ma (MSWD 1.09) and an integrated age of 352.7 ± 3.4 Ma. Unlike run 01, run 02 failed to yield a plateau, with the step-heating spectra displaying a saddle-shape that is typically a result of excess Ar. The integrated age for run 02 is 379.9 ± 3.5 Ma. The step-heating spectra steps D through F for run 01 and step C through G for run 02 have similar geometry and, combined, provide an ideogram age of 349.88 ± 0.59 Ma (MSWD 2.00), which is within error of the plateau age obtained for run 01. An ideogram for run 01 alone produces an age of 350.73 ± 0.77 (MSWD 1.20, n = 9), which is almost identical to the plateau age. The isochron for run 01 gives an age of 347.9 ± 6.0 Ma, which is within error of the plateau, integrated, and ideogram ages from the same run, however the data are clustered, creating a less reliable result. An isochron was not able to be achieved for run 02. The most reliable age for plagioclase from the Granite Springs Granite is 350.7 ± 2.5 Ma, obtained from the plateau for run 01.

3.3.1.2 Hungerford Granite

Two minerals from the Hungerford Granite were analysed: biotite (2122055a) and plagioclase (2122055b). The biotite produced mostly flat step-heating spectra, with both runs 01 and 02 displaying similar geometry. Plateau ages were 361.4 ± 2.6 Ma (MSWD 1.34) for run 01 and 365.5 ± 2.8 Ma (MSWD 1.77) for run 02. The integrated ages were 361.3 ± 3.3 Ma for run 01 and 364.5 ± 3.3 Ma for run 02, so the plateau and integrated ages from both runs are all within error. The ideogram age for run 01 was 361.40 ± 0.68 Ma (MSWD 1.34, n = 12) and 365.49 ± 0.73 Ma (MSWD 1.77, n = 9) for run 02, and an ideogram of combined plateau steps from both runs produce an age of 363.46 ± 0.5 Ma (MSWD 1.92). Isochron for run 01 displays clustered data and ages of 362.7 ± 3.0 Ma, within error of the plateau, integrated, and ideogram ages for run 01. An isochron was not achieved for run 02. The preferred age for the biotite from Hungerford Granite is the ideogram age for the combined plateau steps, 363.46 ± 0.5 Ma.

Plagioclase for the same sample yielded step-heating spectra with a slight saddle- shape, with plateau ages of 332.6 ± 5.7 Ma (MSWD 2.20) for run 01 and 321.6 ± 2.9 Ma (MSWD 2.33) for run 02. Integrated ages were 337.8 ± 6.2 Ma for run 01 and 332.1 ± 3.2 Ma for run 02. Run 01 contained less gas overall than run 02 and is therefore less reliable. Ideogram ages of 332.1 ± 1.7 Ma (MSWD 1.88, n = 6) for run 01 and 325.72 ± 0.77 Ma (MSWD 1.86, n = 5) for run 02 were produced. The saddle- shape of the step-heating spectra can be attributed to excess Ar in the sample, which is also evident in the high atmospheric Ar values from the isochrons. The isochron age for run 01 is 324 ± 10 Ma and 301.4 ± 4.6 Ma for run 02. The preferred age for the plagioclase of the Hungerford Granite is the isochron age obtained from run 02, 301.4 ± 4.6 Ma.

3.3.1.3 Retreat Granite

K-feldspar from sample MLRG01, Retreat Granite, yielded step-heating plateaus of 355.9 ± 3.7 Ma (MSWD 2.71) for run 01, and 344.1 ± 2.6 Ma (MSWD 1.52) for run 02. Integrated ages were 354.9 ± 3.5 Ma for run 01 and 343.5 ± 3.7 Ma for run 02, which are within error of the respective plateau ages. Both runs show an artificially low step A, and steps I through L of run 01 were removed as they were affected by laser decoupling. Run 02 has a longer plateau than run 01, including more high temperature steps and a greater number of total steps. The differences between the two runs could be caused by a number of factors: greater sample mass in one run, differing K content in the feldspar resulting in a staggered K/Ca ratio, and/or multiple K phases within the sample. Ideogram ages of 356.41 ± 0.79 Ma (MSWD 3.88, n = 10) for run 01 and 344.16 ± 0.68 Ma (MSWD 1.68, n = 14) for run 02 were obtained. An isochron age of 357.7 ± 4.0 Ma was achieved for run 01, with no evidence of excess Ar, but the data are clustered and the line of best fit is defined almost entirely by step A, so this age is not considered reliable. The isochron age for run 02 of 346.4 ± 2.8 Ma shows marginally less clustering, although the line of best fit is also defined by step A, and like run 01 shows no evidence of excess Ar. Run 02 contains more gas than run 01, has a longer plateau that includes more high temperature steps, and the ages obtained for run 02 from the plateau, integrated, ideogram, and isochron results are within error. On this basis the preferred age for the Retreat Granite is the plateau age for run 02, 344.1 ± 2.6 Ma.

3.3.1.4 Thunderbolt 1 drillcore

Plagioclase from sample 2130084, taken from the Thunderbolt 1 drill core, yielded a plateau for run 01 of 349.5 ± 2.8 Ma (MSWD 1.86), with integrated ages of 349.4 ± 3.3 Ma and 371.7 ± 7.6 Ma for runs 01 and 02 respectively. The step-heating spectrum for run 01 is roughly flat, with some discordant low temperature steps, and contained significantly more gas than run 02, which was unable to achieve a plateau due to lack of contiguous steps. Ideogram ages for runs 01 and 02 are very different, with run 01 producing 348.86 ± 0.64 Ma (MSWD 1.89, n = 13), compared with 380.8 ± 2.2 Ma (MSWD 1.98, n = 10) for run 02. However, isochrons for both runs provided similar ages, with run 01 producing an isochron age of 347.4 ± 6.6 Ma and run 02 producing 390 ± 18 Ma. All ages for run 01 are within error, as are run 02. The likely cause for the differences between the runs is variation in the compositions of the grains that were analysed, which can be observed in the changing K/Ca ratio. The minimum age for the Thunderbolt 1 sample is the plateau age of run 01 of 349.5 ± 2.8 Ma, and the maximum age is the ideogram age from run 02 of 380.8 ± 2.2 Ma.

3.3.1.5 Ooroonoo 1 drillcore

Three minerals were dated from sample 2152164, which was obtained from granite of the Ooroonoo 1 drill core. The biotite separate is referred to as 2152164a, and two phases of plagioclase are referred to as 2152164b and 2152164c. Step-heating of the biotite yielded integrated ages of 599.4 ± 5.6 Ma and 644.5 ± 7.5 Ma for runs 01 and 02, respectively. No plateaus were achieved. Ideogram ages of 600.1 ± 2.0 Ma (MSWD 1.39, n =5) for run 01 and 613.2 ± 3.0 Ma (MSWD 1.59, n = 4) were obtained, though the spread of data resulted in a lack of support for these ages. The isochron for run 01 produced an age of 598 ± 33 Ma, though the clustering of data prevents this from being a useful age. No isochron was achieved for run 02. The biotite has suffered from chloritisation, and contains excess argon; no reliable ages were obtained. .

Plagioclase sample 2152164b yielded a plateau for run 01 of 585 ± 12 Ma (MSWD 3.85), and integrated ages of 759.8 ± 10 Ma for run 01, and 427.9 ± 4.2 Ma for run 02, though no plateau was achieved for run 02 despite a plateau-like shape to the spectrum at ~380 Ma. The saddle-shape observed in the step-heating spectrum of run 01 is indicative of excess Ar. This shape is present in the step-heating spectrum of run 02 also, although it is less pronounced. Ideograms for 2152164b had a large spread, with little resolution to the data. The ideogram age for run 02 of 426.7 ± 1.9 Ma (MSWD 1.00, n = 4) is within error of the integrated age, although reliability is suspect due to the low number of informing data points. Likewise the ideogram age for run 01 at 585.0 ± 2.9 Ma (MSWD 3.85, n =3) is supported by insufficient data points and is unreliable. The isochron for run 01 produced an age of 640 ± 96 Ma for run 01 and shows evidence of excess Ar. The isochron for run 02 was poor and is therefore not reported.

The second plagioclase sample, 2152164c, has a step-heating spectrum that is saddle- shaped, like sample 2152164b, indicative of excess Ar. The integrated ages are 603 ± 14 Ma for run 01 and 481.1 ± 9.3 Ma for run 02. The steps are discordant, with insufficient contiguous steps to produce a plateau for either run 01 or run 02, though overlap in steps C, D and E of run 01 and steps C & D of run 02, when forced, provide an age of 402.5 ± 9.7 Ma. Ideogram ages for run 01 and 02 are, like sample 2152164b, poorly supported by data points. The ideogram ages are 391.9 ± 6.7 (MSWD 0.69, n =3) for run 01 and 408.5 ± 5.0 (MSWD 0.61, n = 3) for run 02. The isochron for run 01 is unusable, and for run 02 the isochron age is 320 ± 120 Ma, though data clustering is evident.

The differences and difficulties with plagioclase from granite of the Oonoonoo 1 drill core are potentially due to compositional variation in the Ca and K ratios of the analysed grains. Due to excess Ar, the younger isochron age from 2152164b of 306 ± 52 Ma is preferred for the plagioclase age of this sample, despite the large error.

3.3.2 Metamorphic rocks

In addition to the igneous samples described above, metamorphic rocks from the Thomson Orogen were dated as well. Where possible, individual minerals were separated from the metamorphic rocks for $^{40}Ar/^{39}Ar$ analysis. These minerals include amphibole from the Sefton Metamorphics (2152166), muscovite from the Halls Reward Metamorphics (sample NQ37), and muscovite and biotite from the Halls Reward Metamorphics (samples MLHR02a, MLHR02b). The remaining metamorphic samples are whole rock samples dominated by mica and quartz: drill core from the Peak Downs Copper Mine (MLPD01, MLPD02) and Hurleys 5 (MLH501, MLH502, MLH503, MLH505) drillcores of the Anakie Metamorphics, as well as surface samples of the Les Jumelles beds (MLLJ06) and Mt. McLaren beds (AOM03).

3.3.2.1 Sefton Metamorphics

Amphibole from the Sefton Metamorphics (sample 2152166) yielded plateau ages for run 01 of 397.6 ± 3.3 Ma (MSWD 1.26) from steps E through J, and for run 02 of 335.1 ± 3.6 Ma (MSWD = 2.96) from steps C through F. Integrated ages were 388.3 ± 3.8 Ma for run 01 and 325.2 ± 3.1 Ma for run 02. A change in the K/Ca ratio at step G for run 02 may be evidence of alteration or pervasive chloritisation. The ideogram age of 396.19 ± 0.93 Ma (MSWD 2.15, n = 7) for run 01 is preferred over 334.88 ± 0.86 Ma (MSWD 2.61, n = 5) for run 02, due to greater number of informing data points for run 01. The ideogram ages for both runs are within error of the respective plateau ages. Isochrons for both runs are poor and unusable. The preferred age for the Sefton Metamorphics is the plateau age for run 01 of 397.6 ± 3.3 Ma, which incorporates more high-temperature steps than that of run 02, and lacks the irregularity in the K/Ca ratio of run 02.

3.3.2.2 Halls Reward Metamorphics

Two samples (NQ37 and MLHR02) were prepared from different locations within the Halls Reward Metamorphics. Muscovite and biotite separates were obtained from biotite-muscovite-quartz schist (sample MLHR02); muscovite is referred to as MLHR02a and biotite as MLHR02b. Only muscovite was separated from sample NQ37.

Step-heating spectra yielded integrated ages for muscovite from MLHR02a of 441.3 ± 2.3 Ma and 490.4 ± 2.7 Ma for runs 01 and 02, respectively, and plateaus were achieved for both runs. The step-heating spectrum of run 01 is flat, with all steps contiguous, allowing a plateau to be achieved from steps A through J that has an age of 441.5 ± 2.0 Ma (MSWD 1.64). The step-heating spectrum for run 02 is dissimilar to that of run 01, with discordant low temperature steps, and a plateau was only achieved from steps E through G. The age of this plateau, 480.3 ± 4.2 Ma (MSWD 3.04), is significantly older than that of run 01. The discrepancy likely arises from the presence of detrital mica, as seen in thin section, the effects of which may be seen in the erroneously old, discordant steps of B, C and D, which show ages in excess of 500 Ma. The ideogram age for run 01 is 441.48 ± 0.63 Ma (MSWD 1.64, n = 10) and 480.3 ± 1.1 Ma (MSWD 3.04, n = 3) for run 02. Isochrons for both runs are poor. The preferred age for the muscovite from sample MLHR02 is that of the plateau for run 01 (441.5 ± 2.0 Ma), with ideogram and integrated ages within error.

Step-heating spectra for biotite from the same sample (MLHR02b) show similar geometry, although only run 01 achieved a plateau. Integrated ages of 431.4 ± 2.4 Ma for run 01, and 426.5 ± 2.8 Ma for run 02 were achieved, which are within error. A plateau was achieved for run 01 from steps E through K, with an age of 446.6 ± 2.4 Ma (MSWD 1.80). Ideogram ages of 446.57 ± 0.78 Ma (MSWD 1.80, n = 7) for run 01, and 448.1 ± 1.1 Ma (MSWD 1.52, n = 7) for run 02 are within error of the plateau age for run 01. As for the muscovite sample from MLHR02, the biotite sample had poor isochrones. The preferred age for MLHR02b is that of the plateau from run 01, 446.6 ± 2.4 Ma.

NQ37 is a surface sample of muscovite-biotite schist, from which muscovite was separated for analysis. Step-heating spectra for both runs are almost identical, with integrated ages of 447.3 ± 2.2 Ma for run 01 and 444.8 ± 2.0 Ma for run 02. A plateau for run 01 was achieved from steps B through I with an age of 447.8 ± 2.0 Ma (MSWD 1.25), and a similar plateau for run 02 was achieved from steps C through H with an age of 447.4 ± 1.7 Ma (MSWD 1.66). Ideogram ages are likewise similar, with run 01 at 447.81 ± 0.67 Ma (MSWD 1.25, n = 8) and run 02 at 447.61 ± 0.43 Ma (MSWD 1.67, n = 7). The age for run 01 from the isochron at 448.0 ± 2.5 Ma is within error of the step heating spectra and age probability plot ages. The isochron for run 02 is poor. The preferred age for NQ37 is the plateau age from run 01, which has the longer plateau of the two runs, at 447.8 ± 2.0 Ma.

3.3.2.3 Anakie Metamorphic Group

Whole rock samples of the Anakie Metamorphic Group were analysed from drill core that has previously been dated by the K-Ar method (Withnall et al., 1996). The following samples were collected of Hurleys Metamorphics from the Hurleys 5 drillcore: MLH501 at 165.1 m, MLH502 at 164.1 m, MLH503 at 134.6 m, and MLH505 at 93 m (Figure 3.3). All samples are similar and are dominated by quartz and mica, though the presence of feldspars cannot be excluded. Separation of individual minerals was not possible for these samples because they were too fine-grained, so whole rock analyses were conducted. Samples MLPD01 and MLPD02 were collected of Bathampton Metamorphics from the Peak Downs copper mine drillcore DDH6N at depths of 490’8” and 481’4”, respectively. Like the Hurleys 5 drill core samples, the Peak Downs samples are dominated by quartz and mica. A comparison of previous K-Ar and $^{40}Ar/^{39}Ar$ results from this study is provided in Table 3.2.

Runs 01 and 02 from MLH501 had similar geometry, although no plateau was achieved due to lack of contiguous steps. Integrated ages of 485.0 ± 2.4 Ma and 479.8 ± 2.4 Ma were produced for runs 01 and 02, respectively. Ideogram ages are somewhat older: 499.4 ± 1.0 Ma (MSWD 12.08, n = 3) for run 01 and 491.1 ± 1.1 Ma (MSWD 4.89, n = 5) for run 02. Neither achieved an isochron.

Sample MLH502 yielded integrated ages of 480.2 ± 2.5 Ma and 502.3 ± 2.5 Ma for runs 01 and 02, respectively. Run 01 produced a plateau age of 489.7 ± 3.5 Ma (MSWD 2.44), and no plateau was produced for run 02. Ideogram ages of 491.80 ± 0.88 Ma (MSWD 5.16, n = 5) for run 01 and 492.4 ± 1.1 Ma (MSWD 0.33, n = 4) for run 02 are within error of the plateau age. As for MLH501, neither run 01 nor run 02 of MLH502 achieved an isochron.

The step-heating spectra for MLH503 are similar, with integrated ages of 481.4 ± 2.3 Ma for run 01 and 483.1 ± 2.5 Ma for run 02. A plateau of 496.3 ± 3.2 Ma (MSWD 3.11) was achieved from steps E through H of run 01, and an almost identical plateau for run 02 was achieved from steps E through H of 496.9 ± 3.0 Ma (MSWD 1.84). Ideogram ages of 496.25 ± 0.80 Ma (MSWD 1.87, n = 6) for run 01 and 498.65 ± 0.87 Ma (MSWD 3.70, n = 6) are within error of the plateau age. MLH503 is similar to MLH502 and MLH501 in that no isochron was achieved.

Sample MLH505 has almost identical step-heating spectra, however neither runs 01 or 02 achieve a plateau. The integrated ages of 479.5 ± 2.3 Ma for run 01 and 479.8 ± 2.3 Ma for run 02 are within error. Ideogram ages of 488.6 ± 1.1 Ma (MSWD 1.57, n = 3) for run 01 and 492.37 ± 0.92 Ma (MSWD 2.09, n = 3) for run 02 are poorly supported. MLH505 does not achieve an isochron for either run.

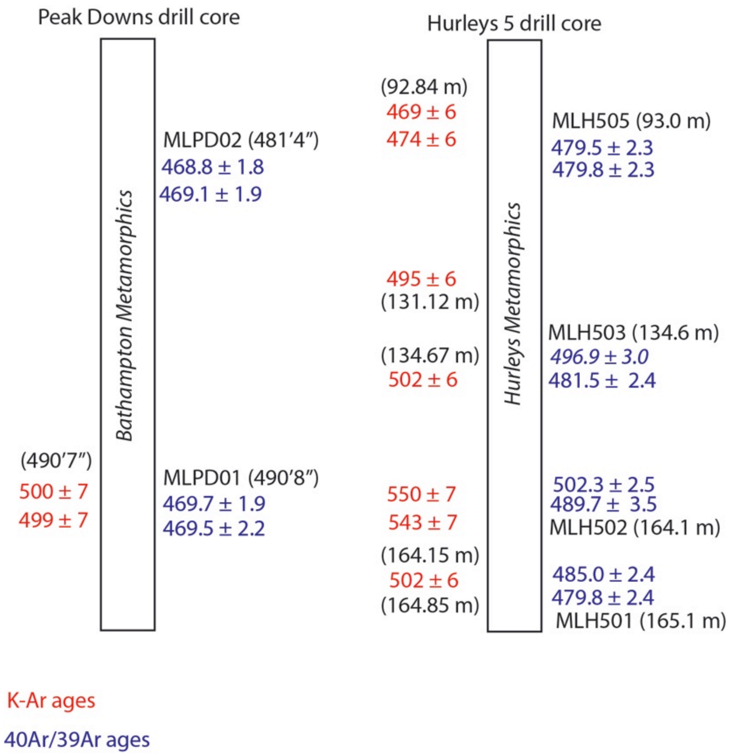

Figure 3.3: *Anakie Metamorphic Group geochronology comparison. Previous K-Ar ages by Withnall et al. (1996) in red, and $^{40}Ar/^{39}Ar$ results from this study in blue.*

MLPD01 has almost identical step-heating spectra, with integrated ages of 468.2 ± 2.1 Ma and 464.9 ± 2.1 Ma for runs 01 and 02 respectively, and plateau ages of 469.7 ± 1.8 Ma (MSWD 1.75) for run 01 and 469.5 ± 2.2 Ma (MSWD 2.49) for run 02. Ideogram ages of 470.37 ± 0.46 Ma (MSWD 5.13, n = 8) for run 01 and 470.27 ± 0.51 Ma (MSWD 3.89. n = 7) for run 02 are within error. The isochron for run 01 provides an age of 470.5 ± 2.6 Ma, although data are clustered. The isochron for run 02 is poor.

Sample MLPD02 has similar step-heating spectra for run 01 and run 02, integrated ages of 465.0 ± 2.1 Ma and 466.7 ± 2.0 Ma for runs 01 and 02 respectively, and plateau ages of 468.8 ± 1.8 Ma (MSWD 1.26) for steps D through I of run 01, and 469.1 ± 1.9 Ma (MSWD 1.17) for steps E through G of run 02. Ideogram ages were 468.79 ± 0.54 (MSWD 1.26, n = 7) for run 01 and 468.41 ± 0.56 Ma (MSWD 2.79, n = 4) for run 02. Isochrons for both runs were poor.

Unit	Sample ID	Run	Plateau Age (Ma)	Error (Ma)	Integrated Age (Ma)	Error (Ma)	K-Ar age	Error (Ma)
Bathampton Metamorphics	MLPD02	1	468.8	1.8	465.0	2.1	499	7
		2	469.1	1.9	466.7	2.0		
	MLPD01	1	469.7	1.9	468.2	2.1		
		2	469.5	2.2	465.0	2.1		
Hurleys Metamorphics	MLH505	1			479.5	2.3	469	6
		2			479.8	2.3	474	6
	MLH503	1	496.3	3.2	481.4	2.3	502	6
		2	496.9	3.0	483.1	2.5		
	MLH502	1	489.7	3.5	480.2	2.5	550	7
		2			502.3	2.5	543	7
	MLH501	1			485.0	2.4	502	6
		2			479.8	2.4		

Table 3.2: *Comparison of $^{40}Ar/^{39}Ar$ ages from this study with K-Ar ages from Withnall et. al. (1996).*

3.3.2.4 Mt. McLaren beds

One whole rock sample (AOM03) with a composition dominated by mica and quartz from the upper part of the Mt McLaren beds was analysed. The step-heating spectra for both run 01 and 02 are similar, as are the integrated ages of 307.1 ± 1.6 Ma (run 01) and 308.0 ± 1.4 Ma (run 02). A plateau was achieved for run 01 from steps B through E and has an age of 312.8 ± 1.8 Ma (MSWD 1.77). Run 02 also produced a plateau from steps B through D with an age of 315.3 ± 1.9 Ma (MSWD 3.54). Ideogram ages were 312.79 ± 0.58 Ma (MSWD 1.35, n = 5) for run 01 and 315.25 ± 0.44 Ma (MSWD 3.54, n = 3) for run 02. An isochron age for run 01 of 307.8 ± 6.2 Ma has low Ar, and the isochron for run 02 is poor. The preferred age for mica from the Mt. McLaren beds is the plateau age from run 01, 312.8 ± 1.8 Ma.

3.3.2.5 Les Jumelles beds

Whole rock analysis of the Les Jumelles beds (MLLJ06) provided a step-heating spectrum with no contiguous steps. An integrated age of 452.0 ± 2.2 Ma was obtained, though step B is erroneously old at 491.4 ± 2.1 Ma, possibly due to the presence of detrital mica. The ideogram age is ~450 Ma.

3.4 Discussion

In general, the new $^{40}Ar/^{39}Ar$ step-heating ages from this study fall into three broad groups. First, the $^{40}Ar/^{39}Ar$ ages from intrusive rocks (all of which are considered cooling ages, as elaborated below) are within a ~90 My interval that spans from ~415 Ma (Early Devonian) to ~325 Ma (middle Carboniferous). Second, metamorphic rocks of the central and northern Thomson Orogen have $^{40}Ar/^{39}Ar$ ages that fall within a ~80 My interval that stretches from ~505 Ma (mid-Cambrian) to ~425 Ma (late Silurian). Third, $^{40}Ar/^{39}Ar$ ages < ~315 Ma from the most easterly sample of this study are significantly younger that other metamorphic rocks that were dated. These three broad intervals are also evident in the results of previous K-Ar and $^{40}Ar/^{39}Ar$ studies, including a number of intrusive K-Ar ages that fall within the ~305 Ma to ~275 Ma band, similar to the easterly metamorphic samples (Figure 3.4).

Included within the previous results are some K-Ar dates of both igneous and metamorphic rocks that were evaluated by re-dating equivalent samples using $^{40}Ar/^{39}Ar$ step-heating. In principle, the original K-Ar dates should equal the integrated ages produced from $^{40}Ar/^{39}Ar$ step-heating, but this is not the case for many of the samples that were re-dated for this study. In those cases where the original K-Ar dates agree with the $^{40}Ar/^{39}Ar$ integrated ages, the $^{40}Ar/^{39}Ar$ ages are frequently more precise.

3.4.1 Igneous rocks

3.4.1.1 Retreat Granite

The Retreat Batholith of the southern Anakie Inlier was dated by the K-Ar method in the 1960s, with resultant ages ranging from 345 - 366 Ma for biotite and 356 - 367 for hornblende, though biotite is typically younger than hornblende from the same sample (Harding, 1969). More recent U-Pb zircon geochronology provides an age of ~390 Ma for the Retreat Granite (Wood, 2006), and 382 ± 7 Ma (Cross et al., 2015) from the Theresa Creek Volcanics. In this study K-feldspar from a sample of the Retreat Granite (MLRG01) produced a $^{40}Ar/^{39}Ar$ step-heating age of 344.1 ± 2.6 Ma. Combined, these data suggest that the Retreat Granite was intruded at ~390 Ma (Middle Devonian) and cooled through the partial retention zone for argon in K-feldspar at ~345 Ma (early Carboniferous).

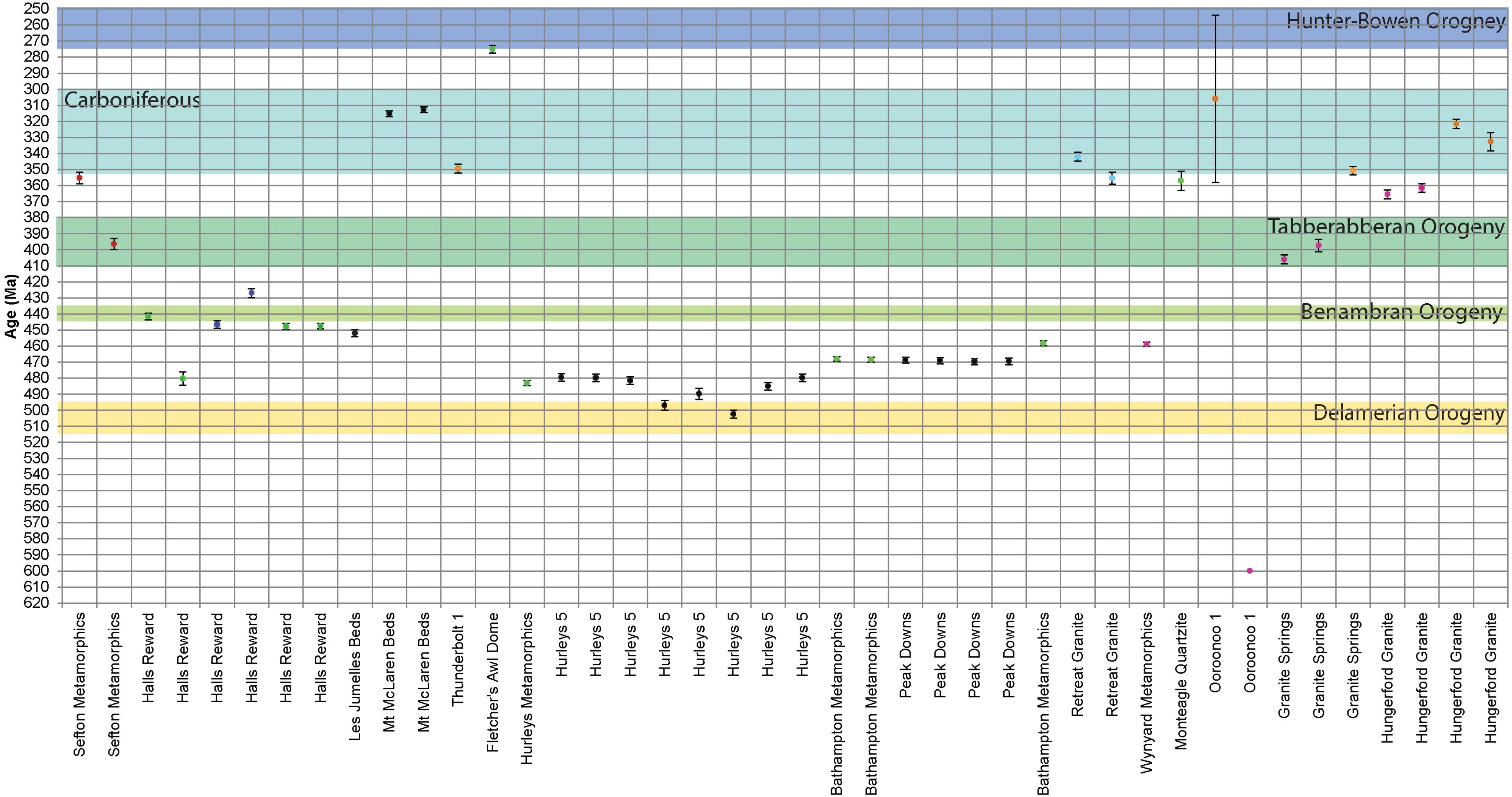

Figure 3.4: *$^{40}Ar/^{39}Ar$ geochronology results and previous K-Ar and 40Ar/39Ar geochronology of Thomson Orogen rocks, with temporally relevant orogenic events. The minerals analysed are categorised by colour; amphibole in red, muscovite in green, biotite in dark blue, plagioclase in orange, potassium feldspar in light blue, biotite in pink, and whole rock analyses are in black.*

3.4.1.2 Granite Springs Granite and Hungerford Granite

Comparison with previous zircon U-Pb dates suggest that $^{40}Ar/^{39}Ar$ results from granites in the southern Thomson Orogen are also cooling ages, as opposed to crystallization ages. U-Pb ages of zircons have previously been obtained from the Granite Springs Granite (sample 2122054) and Hungerford Granite (sample 2122055). Zircons from the Granite Springs Granite have a U-Pb age of 456.3 ± 3.9 Ma (Late Ordovician), but biotite and plagioclase $^{40}Ar/^{39}Ar$ ages of the Granite Springs Granite are 406.0 ± 2.8 Ma (Early Devonian) and 346.6 ± 4.2 Ma (early Carboniferous), respectively. Likewise, zircons in the Hungerford Granite have a U-Pb age of 419.1 ± 2.5 Ma (approximately the Silurian-Devonian boundary), but biotite in the granite has a $^{40}Ar/^{39}Ar$ age of 364.7 ± 2.6 Ma (Late Devonian), and the plagioclase $^{40}Ar/^{39}Ar$ age is younger still at 320.4 ± 2.7 Ma (late Carboniferous). In addition to illustrating that many of the prior K-Ar ages from intrusive rocks of the Thomson Orogen are potentially cooling ages, these combined datasets from the Retreat, Granite Springs, and Hungerford Granites also point toward periods of silicic to intermediate magmatism in the Thomson Orogen during the Late Ordovician to middle Devonian, followed by protracted cooling during the ensuing ~100 My.

3.4.1.3 Mooramin Granite

Seventy kilometres north-east of the Retreat Granite, and immediately to the east of the Anakie Inlier, lies Fletcher's Awl Dome. Zircons from the Mooramin Granite, which crops out in the center of the structural dome, have an age of 463 ± 15 Ma (Middle Ordovician; Mulqueeny, 2010). Unpublished $^{40}Ar/^{39}Ar$ data from muscovite in the Mooramin Granite at Fletcher's Awl Dome have a plateau age of 275.0 ± 2.3 Ma (mid-Permian; Verdel, pers. comm.). As with the examples of other granites of the Thomson Orogen described above, $^{40}Ar/^{39}Ar$ data from the Thomson Orogen therefore seem to reflect a period of cooling, though reheating during this time cannot be excluded. However, this particular period is ≥50 My younger at Fletcher's Dome than in Thomson Orogen rocks farther to the west.

3.4.1.4 Ooroonoo 1 drillcore

The oldest sample from this study was the Ooroonoo1 granite, located in the far west of the Thomson Orogen. Biotite from this drill core was previously dated by the K-Ar method at 860 Ma (Harding, 1969), but the new $^{40}Ar/^{39}Ar$ data from this study suggest that this age previous age was influenced by excess Ar, likely due to chloritisation of biotite, and should not be relied upon. The new $^{40}Ar/^{39}Ar$ age for plagioclase from the same sample is 306 ± 52 Ma, an age that is similar to the results from feldspars from other igneous rocks of this study. Importantly, granite from the

Ooroonoo 1 drill core is much younger than rocks of the Mesoproterozoic Mt. Isa Inlier. The plagioclase $^{40}Ar/^{39}Ar$ results suggest a common late Paleozoic thermal history with other parts of the Thomson Orogen.

3.4.2 Metamorphic rocks

The metamorphic samples from this study can be separated geographically by a NE – SW line that runs parallel to the boundary of the New England Orogen. Areas to the west have $^{40}Ar/^{39}Ar$ ages that fall within a ~80 My interval, whereas samples to the east of the line preserve $^{40}Ar/^{39}Ar$ evidence of cooling <315 Ma (i.e., late Carboniferous and younger).

3.4.2.1 Sefton Metamorphics

One aim of this study was to determine whether metamorphic rocks of the Iron Range Province in the far north of Queensland shared a common thermal history with those of the Thomson Orogen. Previous work on the Sefton Metamorphics of the Iron Range Province provided an estimated Paleozoic depositional age from fossils (Trail 1969 in Purdy et al., 2013), and U-Pb zircon dating of a metaconglomerate component of the Sefton Metamorphics provided a maximum depositional age of ~1200 Ma (late Mesoproterozoic; Blewett et al., 1998). Rocks of similar age found in the Cape River Province to the south (Blewett et al., 1998; Hutton, 2004). To test whether the Sefton Metamorphics share a similar thermal history with the Thomson Orogen, amphibole from the Sefton Metamorphics was dated by $^{40}Ar/^{39}Ar$ geochronology, with a resultant age of 397.6 ± 3.3 Ma. Although dissimilar to the metamorphic samples of the Thomson Orogen, it does share a similar age with igneous samples from this study.

3.4.2.2 Halls Reward Metamorphics

Samples of the Halls Rewards Metamorphics from the northern Thomson Orogen provided $^{40}Ar/^{39}Ar$ ages that contradict some past geochronology results. Monazite U-Pb data, in conjunction with Rb/Sr and K-Ar results, led Nishiya et al. (2003) to conclude that that metamorphism of the Halls Reward Metamorphics occurred around 510 Ma during the Cambrian Delamerian Orogeny. However the youngest detrital zircon from the same study had a U-Pb age 460±90 Ma, which, although imprecise, warranted further investigation because it suggested that the K-Ar ages for muscovite (503±13 and 504±13 Ma) reported by Nishiya et al. (2003) could represent the ages of detrital muscovite. For this study, two samples of the Halls Reward Metamorphics from the northern Thomson Orogen were dated by $^{40}Ar/^{39}Ar$ geochronology. Muscovite produced ages of ~441 to 447 Ma, and biotite had an age of 446.6±2.4 Ma, both considerably younger than the previous K-Ar results of Nishiya et al. (2003). Combined with the prior detrital zircon data, these results suggest that the maximum depositional age of the Halls Reward Metamorphics is 460±90 Ma, and the unit cooled through both the biotite and muscovite closure temperatures at ~446 Ma (latest Ordovician).

3.4.2.3 Les Jumelles and Mt. McLaren beds

The Les Jumelles beds, which are located between the towns of Mount Coolon and Charters Towers in central Queensland, are composed of sandstones and mudstones of early Paleozoic age. They are unconformably overlain by Early Devonian rocks (Fergusson and Henderson, 2013), and are intruded by the Middle Ordovician Coquelicot Tonalite, zircons from which have U-Pb ages of 471±3.6 Ma (OZCHRON, 2007 in Purdy et al., 2013). Previous SHRIMP U-Pb geochronology on detrital zircons from the Les Jumelles beds established a maximum depositional age of 528 ± 9 Ma, though a single detrital zircon produced a younger age of 476 ± 12 Ma. The whole rock $^{40}Ar/^{39}Ar$ integrated age for the Les Jumelles beds of 452.0 ± 2.2 Ma (Late Ordovician) provides a minimum depositional age. Taken together, these data suggest that the Les Jumelles beds were deposited in the latest Cambrian to Early Ordovician, buried and intruded by the Coquelicot Tonalite shortly after burial, then subsequently cooled in the Late Ordovician.

The Mt. McLaren beds, which are located ~60 km north-east of Clermont in central Queensland, are comparable in lithology, depositional environment and age to the Les Jumelles beds. U-Pb detrital zircon ages from Mt. McLaren beds and lithosptratiphic correlations with the Puddler Creek Fm. and Les Jumelles beds, suggest that the Mt. McLaren beds were deposited in the late Cambrian to early Ordovician (Oorloff, 2014). Whole rock $^{40}Ar/^{39}Ar$ geochronology from this study produced an age of 312.8 ± 1.8 Ma (late Carboniferous) for cooling of the Mt. McLaren beds. This age likely represents a period of late Carboniferous extensional exhumation of the Mt. McLaren beds, as suggested by Oorloff (2014).

3.4.2.4 Anakie Metamorphic Group

One of the aims of this study was to re-date drill core of the Anakie Metamorphic Group that was previously dated by the K-Ar method. Previous K-Ar dating of the Peak Downs core provided ages of 499 ± 7 Ma and 500 ± 7 Ma, and Hurleys 5 drill core which yielded ages from 550 ± 7 Ma to 469 ± 6 Ma (Withnall et al., 1996). These previous results have been interpreted as evidence that deformation during the Cambrian Delamerian Orogeny, which is most prominent in southern Australia, extended as far north as the northern Thomson Orogen (Withnall et al., 1996). As described above, drill core was re-sampled at the same or similar intervals to facilitate a comparison of previous K-Ar and new $^{40}Ar/^{39}Ar$ results. Overall, the new $^{40}Ar/^{39}Ar$ results from the Peak

Downs drill core (Bathampton Metamorphics) are ~30 My younger than the K-Ar results of Withnall et al. (1996), and the new $^{40}Ar/^{39}Ar$ ages post-date the Delamerian Orogeny. Results from the Hurleys 5 drill core (Hurleys Metamorphics) are similar: sample MLH501 is ~20 My younger than the associated K-Ar sample, MLH502 is 40-60 My younger than the associated K-Ar sample, and the integrated age from MLH503 is ~20 My younger than the associated K-Ar age (although the plateau age is within error of the K-Ar age). In contrast, the shallowest sample from the Hurleys 5 drill core (sample MLH505) has an integrated $^{40}Ar/^{39}Ar$ age that is older than the associated K-Ar age.

Despite the K-Ar vs. $^{40}Ar/^{39}Ar$ discrepancies for the Anakie Metamorphic Group, the general conclusions of Withnall et al. (1996) seem to hold true; the Delamerian Orogeny is likely to have affected the Anakie Metamorphic Group. Age spectra from these samples show high temperature steps approaching 490 Ma, potentially being metamorphosed during this orogenic event which is estimated to have concluded by ~495 Ma (late Cambrian; Foden et al., 2006; Turner et al., 2009). In particular, the integrated age of 502.3±2.5 Ma for one run from sample MLH502, in addition to the plateau age of 496.9±3.0 Ma from sample MLH503, add further solidity to this hypothesis. The younger ages from these samples, seeming to record Middle and Early Ordovician events, are likely caused by argon loss. A comparison of the $^{40}Ar/^{39}Ar$ and K-Ar geochronology results for the Anakie Metamorphic Group are shown in Table 3.2.

3.4.3 Implications for the tectonic history of the Thomson Orogen

The $^{40}Ar/^{39}Ar$ ages obtained during this study range from Neoproterozoic to the Carboniferous-Permian boundary. The majority of $^{40}Ar/^{39}Ar$ ages from metamorphic rocks range from late Cambrian to Silurian, and the $^{40}Ar/^{39}Ar$ ages from igneous rocks range from Early Devonian to middle Carboniferous. As elaborated below, the new results facilitate comparison with previous results in other parts of eastern Australia.

3.4.3.1 Rodinia rifting

Rifting of the supercontinent Rodinia is believed to have occurred in two phases: the first at 800-750 Ma (Fergusson and Henderson, 2015), and the second at 600-580 Ma (Glen, 2013). Following rifting, the eastern margin of the Australian continent is approximated by the Tasman Line, which forms the western boundary of the Thomson Orogen. The Ooroonoo 1 drill core is located along the western border of the Thomson Orogen, and a previous K-Ar age for biotite from the granite produced an unreliable 840 Ma age, shown in this study as affected by excess argon as a result of chloritisation. Plagioclase from the same granite has an $^{40}Ar/^{39}Ar$ age of 306±52 Ma. Given the large uncertainties of the plagioclase age, it could be attributable to a variety of Carboniferous to Permian tectonic events that affected the Thomson Orogen.

3.4.3.2 Delamerian Orogeny

As described above, the previous K-Ar geochronology by Withnall et al. (1996) suggested that rocks of the Anakie Metamorphic Group were deformed during the Cambrian Delamerian Orogeny, which is characterized in southern Australia by E-W contraction from 514 to 495 Ma (Foden et al., 2006). The only samples from this study that are temporal equivalents to the Delamerian Orogeny are three samples from one drill hole into the Hurleys Metamorphics of the Anakie Inlier, although those ages are similar to previous $^{40}Ar/^{39}Ar$ and K-Ar results (Withnall et al., 1996; Wood, 2006; Wood and Lister, 2013). The reminder of these new $^{40}Ar/^{39}Ar$ data appear to show that the Anakie Metamorphic Group was affected by metamorphism during the Ordovician and, therefore, post-dates the Delamerian Orogeny, however these younger ages are likely affected by argon loss and should be used with caution. A study aiming to date micro-structures of the Anakie Inlier by $^{40}Ar/^{39}Ar$ geochronology, also showed Delamerian ages and an additional observation that ages decreased from NE to SW across the Anakie Inlier at Clermont (Wood, 2006).

Work on the Halls Reward Metamorphics from the northern Thomson Orogen by Nishiya et al. (2003) used Rb/Sr and K-Ar dates to conclude that peak metamorphism was reached before 490 Ma, however $^{40}Ar/^{39}Ar$ geochronology from this study show that the closure temperature for muscovite was reached at ~ 441 – 447 Ma, which is ~ 60 Ma later than previously thought. This places the latest metamorphism of the Halls Reward Metamorphics as occurring after the Delamerian Orogeny, and more akin to the Benambran Orogeny.

3.4.3.3 Benambran Orogeny

The Late Ordovician to Early Silurian Benambran Orogeny has been documented in the Lachlan Orogen (e.g., Glen, 2013) and Thomson Orogen (Kotischin, et al), but the extent to which it affected the Thomson Orogen is not well defined (Spampinato et al., 2015a). In the north, the Thomson Orogen has been delineated from the Silurian-Devonian Mossman Orogen (Withnall and Henderson, 2012). This separation represents a division of pre-Benambran rocks (i.e., the Thomson Orogen) from those that were deposited after the Benambran Orogeny (i.e., the Mossman Orogen; Glen, 2013).

$^{40}Ar/^{39}Ar$ cooling ages reported in this study from granites are similar to ages reported in metasediments of the Lachlan Orogen (Foster et al., 1999), suggesting that igneous intrusions into the Thomson Orogen may be related to the Benambran Orogeny. The effects of the Benambran Orogeny may also be shown in the metamorphic rocks from this study, contrary to suggestions that deformation due to the Benambran Orogeny was minimal in the central Thomson Orogen (Spampinato et al., 2015a), re-dating of drill core from the Anakie Metamorphic Group has resulted in ages that are at least partly Benambran in affinity, and the Halls Reward Metamorphics also have $^{40}Ar/^{39}Ar$ ages coincident with the Benambran ages.

3.4.3.4 Tabberabberan Orogeny

Igneous rocks from the Thomson Orogen dated for this study show emplacement occurred prior to 400 Ma, with slow cooling over the subsequent ~90 My. This timing is similar to that of the Tabberabberan cycle (430-380 Ma; Glen, 2005), which affected the Lachlan Orogen, though this study has revealed no Tabberabberan Orogeny (395-380 Ma) ages, which marks the end of the Tabberabberan cycle, in the Thomson Orogen. Apart from one $^{40}Ar/^{39}Ar$ age from the Sefton Metamorphics in Cape York, there are no corresponding Tabberabberan ages from metamorphic rocks in this study.

3.4.3.5 Hunter-Bowen Orogeny

The Hunter-Bowen Orogeny (HBO) is characterized by E-W shortening during the late Permian to Triassic (265-230 Ma; Rosenbaum et al., 2012) and had a significant influence on the rocks of the New England Orogen. The earliest stages of the HBO overlap with the Kanimblan cycle in the Lachlan Orogen (Glen, 2013). $^{40}Ar/^{39}Ar$ ages of ~270 – 275 Ma, similar to those from the easternmost Thomson Orogen rocks (Fletcher's Awl Dome), have been widely reported from the New England Orogen (NEO), where they are attributed to the onset of the HBO (Shaanan et al., 2014). Considering the close proximity of the NEO, it is not unrealistic to suggest that the HBO may have affected at least the eastern portions of the Thomson Orogen. However, there seem to be no rocks within the Anakie Inlier that have $^{40}Ar/^{39}Ar$ ages as young as the HBO, though zircon (U-Th)/He ages from the Anakie Inlier may be attributable to the HBO (Verdel et al., 2016). These results therefore suggest a division between eastern Thomson Orogen rocks that were relatively strongly affected by the HBO, and central and western Thomson Orogen rocks that were less affected. This division roughly corresponds with a covered area between Fletcher's Awl Dome and the southern Anakie Inlier, and the existence of this division may hint at a major and unidentified structure in this area.

3.5 Conclusions

The Thomson Orogen was influenced by a number of orogenic events that affected other elements of the Tasmanides. In particular, new $^{40}Ar/^{39}Ar$ results reveal similarities with the New England, Lachlan, and, Delamerian Orogens. $^{40}Ar/^{39}Ar$ ages from Ordovician granite at Fletcher's Awl Dome in the eastern Thomson Orogen suggest that it was affected by late Permian deformation during the early Hunter Bowen Orogeny, as were many parts of the New England Orogeny. The new results illustrate a discrepancy in $^{40}Ar/^{39}Ar$ ages between Fletcher's Awl Dome and the southern Anakie Inlier <100 km to the west. Areas to the west seem to show no $^{40}Ar/^{39}Ar$ influence from the Hunter Bowen Orogeny. Instead, they preserve $^{40}Ar/^{39}Ar$ records of older tectonic events.

$^{40}Ar/^{39}Ar$ ages equivalent to the Delamerian Orogeny are recorded in the Hurleys Metamorphics of the Anakie Inlier, although elsewhere in the Thomson Orogen this study found no evidence of Delamerian deformation. The majority of new $^{40}Ar/^{39}Ar$ ages from metamorphic rocks of the Thomson Orogen are Ordovician to Silurian, and they likely record periods of deformation that correspond with the Benambran and Kanimblan Orogenies of the Lachlan Orogen. $^{40}Ar/^{39}Ar$ ages that may be attributable to the Benambran Orogeny were found in samples of the Anakie Metamorphics and Halls Reward Metamorphics, and igneous cooling ages from this study are similar to the age of the early Tabberabberan cycle. An open question is how these orogenic events of eastern Australia relate to the coincident Alice Springs Orogeny of central Australia, from which similar ages have been obtained (Haines et al., 2001; Quentin de Gromard, 2013).

Chapter 4: Summary

This project aimed to (1) improve understanding of the stratigraphy and thermal history of the Thomson Orogen and (2) place more accurate radiometric age constraints on rocks previously dated by the K-Ar method.

4.1 Cambrian-Ordovician stratigraphy of the northern Thomson Orogen

Neoproterozoic-Cambrian metasedimentary rocks of the Anakie Metamorphic Group, which are exposed in the Anakie Inlier of east-central Queensland, are the oldest part of the Thomson Orogen. They are overlain by late Cambrian to Early Ordovician metasediments, some of which were deposited in the Larapintine Sea, an inland seaway that may have stretched east-to-west across the Australian continent. Based on detrital zircon data, the Ross-Delamerian Orogen appears to have been a significant source of material for the Thomson Orogen Cambrian-Ordovician metasediments (e.g., Maidment et al., 2007; Fergusson and Henderson, 2015).

A newly described, ~2000 m-thick accumulation of metasediments at Mt. McLaren, which lies to the east of the Anakie Inlier, seems to correlate with previously described Cambrian-Orodovician strata in the northern Thomson Orogen. Deposited from a vast shallow, clastic sea, the Mt McLaren beds, Les Jumelles beds and Puddler Creek Fm. are similar in age and depositional environment (Oorloff, 2014; Lee et al., 2015). In addition to Thomson Orogen correlations, the Mt. McLaren beds also seem to have stratigraphic equivalents in the Centralian Superbasin, in particular the Pacoota Sandstone of the Amadeus Basin and the Tomahawk Formation of the Georgina Basin (Oorloff, 2014).

The first-order sedimentology of the Mt. McLaren beds suggests that they were deposited in a shallow-marine environment, possibly the precursor to the deeper marine environment in which Ordovician turbidites of the Lachlan Orogen were subsequently deposited (Oorloff, 2014; Lee et al., 2015). The Mt. McLaren beds contrast, therefore, with rocks that have been described in the southern Thomson Orogen and the Lachlan Orogen (Murray, 1994; Glen, 2005). The set of stratigraphic correlations described above suggest significant variation in depositional environments during Cambrian to Ordovician time in various components of the Tasmanides.

4.2 Thermal history of the Thomson Orogen

New $^{40}Ar/^{39}Ar$ results from this study help establish a broad thermal history of both intrusive and metamorphic rocks of the Thomson Orogen. Much of the Thomson Orogen was emplaced or deformed in the Devonian and Carboniferous, therefore post-dating the Cambrian Delamerian Orogeny. Peviously considered as a major control on Thomson Orogen metamorphism and deformation (Withnall et al., 1996; Nishiya et al., 2003), the Delamerian Orogeny is recorded in $^{40}Ar/^{39}Ar$ ages from this study obtained from rocks of the Anakie Metamorphic Group. Additionally, $^{40}Ar/^{39}Ar$ data from granites that were emplaced in the central and southern Thomson Orogen during Silurian to Devonian time illustrate that they underwent protracted cooling over a ~90 My period. $^{40}Ar/^{39}Ar$ results indicate that Thomson Orogen rocks to the east of the Anakie Inlier were strongly affected by mid to late Permian deformation, unlike most Thomson Orogen rocks to the west. These new results are therefore helpful in delineating a broad-scale division between eastern Thomson Orogen-New England Orogen rocks that were strongly affected by the Hunter-Bowen Orogeny, and western Thomson Orogen rocks that preserve $^{40}Ar/^{39}Ar$ records of older periods of deformation.

4.3 Summary of the stratigraphic and tectonic development of the Thomson Orogen

The earliest evidence of the origins of the Thomson Orogen is found in the detrital zircon record from the Anakie Inlier. The oldest component of the Thomson Orogen, these late Neoproterozoic to early Paleozoic sediments form the Anakie Metamorphic Group, and have been linked to the development of the Gondwanan margin after rifting of the supercontinent Rodinia (Fergusson et al., 2001). The breakup of Rodinia was the precursor to the development of the Terra Australis Orogen of Gondwana, with a ~600 – 580 Ma rifting event linked to clastic sedimentation (Fergusson and Henderson, 2015). In the far west of the Thomson Orogen a ~600 Ma $^{40}Ar/^{39}Ar$ age from this study is potentially due to Rodinia rifting. By the middle to late Cambrian Gondwana had assembled, with associated contraction during the late Cambrian to early Ordovician Delamerian Orogeny recorded as far north as the Anakie Inlier (Withnall et al., 1996; Wood, 2006).

Distinctly younger than the Anakie Metamorphic Group, the sediments which make up the northern Thomson Orogen were deposited in late Cambrian to Ordovician time (Oorloff, 2014; Cross et al., 2015), and are temporally similar to deposits from central Australia (Li and Powell, 2001; Haines and Wingate, 2007; Maidment et al., 2007). $^{40}Ar/^{39}Ar$ ages of this study, obtained from northern Thomson Orogen rocks, are Ordovician to Silurian in age, therefore post-dating the Delamerian Orogeny and are more inline with ages attributed to the Benambran Orogeny, which has been linked to the Mossman Orogenic event of north Queensland (Fergusson et al., 2013). In the southern Thomson Orogen and Lachlan Orogen a deeper marine environment resulted in turbidite deposition (Murray, 1994; Veevers, 2015), associated with the Ordovician to Silurian Benambran cycle (Glen, 2005). The shallower environment of the northern Thomson Orogen may have been a precursor to this deeper environment to the south. Contractile deformation during the latter stages of the Benambran Orogeny is associated with intrusions in the Lachlan Orogen (Draper, 2006; Kositcin et al., 2009), and marine sedimentation continued into the Silurian and early Devonian (Li and Powell, 2001).

The Tabberabberan Orogeny of the middle Devonian is recorded in the New England Orogen and resulted in intrusions throughout the Lachlan Orogen (Glen, 2005), and possibly the central and southern Thomson Orogen (Kositcin et al., 2009). $^{40}Ar/^{39}Ar$ ages from igneous rocks of the central and southern Thomson Orogen are attributed to cooling over ~90 My, with ages similar to those attributed to the Tabberabberan cycle (Glen, 2005), though no late Tabberabberan ages, which would be attributable to the Tabberabberan Orogeny, are recorded in this study. The Kanimblan Orogeny followed in the late Devonian to Carboniferous, however due to temporal overlap of the Benambran, Tabberabberan and Kanimblan Orogenies with the central Australian Alice Springs Orogeny there are difficulties in deciphering the influence of each of these events.

Carboniferous extension is recorded in the eastern Thomson Orogen, with $^{40}Ar/^{39}Ar$ ages from the Mt McLaren beds recording this much younger deformation event, which is not seen in rocks of the nearby Anakie Inlier, <100km to the west. Fletcher’s Awl Dome records evidence of the subsequent Permian Hunter-Bowen Orogeny, with ages similar to those reported from the New England Orogen (Shaanan et al., 2014), which is the final tectonic event recorded in the Thomson Orogen.

References

Berry, R.F., Huston, D.L., Stolz, A.J., Hill, A.P., Beams, S.D., Kuronen, U., and Taube, A., 1992, Stratigraphy, structure, and volcanic-hosted mineralization of the Mount Windsor Subprovince, North Queensland, Australia: Economic Geology, v. 87, no. 3, p. 739–763, doi: 10.2113/gsecongeo.87.3.739.

Blake, P., Withnall, I., Fitzell, M., Kyriakis, Z., and Purdy, D., 2012, Geology of the western part of the Drummond Basin. Queensland Geological Record 2012/17:.

Blewett, R.S., Black, L.P., Sun, S.S., Knutson, J., Hutton, L.J., and Bain, J.H.C., 1998, U-Pb zircon and Sm-Nd geochronology of the Mesoproterozoic of North Queensland: implications for a Rodinian connection with the Belt supergroup of North America: Precambrian Research, v. 89, p. 101–127, doi: 10.1016/S0301-9268(98)00030-8.

Bourgeois, J., 1980, A transgressive shelf sequence exhibiting hummocky stratification: The Cape Sebastian sandstone (Upper Cretacious), southwestern Oregon: Journal of Sedimentary Petrology, v. 50, no. 3, p. 681–702.

Boyd, R., Ruming, K., Goodwin, I., Sandstrom, M., and Schröder-Adams, C., 2008, Highstand transport of coastal sand to the deep ocean: A case study from Fraser Island, southeast Australia: Geology, v. 36, no. 1, p. 15–18, doi: 10.1130/G24211A.1.

Burton, G.R., 2010, New structural model to explain geophysical features in northwestern New South Wales: implications for the tectonic framework of the Tasmanides: Australian Journal of Earth Sciences, v. 57, no. 1, p. 23–49, doi: 10.1080/08120090903416195.

Cawood, P. a., 2005, Terra Australis Orogen: Rodinia breakup and development of the Pacific and Iapetus margins of Gondwana during the Neoproterozoic and Paleozoic: Earth-Science Reviews, v. 69, no. 3-4, p. 249–279, doi: 10.1016/j.earscirev.2004.09.001.

Champion, D.C., Kositcin, N., Huston, D.L., Mathews, E., and Brown, C., 2009, Geodynamic synthesis of the Phanerozoic of Eastern Australia and implications for metallogeny:.

Coney, P.J., Edwards, A., Hine, R., Morrison, F., and Windrim, D., 1990, The regional tectonics of the Tasman orogenic system, eastern Australia: Journal of Structural Geology, v. 12, no. 5–6, p. 519–543, doi: http://dx.doi.org/10.1016/0191-8141(90)90071-6.

Cook, P.J., 1972, Sedimentological studies on the Stairway Sandstone of Central Australia, *in* Bulletin 95, Adelaide, S.A., p. 73.

Cross, A., Dunkley, D., Bultitude, R., Brown, D., Purdy, D., Withnall, I.W., von Gnielinski, F., and Blake, P., 2015, Summary of results Joint GSQ – GA geochronology project: Thomson Orogen, New England Orogen and Mount Isa region, 2010-2012:.

Davis, B.K., Henderson, R.A., and Bultitude, R.J., 1998, Evidence for a major crustal dislocation in the Hodgkinson Province, north Queensland: Australian Journal of Earth Sciences, v. 45, no. 6, p. 937–942, doi: 10.1080/08120099808728447.

Direen, N.G., and Crawford, a. J., 2003a, Fossil seaward-dipping reflector sequences preserved in southeastern Australia: a 600 Ma volcanic passive margin in eastern Gondwanaland: Journal of the Geological Society, London, v. 160, no. 6, p. 985–990, doi: 10.1144/0016-764903-010.

Direen, N.G., and Crawford, a. J., 2003b, The Tasman Line: Where is it, what is it, and is it Australia's Rodinian breakup boundary? Australian Journal of Earth Sciences, v. 50, no. 4, p. 491–502, doi: 10.1046/j.1440-0952.2003.01005.x.

Draper, J.J., 2006, The Thomson Fold Belt in Queensland revisited: ASEG Extended Abstracts, v. 2006, no. 1, p. 1–6, doi: doi:10.1071/ASEG2006ab038.

Dumas, S., and Arnott, R.W.C., 2006, Origin of hummocky and swaley cross-stratification— The controlling influence of unidirectional current strength and aggradation rate: Geology, v. 34, no. 12, p. 1073–1076, doi: 10.1130/g22930a.1.

Fergusson, C.L., Carr, P.F., Fanning, C.M., and Green, T.J., 2001, Proterozoic-Cambrian detrital zircon and monazite ages from the Anakie Inlier, central Queensland: Grenville and Pacific-Gondwana signatures: Australian Journal of Earth Sciences, v. 48, no. 6, p. 857–866, doi: 10.1046/j.1440-0952.2001.00904.x.

Fergusson, C.L., and Henderson, R.A., 2015, Early Palaeozoic continental growth in the Tasmanides of northeast Gondwana and its implications for Rodinia assembly and rifting: Gondwana Research, v. 28, no. 3, p. 933–953, doi: 10.1016/j.gr.2015.04.001.

Fergusson, C.L., and Henderson, R.A., 2013, Thomson Orogen, *in* Jell, P.A. ed., Geology of Queensland, Geological Survey of Queensland, Brisbane, Queensland, p. 113–224.

Fergusson, C., Henderson, R., Fanning, C., and Withnall, I., 2007a, Detrital zircon ages in Neoproterozoic to Ordovician siliciclastic rocks, northeastern Australia: implications for the tectonic history of the East Gondwana continental margin: Journal of the Geological Society, v. 164, no. 1, p. 215–225, doi: 10.1144/0016-76492005-136.

Fergusson, C., Henderson, R., Lewthwaite, K., Phillips, D., and Withnall, I., 2005, Structure of the Early Palaeozoic Cape River Metamorphics, Tasmanides of north Queensland: evaluation of the roles of convergent and extensional tectonics: Australian Journal of Earth Sciences, v. 52, no. 2, p. 261–277, doi: 10.1080/08120090500139372.

Fergusson, C.L., Henderson, R.A., Withnall, I.W., and Fanning, C.M., 2007b, Structural history of the Greenvale Province, north Queensland: Early Palaeozoic extension and convergence on the Pacific margin of Gondwana*: Australian Journal of Earth Sciences, v. 54, no. 4, p. 573–595, doi: 10.1080/08120090701188970.

Fergusson, C.L., Henderson, R. a., Withnall, I.W., Fanning, C.M., Phillips, D., and Lewthwaite, K.J., 2007c, Structural, metamorphic, and geochronological constraints on alternating compression and extension in the Early Paleozoic Gondwanan Pacific margin, northeastern Australia: Tectonics, v. 26, no. 3, p. 1–20, doi: 10.1029/2006TC001979.

Fergusson, C.L., Nutman, A.P., Kamiichi, T., and Hidaka, H., 2013, Evolution of a Cambrian active continental margin: The Delamerian–Lachlan connection in southeastern Australia from a zircon perspective: Gondwana Research, v. 24, no. 3–4, p. 1051–1066, doi: http://dx.doi.org/10.1016/j.gr.2013.03.006.

Foden, J., Elburg, M.A., Dougherty-Page, J., and Burtt, A., 2006, The Timing and Duration of the Delamerian Orogeny: Correlation with the Ross Orogen and Implications for Gondwana Assembly: The Journal of Geology, v. 114, no. 2, p. 189–210, doi: 10.1086/499570.

Foster, D., and Ehlers, K., 1998, 40Ar-39Ar thermochronology of the southern Gawler Craton, Australia: Implications for Mesoproterozoic and Neoproterozoic tectonics of East Gondwana and Rodinia: Journal of Geophysical Research, v. 103, no. B5, p. 10,177–10,193.

Foster, D. a., Gray, D.R., and Bucher, M., 1999, Chronology of deformation within the turbidite-dominated, Lachlan orogen: Implications for the tectonic evolution of eastern Australia and Gondwana: Tectonics, v. 18, no. 3, p. 452–485, doi: 10.1029/1998TC900031.

Glen, R.A., 2013, Refining accretionary orogen models for the Tasmanides of eastern Australia: Australian Journal of Earth Sciences, v. 60, no. 3, p. 315–370, doi: 10.1080/08120099.2013.772537.

Glen, R.A., 2005, The Tasmanides of eastern Australia: Geological Society, London, Special Publications, v. 246, no. 1, p. 23–96, doi: 10.1144/gsl.sp.2005.246.01.02.

Glen, R. a., Percival, I.G., and Quinn, C.D., 2009, Ordovician continental margin terranes in the Lachlan Orogen, Australia: Implications for tectonics in an accretionary orogen along the east Gondwana margin: Tectonics, v. 28, no. 6, p. 1–17, doi: 10.1029/2009TC002446.

Haines, P.W., Hand, M., and Sandiford, M., 2001, Palaeozoic synorogenic sedimentation in Central and Northern Australia: A review of distribution and timing with implications for the evolution of intracontinental orogens: Australian Journal of Earth Sciences, v. 48, no. November 2015, p. 911–928, doi: 10.1046/j.1440-0952.2001.00909.x.

Haines, P.W., and Wingate, M.T.D., 2007, Contrasting depositional histories, detrital zircon provenance and hydrocarbon systems: did the Larapintine Seaway link the Canning and Amadeus basins during the Ordovician? Northern Territory Geological Survey Special Publication, v. 2, p. 36–51.

Harding, R., 1969, Catalogue of Age Determinations on Australian Rocks, 1962-1965:.

Henderson, R.A., 1986, Geology of the Mt Windsor subprovince—a lower Palaeozoic volcano-sedimentary terrane in the northern Tasman orogenic zone: Australian Journal of Earth Sciences, v. 33, no. 3, p. 343–364, doi: 10.1080/08120098608729371.

Henderson, R.A., Davis, B.K., and Fanning, C.M., 1998, Stratigraphy, age relationships and tectonic setting of rift-phase infill in the Drummond Basin, central Queensland: Australian Journal of Earth Sciences, v. 45, no. 4, p. 579–595, doi: 10.1080/08120099808728414.

Higgs, R., 1996, A new facies model for the Misoa Formation (Eocene), Venezuela's main oil reservoir: Journal of Petroleum Geology, v. 19, no. July, p. 249–269, doi: 10.1306/BF9AB770-0EB6-11D7-8643000102C1865D.

Hutton, L., 2004, Petrogenesis of I- and S-type Granites in the Cape River - Lolworth area, northeastern Queensland: Their contribution to an understanding of the Early Palaeozoic Geological History of northeastern Queensland: The Queensland University of Technology, 0-308 p.

Johnson, H.D., and Baldwin, C.T., 1996, Shallow clastic seas, *in* Reading, H.G. ed., Sedimentary environments: processes, facies and stratigraphy, Blackwell Science Ltd, Oxford, p. 232–280.

Kositcin, N., Champion, D.C., and Huston, D.L., 2009, Geodynamic Synthesis of the North Queensland Region and Implications for Metallogeny Geodynamic: Geoscience Australia.

Lee, M., Verdel, C., Welsh, K., and Oorloff, A., 2015, Stratigraphy of the Thomson Orogen – New Insights from Mount McLaren, North-east Australia, *in* PACRIM2015 Proceedings, The

Australasian Institute of Mining and Metallurgy, Carlton, Victoria, p. 551–556.

Leitch, E.C., 1978, Structural succession in a Late Palaeozoic slate belt and its tectonic significance: v. 47, p. 311–323.

Levell, B.K., 1980, A late Precambrian tidal shelf deposit, the Lower Sandfjord Formation, Finnmark, North Norway: Sedimentology, v. 27, no. 5, p. 539–557, doi: 10.1111/j.1365-3091.1980.tb01646.x.

Li, Z.X., Bogdanova, S. V, Collins, A.S., Davidson, A., De Waele, B., Ernst, R.E., Fitzsimons, I.C.W., Fuck, R.A., Gladkochub, D.P., Jacobs, J., Karlstrom, K.E., Lu, S., Natapov, L.M., Pease, V., et al., 2008, Assembly, configuration, and break-up history of Rodinia: A synthesis: Precambrian Research, v. 160, no. 1–2, p. 179–210, doi: http://dx.doi.org/10.1016/j.precamres.2007.04.021.

Li, Z.X., and Powell, C.M., 2001, An outline of the palaeogeographic evolution of the Australasian region since the beginning of the Neoproterozoic: Earth-Science Reviews, v. 53, no. 3–4, p. 237–277, doi: http://dx.doi.org/10.1016/S0012-8252(00)00021-0.

Li, P.-F., Rosenbaum, G., and Rubatto, D., 2012, Triassic asymmetric subduction rollback in the southern New England Orogen (eastern Australia): the end of the Hunter-Bowen Orogeny: Australian Journal of Earth Sciences, v. 59, no. 6, p. 965–981, doi: 10.1080/08120099.2012.696556.

Lindsey, K. a., and Gaylord, D.R., 1992, Fluvial, coastal, nearshore, and shelf deposition in the Upper Proterozoic (?) to Lower Cambrian Addy Quartzite, northeastern Washington: Sedimentary Geology, v. 77, no. 1-2, p. 15–35, doi: 10.1016/0037-0738(92)90101-V.

Maidment, D.W., Williams, I.S., and Hand, M., 2007, Testing long-term patterns of basin sedimentation by detrital zircon geochronology, Centralian Superbasin, Australia: Basin Research, v. 19, no. 3, p. 335–360, doi: http://dx.doi.org/10.1111/j.1365-2117.2007.00326.x.

McDougall, I., and Harrison, T.M., 1999, Geochronology and Thermochronology by the 40Ar/39Ar Method: Oxford University Press on Demand.

McDougall, I., and Wellman, P., 2011, Calibration of GA1550 biotite standard for K / Ar and Ar / 39 Ar dating: Chemical Geology, v. 280, no. 1-2, p. 19–25, doi: 10.1016/j.chemgeo.2010.10.001.

Murray, C.G., 1994, Basement cores from the Tasman Fold Belt system beneath the Great Artesian Basin in Queensland, Queensland Geological Record, 1994/10:.

Murray, C.G., 1986, Metallogeny and tectonic development of the Tasman Fold Belt System in Queensland: Ore Geology Reviews, v. 1, no. 2-4, p. 315–400.

Murray, C.G., and Kirkegaard, A.G., 1978, The Thomson Orogen of the Tasman Orogenic Zone: Tectonophysics, v. 48, no. 3–4, p. 299–325, doi: http://dx.doi.org/10.1016/0040-1951(78)90122-1.

Mutti, E., and Ricci Lucchi, F., 1972, Le torbiditi dell'Appennino settentrionale: introduzione all'analisi di facies: Memorie della Societa Geologica Italiana, v. 11, no. 2, p. 161–199.

Myrow, P.M., and Southard, J.B., 1996, Tempestite deposition: Journal of Sedimentary Research, v. 66, no. 5.

Nishiya, T., Watanabe, T., Yokoyama, K., and Kuramoto, Y., 2003, New Isotopic Constraints on the Age of the Halls Reward Metamorphics , North Queensland , Australia: Delamerian Metamorphic Ages and Grenville Detrital Zircons: , no. 2, p. 241–249.

Offler, R., Phillips, G., Fergusson, C.L., and Green, T.J., 2011, Tectonic Implications of Early Paleozoic Metamorphism in the Anakie Inlier, Central Queensland, Australia: The Journal of Geology, v. 119, no. 5, p. 467–485, doi: 10.1086/661191.

Oorloff, A., 2014, Geology of Mt. McLaren: Deposition and exhumation of a Thomson Orogen Inlier: University of Queensland.

Purdy, D., and Brown, D., 2011, Peeking under the covers - The new "Geology of the Thomson Orogen" project: v. Queensland, p. 39–48.

Purdy, D.J., Carr, P.A., and Brown, D.D., 2013, A review of the geology, mineralisation, and geothermal energy potential of the Thomson Orogen in Queensland. Queensland Geological Record 2013/01.: Department of Natural Resources and Mines.

Quentin de Gromard, R., 2013, The significance of E–W structural trends for the Alice Springs Orogeny in the Charters Towers Province, North Queensland: Tectonophysics, v. 587, no. 0, p. 168–187, doi: http://dx.doi.org/10.1016/j.tecto.2012.09.002.

Rosenbaum, G., Li, P., and Rubatto, D., 2012, The contorted New England Orogen (eastern Australia): New evidence from U-Pb geochronology of early Permian granitoids: Tectonics, v. 31, no. 1, doi: 10.1029/2011TC002960.

Shaanan, U., Rosenhaum, G., Li, P., and Vasconcelos, P., 2014, Structural evolution of the early Permian Nambucca Block (New England Orogen, eastern Australia) and implications for oroclinal bending: Tectonics, v. 33, p. 1425–1443, doi: 10.1002/2013TC003426.Received.

Spampinato, G.P.T., Ailleres, L., Betts, P.G., and Armit, R.J., 2015a, Crustal architecture of the Thomson Orogen in Queensland inferred from potential field forward modelling: Australian Journal of Earth Sciences, , no. August 2015, p. 1–23, doi: 10.1080/08120099.2015.1063546.

Spampinato, G.P.T., Betts, P.G., Ailleres, L., and Armit, R.J., 2015b, Early tectonic evolution of the Thomson Orogen in Queensland inferred from constrained magnetic and gravity data: Tectonophysics, v. 651-652, p. 99–120, doi: 10.1016/j.tecto.2015.03.016.

Spell, T.L., and McDougall, I., 2003, Characterization and calibration of Ar / 39 Ar dating standards: Chemical Geology, v. 198, p. 189–211, doi: 10.1016/S0009-2541(03)00005-6.

Squire, R.J., Campbell, I.H., Allen, C.M., and Wilson, C.J.L., 2006, Did the Transgondwanan Supermountain trigger the explosive radiation of animals on Earth? Earth and Planetary Science Letters, v. 250, no. 1–2, p. 116–133, doi: http://dx.doi.org/10.1016/j.epsl.2006.07.032.

VandenBerg, A.H.M., 1999, Timing of orogenic events in the Lachlan Orogen: Australian Journal of Earth Sciences, v. 46, no. 5, p. 691–701, doi: 10.1046/j.1440-0952.1999.00738.x.

Veevers, J.J., 2015, Beach sand of SE Australia traced by zircon ages through Ordovician turbidites and S-type granites of the Lachlan Orogen to Africa/Antarctica: a review: Australian Journal of Earth Sciences, v. 62, no. 4, p. 385–408, doi: 10.1080/08120099.2015.1053985.

Veevers, J.J., 2004, Gondwanaland from 650–500 Ma assembly through 320 Ma merger in Pangea to 185–100 Ma breakup: supercontinental tectonics via stratigraphy and radiometric dating:

Earth-Science Reviews, v. 68, no. 1–2, p. 1–132, doi: http://dx.doi.org/10.1016/j.earscirev.2004.05.002.

Walter, M.R., Desmarais, D., Farmer, J.D., and Hinman, N.W., 1996, Lithofacies and biofacies of mid-Paleozoic thermal spring deposits in the Drummond Basin, Queensland, Australia.: Palaios, v. 11, no. 6, p. 497–518.

Walter, M.R., Veevers, J.J., Calver, C.R., Grey, K., and Hilyard, D., 1992, The Proterozoic Centralian Superbasin: a frontier petroleum province: Bull. Am. Ass. Petrol. Geol, v. 76, p. 1132.

Webb, a. W., and McDougall, I., 1968, The geochronology of the igneous rocks of Eastern Queensland: Journal of the Geological Society of Australia, v. 15, no. 2, p. 313–346, doi: 10.1080/00167616808728701.

Withnall, I.W., Blake, P.R., Crouch, S.B.S., Woods, K.T., Grimes, K.G., Hayward, M.A., Lam, J.S., Garrad, P., and Rees, I.D., 1995, Geology of the southern part of the Anakie Inlier, central Queensland: Queensland Geology, p. 245.

Withnall, I.W., Golding, S.D., Rees, I.D., and Dobos, S.K., 1996, K—Ar dating of the Anakie Metamorphic Group: Evidence for an extension of the Delamerian Orogeny into central Queensland: Australian Journal of Earth Sciences, v. 43, no. 5, p. 567–572, doi: 10.1080/08120099608728277.

Withnall, I.W., and Henderson, R.A., 2012, Accretion on the long-lived continental margin of northeastern Australia: Episodes, v. 35, no. 1, p. 166–176.

Wood, D.G., 2006, Strucutral geology, tectonics and gold mineralisation of the southern Anakie Inlier: Australian National University, 281 p.

Wood, D., and Lister, G., 2004, Age and implications of core complex formation in Central East Queensland, *in* 17th Australian Geological Convention, Hobart.

Wood, D.G., and Lister, G.S., 2013, Dating deformation in the Anakie Metamorphic Group and Gem Park Granite, *in* Jell, P. ed., Queensland Geology, Geological Survey of Queensland, Brisbane, p. 133–135.

Appendix A: Sample location information, including coordinates.

Sample #	*Name*	*Lat*	*Long*	*Sample Type*	*Depth*	*Rock Type*
2122055	Hungerford Granite	-28.99578223	144.4615304	Surface		Monzogranite
2152164	Ooroonoo1	-23.17913543	141.5536758	Drill core	3849'-3849.2'	Granite
2122054	Granite Springs Granite	-28.33065565	144.5473222	Surface		Monzogranite
2152166	Sefton Metamorphics	-12.6992	143.3039	Drill core	78.5-79.5m	Schist
2130084	Thunderbolt1	-22.36568611	145.0027972	Drill core	5282'-5285'	Rhyolitic Ignimbrite
MLRG01	Retreat Granite	-22.97414	147.54268	Surface		Granite
MLLJ06	Les Jumelles beds	-21.09137398	146.879378	Surface		Metasediments
MLHR02	Halls Reward Metamorphics	-18.94215502	144.976643	Surface		Schist
NQ37	Halls Reward Metamorphics	-18.96701045	144.9644444	Surface		Schist
AOM03	Mt McLaren beds	-22.34805	147.78633	Surface		Metasediments
MLPD01	Newmont Peak Downs DDH6N (bore # 51382)	-22.86570439	147.5982609	Drill core	490'8"	Metasediments
MLPD02	Newmont Peak Downs DDH6N (bore # 51382)	-22.86570439	147.5982609	Drill core	481'4"	Metasediments
MLH501	Hurleys 5 (bore #51814)	-22.72266089	147.4835687	Drill core	165.10m	Metasediments
MLH502	Hurleys 5 (bore #51814)	-22.72266089	147.4835687	Drill core	164.10m	Metasediments
MLH503	Hurleys 5 (bore #51814)	-22.72266089	147.4835687	Drill core	134.60m	Metasediments
MLH504	Hurleys 5 (bore #51814)	-22.72266089	147.4835687	Drill core	131.0m	Metasediments
MLH505	Hurleys 5 (bore #51814)	-22.72266089	147.4835687	Drill core	93.0m	Metasediments

Appendix B: $^{40}Ar/^{39}Ar$ geochronology data tables.

Sample	Run ID	Laser (W)	Age (Ma)	±	36Ar/39Ar	±	37Ar/39Ar	±	38Ar/39Ar	±	40Ar/39Ar	±	40Ar*/39Ar	±	% Rad	±	39Ar (moles)	40Ar (moles)	Fit Type
8631-01A	2152164a	0.1	595.3311	4.207294	0.0381208	0.0004824	0.0641674	0.0128554	0.0260595	0.0006662	112.3424	0.8254177	100.9703	0.8377725	89.87398	0.1612452	2.71E-15	3.04E-13	PPLLLL
8631-01B	2152164a	0.15	666.3386	3.958647	0.0091555	0.0002352	0.0860693	0.0083688	0.0215372	0.0005284	118.1116	0.816174	115.3915	0.8199052	97.69192	0.1061693	4.74E-15	5.60E-13	PPLLLL
8631-01C	2152164a	0.2	600.2529	3.442994	0.005479	0.000223	0.0508855	0.0059728	0.0210961	0.0004558	103.58	0.6827993	101.9517	0.6874552	98.42525	0.1157182	4.76E-15	4.93E-13	PPLLLL
8631-01D	2152164a	0.25	562.5511	4.116221	0.0114691	0.0003532	0.0956759	0.011327	0.0222309	0.000564	97.91263	0.8049105	94.50197	0.8048795	96.51106	0.1797543	3.12E-15	3.05E-13	PPLLLL
8631-01E	2152164a	0.3	549.7203	3.561757	0.0107741	0.0004249	0.0656914	0.0134495	0.0209735	0.0006568	95.2096	0.6796417	92.00196	0.6915247	96.62742	0.2242208	2.30E-15	2.19E-13	PPLLLL
8631-01F	2152164a	0.35	558.1492	3.406299	0.0094907	0.0003676	0.0633006	0.0125181	0.0209999	0.0005944	96.46697	0.6532399	93.64228	0.6644392	97.06844	0.2027755	2.14E-15	2.07E-13	PPLLLL
8631-01G	2152164a	0.4	583.4205	3.604863	0.0054251	0.0003475	0.0755054	0.01252	0.0206924	0.0006974	100.2153	0.7052677	98.60643	0.7130906	98.3903	0.2122622	2.16E-15	2.16E-13	PPLLLL
8631-01H	2152164a	0.45	605.6791	3.833666	0.0031995	0.0003927	0.0937938	0.0198198	0.0217944	0.0008	103.978	0.7592019	103.0368	0.7677656	99.0891	0.1809937	1.54E-15	1.60E-13	PPLLLL
8631-01I	2152164a	0.5	624.6644	5.422157	0.003409	0.0007319	0.0909114	0.0308377	0.0159391	0.0013437	107.8636	1.080321	106.859	1.097379	99.06315	0.2885735	7.86E-16	8.48E-14	PPLLLL
8631-01J	2152164a	0.6	616.3675	7.36787	0.005645	0.0011164	0.2073959	0.0461631	0.0212647	0.0019499	106.8381	1.4624	105.1837	1.484326	98.43815	0.4466252	5.30E-16	5.66E-14	PPLLLL
8631-01K	2152164a	0.8	628.8027	8.363989	0.0036405	0.0012174	0.1464638	0.0599644	0.0191956	0.0021189	108.7625	1.669766	107.6975	1.696658	99.01157	0.4506352	4.62E-16	5.03E-14	PPLLLL
8631-01L	2152164a	1	667.7826	17.80258	-0.0070974	0.0028241	0.0521875	0.1485264	0.0085219	0.0047838	113.5646	3.530265	115.6907	3.690179	101.8692	0.8111169	1.85E-16	2.10E-14	PPLLLL
8631-01M	2152164a	2.5	602.7344	8.627183	0.006362	0.0013866	0.240785	0.0604884	0.0153331	0.0023338	104.3121	1.698477	102.4475	1.724942	98.19694	0.521282	4.07E-16	4.25E-14	PPLLLL
8631-02A	2152164a	0.1	608.9846	3.93366	0.0334768	0.0005387	0.0718597	0.0108184	0.0225743	0.0006166	113.6839	0.7601752	103.6994	0.789236	91.21338	0.1750208	2.40E-15	2.73E-13	PPLLLL
8631-02B	2152164a	0.15	740.4253	5.783043	0.0138765	0.000558	0.0540773	0.0208722	0.0226463	0.0009972	135.1896	1.252559	131.0556	1.247982	96.93907	0.1986808	1.51E-15	2.05E-13	PPLLLL
8631-02C	2152164a	0.2	617.054	5.279303	0.0298651	0.0009287	0.0443417	0.028141	0.0246505	0.0011374	114.232	1.057966	105.322	1.063969	92.1979	0.3156929	1.00E-15	1.14E-13	PPLLLL
8631-02D	2152164a	0.25	561.0474	5.317496	0.03135	0.0009735	0.0480336	0.0355572	0.0229591	0.0014079	103.5614	1.041141	94.20807	1.038909	90.96598	0.3446223	8.17E-16	8.46E-14	PPLLLL
8631-02E	2152164a	0.3	653.5077	7.418978	0.0198482	0.0010739	0.0919531	0.0447756	0.0211877	0.001578	118.6554	1.545023	112.7435	1.52571	95.01217	0.3684089	5.58E-16	6.62E-14	PPLLLL
8631-02F	2152164a	0.35	700.1343	9.791207	0.0131181	0.0016181	-0.0659217	0.076623	0.0238338	0.0022698	126.3842	2.060289	122.4572	2.066278	96.89781	0.5218634	3.26E-16	4.12E-14	PPLLLL
8631-02G	2152164a	0.4	662.3494	25.13643	0.0296273	0.0061759	0.308647	0.236849	0.0240801	0.0085304	123.3638	5.228564	114.5662	5.194697	92.84939	1.529698	9.63E-17	1.19E-14	PPLLLL
8631-02H	2152164a	0.5	559.0365	31.92275	0.0297147	0.0083587	0.8643325	0.3486637	0.0512463	0.0124956	102.562	6.250241	93.81541	6.229975	91.41799	2.477347	6.42E-17	6.58E-15	PPLLLL
8631-02I	2152164a	0.8	622.7467	10.91688	0.0181033	0.0027908	-0.1341649	0.1021548	0.0218778	0.0030044	111.8964	2.134439	106.4711	2.207097	95.16104	0.764247	2.38E-16	2.67E-14	LPLLLL
8631-02J	2152164a	1	662.3985	41.66217	0.0017447	0.0089995	-0.2079657	0.4325812	0.0094093	0.0153742	115.1308	8.220087	114.5764	8.610139	99.5334	2.445149	5.82E-17	6.70E-15	PPLLLL
8631-02K	2152164a	2.5	225.8984	267.9932	0.2228812	0.1907279	3.184583	5.772512	0.1029458	0.1638713	100.6696	65.94196	34.45059	43.48242	34.14643	36.86673	4.61E-18	4.64E-16	PPLLLL
8632-01A	2130084	0.1	362.7237	2.140141	0.0143305	0.0003125	0.0912628	0.0098112	0.015277	0.0005614	61.78298	0.3470283	57.5143	0.3746021	93.0862	0.2170992	2.73E-15	1.69E-13	PPLLLL
8632-01B	2130084	0.15	347.8937	2.344622	0.0027099	0.0003932	0.1410408	0.0191493	0.0131345	0.0007369	55.72283	0.3895387	54.92915	0.407034	98.5675	0.2709465	1.46E-15	8.15E-14	PPLLLL
8632-01C	2130084	0.2	352.7372	2.853334	0.0068201	0.0005641	0.1004022	0.0230608	0.0163867	0.0008386	57.7963	0.470716	55.77113	0.4966796	96.49068	0.3694134	1.08E-15	6.24E-14	PPLLLL
8632-01D	2130084	0.25	344.6099	3.230818	0.0045558	0.0006471	0.0690639	0.0271555	0.0109266	0.0010945	55.71294	0.5308608	54.3596	0.5598605	97.56764	0.4398146	9.16E-16	5.10E-14	PPLLLL
8632-01E	2130084	0.3	347.7142	2.913782	0.0041175	0.0005364	-0.0172637	0.0257319	0.0115547	0.0011091	56.13028	0.4827255	54.898	0.5057916	97.80719	0.4147167	9.66E-16	5.42E-14	PPLLLL
8632-01F	2130084	0.35	341.4511	2.188748	0.0066382	0.0004113	-0.0166077	0.0170055	0.0119144	0.0007168	55.79746	0.3546809	53.8127	0.3786192	96.44541	0.2959841	1.38E-15	7.69E-14	PPLLLL
8632-01G	2130084	0.4	341.7592	2.194301	0.0067195	0.0003604	0.0009757	0.0139404	0.0146253	0.0005754	55.87274	0.3613337	53.86599	0.3796447	96.40967	0.238802	1.71E-15	9.53E-14	PPLLLL
8632-01H	2130084	0.5	346.3035	2.454499	0.0055559	0.0002343	0.0199952	0.0085489	0.0138144	0.0003844	56.31048	0.4211129	54.65322	0.4257334	97.05698	0.2034882	3.27E-15	1.84E-13	PPLLLL
8632-01I	2130084	0.6	346.7593	1.942207	0.0040616	0.0001721	0.0151977	0.0059456	0.0130909	0.0003229	55.94399	0.3299689	54.73229	0.3369614	97.83446	0.1555328	6.03E-15	3.38E-13	PPLLLL
8632-01J	2130084	0.7	353.1158	1.999877	0.0033265	0.0001735	0.0221702	0.0067476	0.0131394	0.0003278	56.82844	0.3421676	55.83703	0.3481915	98.25533	0.1430997	4.40E-15	2.50E-13	PPLLLL
8632-01K	2130084	0.8	353.6908	2.076389	0.00241	0.000269	0.0148228	0.0127332	0.0130694	0.0004979	56.65576	0.3512729	55.93717	0.361628	98.73204	0.2185076	2.47E-15	1.40E-13	PPLLLL
8632-01L	2130084	1	353.6809	1.982418	0.0030639	0.0001963	0.0135973	0.0082151	0.0129226	0.0004294	56.84945	0.3380975	55.93544	0.3452599	98.3927	0.160612	3.31E-15	1.88E-13	PPLLLL
8632-01M	2130084	1.2	371.3235	7.662512	0.0037807	0.0018789	-0.1607044	0.0824822	0.0108957	0.0031216	60.17188	1.246312	59.02318	1.347625	98.10318	0.9994172	2.97E-16	1.79E-14	PPLLLL
8632-01N	2130084	1.4	352.415	2.681429	0.0028334	0.0004061	0.0436333	0.0194584	0.0106126	0.0008722	56.55701	0.451914	55.71506	0.4666729	98.50976	0.3273828	1.38E-15	7.79E-14	PPLLLL
8632-01O	2130084	1.6	355.4246	2.102074	0.0021804	0.0002191	0.0055117	0.0087604	0.0128924	0.0004634	56.89042	0.359559	56.23927	0.3664534	98.85646	0.2012277	3.49E-15	1.98E-13	PPLLLL
8632-01P	2130084	2	351.8855	1.995611	0.002343	0.000161	0.0025656	0.0066817	0.0123105	0.0003288	56.32301	0.3424941	55.62291	0.3472118	98.75822	0.1312567	5.38E-15	3.03E-13	PPLLLL
8632-01Q	2130084	2.5	362.4002	2.036022	0.0012743	0.0002332	0.028478	0.0109979	0.0133286	0.0004535	57.83556	0.3486281	57.45768	0.3563137	99.34606	0.1853686	2.47E-15	1.43E-13	PPLLLL
8632-01R	2130084	3	366.008	26.63479	0.0105956	0.0068364	-0.4329084	0.3000649	0.0196761	0.0116644	61.30397	4.43628	58.08969	4.670547	94.78641	3.459039	8.08E-17	4.95E-15	PPLLLL
8632-02A	2130084	0.1	281.3325	11.28607	0.3134821	0.0063046	0.0818075	0.0614043	0.0638224	0.0026899	137.1706	2.461653	43.58449	1.888327	31.77233	0.6924611	4.48E-16	6.15E-14	PPLLLL
8632-02B	2130084	0.2	387.858	4.623842	0.0371856	0.0010271	0.5426386	0.0376185	0.0160349	0.0012154	72.98294	0.8338206	61.9445	0.8206941	84.84444	0.4421135	8.19E-16	5.98E-14	PPLLLL
8632-02C	2130084	0.3	375.0713	3.866803	0.04339	0.000844	0.2011454	0.0234219	0.0200302	0.0009611	72.61464	0.6697936	59.68299	0.6814787	82.18089	0.3732948	1.17E-15	8.50E-14	PPLLLL
8632-02D	2130084	0.4	365.5943	4.511778	0.0468683	0.00118	0.15496	0.0346197	0.0205634	0.0014771	71.99294	0.7864553	58.01716	0.7909819	80.57957	0.502593	8.09E-16	5.83E-14	PPLLLL
8632-02E	2130084	0.5	348.4448	5.243481	0.0778327	0.0017364	0.2513476	0.0443901	0.0227658	0.0018698	78.23499	0.8811715	55.02485	0.9105633	70.3213	0.6313742	6.82E-16	5.34E-14	PPLLLL
8632-02F	2130084	0.6	371.3084	7.403334	0.1248346	0.002863	0.3545594	0.0645562	0.0396316	0.0025321	96.2499	1.40385	59.02052	1.302032	61.30558	0.7404464	4.68E-16	4.51E-14	PPLLLL
8632-02G	2130084	0.7	393.5654	7.015265	0.0913779	0.0022551	0.2311067	0.0655663	0.0292795	0.0028349	90.21395	1.391702	62.95912	1.249098	69.77816	0.6609158	4.47E-16	4.03E-14	PPLLLL
8632-02H	2130084	0.8	377.613	6.058044	0.0909519	0.0018908	0.1840817	0.0521299	0.0245129	0.0019635	87.26543	1.151089	60.13126	1.069164	68.89804	0.5702233	5.46E-16	4.76E-14	PPLLLL
8632-02I	2130084	0.9	394.2279	5.38637	0.098987	0.0017396	0.3340051	0.0394788	0.0356222	0.0012414	92.59081	0.8897483	63.07711	0.9594182	68.10946	0.5104098	8.35E-16	7.73E-14	PPLLLL
8632-02J	2130084	1	369.7123	9.439974	0.1119103	0.003707	0.3476635	0.108354	0.0308434	0.0037421	92.11218	1.99132	58.73993	1.65875	63.75524	0.9485714	2.65E-16	2.44E-14	PPLLLL
8632-02K	2130084	1.2	388.2318	10.6957	0.1140372	0.0043979	0.0233091	0.1146154	0.0282908	0.0037309	96.05641	2.204487	62.01086	1.898792	64.55622	1.13801	2.30E-16	2.21E-14	PPLLLL
8632-02L	2130084	1.6	383.6298	10.20789	0.1116784	0.0040712	0.2563402	0.1206842	0.039625	0.0040557	94.50725	2.12159	61.19491	1.807576	64.74064	1.071755	2.27E-16	2.15E-14	PPLLLL
8632-02M	2130084	2	69.5571	82.10601	0.1362352	0.0568134	0.7141255	2.005488	0.0346383	0.0624465	50.76769	15.40166	10.15197	12.216	19.98735	23.25963	1.41E-17	7.15E-16	PPLLLL
8632-02N	2130084	2.5	375.2615	36.40552	0.1091323	0.0154337	0.9640285	0.5189936	0.0433001	0.0185383	92.18501	8.087346	59.71651	6.416723	64.7364	3.992196	5.03E-17	4.64E-15	PPLLLL
8632-02O	2130084	3	410.1927	33.00977	0.1168179	0.0134234	-1.120198	0.4623613	0.0103857	0.0155981	100.9508	7.766812	65.93337	5.931949	65.36343	3.018349	5.65E-17	5.71E-15	PPLLLL
8634-01A	2122055b	0.1	472.3983	21.28082	0.528307	0.016516	1.032327	0.1748354	0.1189278	0.0074526	234.9039	6.737399	77.30685	3.958386	32.88663	0.9032458	1.50E-16	3.53E-14	PPLLLL
8634-01B	2122055b	0.2	314.6544	5.842713	0.1033044	0.0021767	2.44729	0.0675467	0.0330267	0.0014241	79.78377	0.9208062	49.21155	0.9957967	61.57747	0.7284652	5.46E-16	4.36E-14	PPLLLL
8634-01C	2122055b	0.3	341.9811	4.633166	0.0702293	0.0015096	2.609853	0.0641449	0.0198001	0.0014757	74.57597	0.7017976	53.90438	0.8017008	72.15159	0.6098981	6.84E-16	5.10E-14	PPLLLL
8634-01D	2122055b	0.4	333.883	3.341607	0.0234299	0.0008413	1.985151	0.0517551	0.0156459	0.0010509	59.27808	0.5308834	52.50627	0.5756259	88.4559	0.5008621	7.14E-16	4.23E-14	PPLLLL
8634-01E	2122055b	0.5	334.9845	4.96252	0.0094728	0.0014826	1.484728	0.0697281	0.0096419	0.0021977	55.35757	0.7559069	52.69607	0.8553668	95.09589	0.8636746	3.85E-16	2.13E-14	PPLLLL

8634-01F	2122055b	0.7	328.917	4.14345	0.0107289	0.0010532	0.9290212	0.0588165	0.0191031	0.001627	54.75108	0.6611237	51.652	0.7117895	94.28052	0.6193239	5.71E-16	3.12E-14	PPLLLL
8634-01G	2122055b	1	341.7973	4.087812	0.0549984	0.0012531	1.926209	0.0547269	0.0235524	0.0012582	70.07411	0.6200882	53.87258	0.7072632	76.77799	0.5481242	7.30E-16	5.12E-14	PPLLLL
8634-01H	2122055b	1.5	354.2333	3.742427	0.0594797	0.0009784	3.197856	0.0491023	0.0242677	0.0011425	73.42146	0.5623804	56.03167	0.6519846	76.14732	0.4166324	9.96E-16	7.31E-14	PPLLLL
8634-01I	2122055b	2	338.6025	5.30291	0.02155	0.0016481	1.761322	0.0903327	0.0161489	0.0023593	59.55507	0.8335405	53.32032	0.9158733	89.42336	0.8587805	3.64E-16	2.17E-14	PPLLLL
8634-01J	2122055b	2.5	338.4689	10.01307	0.0116276	0.0030087	1.172787	0.1719595	0.0092631	0.0045056	56.63695	1.562016	53.29724	1.729243	94.02838	1.670065	1.82E-16	1.03E-14	PPLLLL
8634-02A	2122055b	0.1	1786.792	53.7817	0.4454126	0.0220734	-0.3388473	0.2463841	0.0855211	0.0092084	570.1898	26.57163	437.077	20.72896	76.67273	0.4388086	1.01E-16	5.78E-14	PPLLLL
8634-02B	2122055b	0.2	423.0065	3.120882	0.0292912	0.0004887	0.0443781	0.0131125	0.0172232	0.0005209	76.98479	0.533567	68.24424	0.564829	88.6446	0.2038313	2.32E-15	1.79E-13	PPLLLL
8634-02C	2122055b	0.3	324.3863	1.750074	0.0037242	0.0001542	0.0360567	0.0051296	0.0121946	0.0003031	51.98343	0.2922189	50.87466	0.2998853	97.86616	0.1394094	5.78E-15	3.01E-13	PPLLLL
8634-02D	2122055b	0.4	321.0819	1.83649	0.0037395	0.0001483	0.0562266	0.0072582	0.0126867	0.0002656	51.41998	0.3078632	50.30895	0.3141174	97.83704	0.140745	5.23E-15	2.69E-13	PPLLLL
8634-02E	2122055b	0.5	325.3853	2.084935	0.005197	0.0002416	0.0744403	0.0069904	0.0137101	0.0003931	52.58994	0.3478502	51.0459	0.3574635	97.0605	0.1918394	4.22E-15	2.22E-13	PPLLLL
8634-02F	2122055b	0.7	324.7672	1.69234	0.0052265	0.0001725	0.0595609	0.0058453	0.0130345	0.0002621	52.49454	0.2781717	50.93994	0.2900536	97.03605	0.153381	5.62E-15	2.95E-13	PPLLLL
8634-02G	2122055b	1	319.6053	1.791532	0.0027091	0.0001609	0.0302396	0.0056415	0.0123119	0.0003955	50.86282	0.3000209	50.0565	0.306177	98.41423	0.1303204	4.65E-15	2.36E-13	PPLLLL
8634-02H	2122055b	1.5	319.9834	1.688149	0.0048766	0.0001488	0.0482945	0.0043724	0.0134175	0.0002952	51.5725	0.2788213	50.12112	0.288569	97.18402	0.1381257	7.15E-15	3.69E-13	PPLLLL
8634-02I	2122055b	2	326.8084	1.585724	0.005598	0.0001164	0.0455488	0.0046731	0.0133423	0.0001921	52.95702	0.2602284	51.28999	0.2720881	96.85053	0.1185664	1.23E-14	6.51E-13	PPLLLL
8634-02J	2122055b	2.5	330.1948	1.670717	0.0049317	0.0001404	0.0286708	0.0045549	0.0137596	0.0002495	53.34151	0.2769303	51.87158	0.2872103	97.24385	0.1182686	1.00E-14	5.34E-13	PPLLLL
8635-01A	2122054b	0.1	-1041.903	936.2023	0.1100614	0.0972771	0.275268	3.021511	0.1059564	0.1245111	-80.45111	51.52441	-113.3045	75.22506	140.8083	26.08217	-8.25E-18	6.64E-16	PPLLLL
8635-01B	2122054b	0.2	600.584	29.83421	0.0010368	0.0060254	-0.6147527	0.250126	-0.0144509	0.0089346	102.4215	5.704371	102.0178	5.958025	99.64891	1.855352	9.23E-17	9.46E-15	PPLLLL
8635-01C	2122054b	0.3	352.2208	2.13377	0.002997	0.0003768	-0.0541192	0.0164427	0.0132515	0.0005862	56.58306	0.3518402	55.68125	0.3713189	98.41132	0.2529616	1.64E-15	9.29E-14	PPLLLL
8635-01D	2122054b	0.4	349.7857	1.993537	0.0021596	0.00023	0.007023	0.0087674	0.0130203	0.0004314	55.90254	0.3378543	55.25779	0.3464475	98.8476	0.2009879	2.83E-15	1.58E-13	PPLLLL
8635-01E	2122054b	0.5	349.6693	2.302796	0.000179	0.0003565	-0.044449	0.0158572	0.0124744	0.0007156	55.29691	0.3857316	55.23756	0.4001664	99.89718	0.2695158	1.62E-15	8.95E-14	PPLLLL
8635-01F	2122054b	0.7	351.8446	2.666609	0.0008722	0.0003793	-0.0224714	0.0173657	0.013319	0.0007093	55.87953	0.4502879	55.6158	0.4639469	99.53102	0.3061273	1.53E-15	8.53E-14	PPLLLL
8635-01G	2122054b	1	345.5888	2.414943	0.0012978	0.000361	0.014661	0.0155252	0.0130437	0.0006761	54.91585	0.404632	54.52928	0.4187066	99.29653	0.2891747	1.57E-15	8.62E-14	PPLLLL
8635-01H	2122054b	1.5	351.8818	2.089629	0.0026951	0.0002421	0.0182099	0.0120102	0.0121148	0.0005148	56.42572	0.3546359	55.62227	0.3635692	98.57627	0.1931835	2.35E-15	1.33E-13	PPLLLL
8635-01I	2122054b	2	349.7593	2.080965	0.0035187	0.0002019	0.0095959	0.0099502	0.0134018	0.0004082	56.30339	0.3543618	55.2532	0.361636	98.13551	0.1834958	2.84E-15	1.60E-13	PPLLLL
8635-01J	2122054b	2.5	353.2898	2.172917	0.0029074	0.000217	0.0061756	0.0090179	0.0128743	0.0004188	56.73546	0.3714917	55.86733	0.3783553	98.47085	0.175247	3.13E-15	1.78E-13	PPLLLL
8635-02A	2122054b	0.1	909.9499	33.82048	0.0274454	0.0045785	-0.1876183	0.1905223	0.0275233	0.0064061	177.6432	8.283351	169.413	8.017538	95.37981	0.7965126	1.35E-16	2.40E-14	PPLLLL
8635-02B	2122054b	0.2	381.0836	2.078018	0.0029706	0.0001776	0.0331028	0.0077105	0.013052	0.0004017	61.62814	0.3608816	60.74436	0.3674488	98.56499	0.1483153	4.71E-15	2.90E-13	PPLLLL
8635-02C	2122054b	0.3	352.6127	2.046622	0.0022189	0.0001724	0.0380862	0.0061805	0.0140185	0.0003104	56.40824	0.3510641	55.74946	0.3562308	98.83094	0.1466019	4.28E-15	2.41E-13	PPLLLL
8635-02D	2122054b	0.4	347.602	2.318517	0.0026692	0.0002618	0.0672101	0.0116009	0.0138872	0.0005024	55.66842	0.3944	54.87852	0.402437	98.57792	0.2317007	2.46E-15	1.37E-13	PPLLLL
8635-02E	2122054b	0.5	347.2534	2.426067	0.0012188	0.0003802	0.0096151	0.0142525	0.0132368	0.0005862	55.18153	0.4053987	54.81802	0.4210237	99.34204	0.3311438	1.77E-15	9.78E-14	PPLLLL
8635-02F	2122054b	0.7	348.8182	1.834981	0.0016144	0.000221	0.015377	0.0098606	0.0137906	0.0004261	55.57062	0.3099207	55.0897	0.3187219	99.13496	0.229686	2.78E-15	1.54E-13	PPLLLL
8635-02G	2122054b	1	355.1534	2.175999	0.0033747	0.0001975	0.0245471	0.0074992	0.0128136	0.0003829	57.19756	0.3731122	56.192	0.3792836	98.24168	0.1670605	4.34E-15	2.48E-13	PPLLLL
8635-02H	2122054b	1.5	381.872	1.958308	0.0031204	0.000119	0.0268182	0.0053569	0.0132018	0.0002412	61.81301	0.3409857	60.8838	0.3464323	98.49621	0.1028395	8.08E-15	5.00E-13	PPLLLL
8635-02I	2122054b	2	403.1375	2.074494	0.0028088	0.0001354	0.0382421	0.0052788	0.0131031	0.0002617	65.50274	0.3660202	64.668	0.3713375	98.72424	0.1216231	8.76E-15	5.74E-13	PPLLLL
8635-02J	2122054b	2.5	408.4895	2.095467	0.0022672	0.0001624	0.0221394	0.0069764	0.0125807	0.0003586	66.30249	0.3705657	65.62745	0.376206	98.98158	0.1341117	6.75E-15	4.48E-13	PPLLLL
8641-01A	2152166	0.1	212.9382	7.35787	0.0046912	0.0026067	0.13967	0.1030517	0.0157876	0.0043152	33.74259	0.928648	32.3553	1.185283	95.88166	2.407488	2.27E-16	7.67E-15	PPLLLL
8641-01B	2152166	0.2	291.9451	3.506522	0.059254	0.0009736	0.0821808	0.0185346	0.024268	0.0008126	63.04808	0.504619	45.36537	0.5901546	71.95045	0.4438833	1.38E-15	8.71E-14	PPLLLL
8641-01C	2152166	0.3	365.3998	2.417211	0.0150962	0.0003299	0.0437525	0.0081938	0.0155022	0.0004546	62.48583	0.4020939	57.98306	0.4237274	92.79232	0.2103609	3.24E-15	2.02E-13	PPLLLL
8641-01D	2152166	0.4	392.1953	1.817513	0.0072395	0.0001638	0.0309709	0.0047408	0.013977	0.0002984	64.87376	0.3087982	62.71527	0.3233703	96.67193	0.1190166	7.03E-15	4.56E-13	PPLLLL
8641-01E	2152166	0.5	401.1807	2.14294	0.0041441	0.0001431	0.0480567	0.0054853	0.013567	0.0002942	65.55012	0.3779489	64.31792	0.3831736	98.11818	0.1285496	6.55E-15	4.29E-13	PPLLLL
8641-01F	2152166	0.6	395.711	2.249147	0.0045434	0.0001744	0.0660912	0.006369	0.0130969	0.0003518	64.69072	0.3955557	63.34138	0.4009467	97.91092	0.1163361	5.97E-15	3.86E-13	PPLLLL
8641-01G	2152166	0.7	395.2919	1.983042	0.0034504	0.0001803	0.0598612	0.0065673	0.0131362	0.0003187	64.29042	0.3460389	63.26668	0.3534272	98.40481	0.118915	6.02E-15	3.87E-13	PPLLLL
8641-01H	2152166	0.9	397.6726	2.798413	0.0026122	0.0002267	0.0836465	0.0077923	0.013351	0.0004321	64.46181	0.4960263	63.69126	0.499405	98.80018	0.173281	3.41E-15	2.20E-13	PPLLLL
8641-01I	2152166	1.2	399.5462	5.427952	0.0010804	0.0009697	0.238398	0.0460577	0.0155695	0.0018912	64.32	0.9284399	64.0258	0.9696791	99.52745	0.5612435	5.17E-16	3.33E-14	PPLLLL
8641-01J	2152166	2.5	408.1093	9.069887	0.0007601	0.0018144	0.1532606	0.0942068	0.0132534	0.0025878	65.76817	1.539368	65.55919	1.628003	99.67293	0.9209675	2.91E-16	1.92E-14	PPLLLL
8641-02A	2152166	0.1	189.716	1.95754	0.0193038	0.0005339	0.1147591	0.024234	0.0155686	0.0008634	34.39151	0.2716824	28.6384	0.3113081	83.26707	0.5088637	1.26E-15	4.34E-14	PPLLLL
8641-02B	2152166	0.2	304.3016	1.746301	0.0080896	0.0001841	0.1098304	0.0073694	0.0139405	0.0003279	49.85612	0.2842229	47.45212	0.2959259	95.17243	0.1660312	5.50E-15	2.74E-13	PPLLLL
8641-02C	2152166	0.3	333.2172	1.459635	0.0032202	0.0000991	0.0314785	0.0035895	0.0131457	0.0001756	53.35026	0.2443127	52.39161	0.2513442	98.20245	0.1275834	1.35E-14	7.19E-13	PPLLLL
8641-02D	2152166	0.4	332.9209	1.913557	0.0031891	0.0001381	0.037991	0.0056839	0.0132192	0.0002577	53.28921	0.3254506	52.34058	0.3294539	98.21874	0.1269216	8.39E-15	4.47E-13	PPLLLL
8641-02E	2152166	0.5	339.6034	1.872466	0.0028256	0.0001488	0.0218078	0.0055466	0.012215	0.000273	54.33526	0.3187079	53.49324	0.3235758	98.45031	0.1817965	6.82E-15	3.71E-13	PPLLLL
8641-02F	2152166	0.6	335.7599	1.899188	0.0028691	0.0002355	0.0327773	0.0102549	0.0128273	0.000376	53.68345	0.3181359	52.82975	0.3274951	98.409	0.210355	2.80E-15	1.50E-13	PPLLLL
8641-02G	2152166	0.7	318.9075	2.615902	0.0036798	0.0004783	0.0111452	0.0199963	0.012432	0.0007479	51.03556	0.4263195	49.93728	0.4468909	97.8488	0.3447787	1.31E-15	6.69E-14	PPLLLL
8641-02H	2152166	0.9	315.3227	3.898834	0.0028589	0.0007809	0.0019714	0.0388119	0.0131178	0.0013983	50.17958	0.6296606	49.32546	0.6647398	98.29934	0.5967536	6.69E-16	3.36E-14	PPLLLL
8641-02I	2152166	1.2	313.9451	3.063099	0.0032111	0.0006238	0.0712106	0.0288014	0.0126087	0.001099	50.04234	0.4920479	49.09067	0.5218509	98.09503	0.4529523	9.17E-16	4.59E-14	PPLLLL
8641-02J	2152166	2.5	329.2243	4.582792	0.0026583	0.0010472	0.0784542	0.0472594	0.0145414	0.0017926	52.49025	0.7307387	51.7048	0.7873968	98.4998	0.6611676	5.35E-16	2.81E-14	PPLLLL
8642-01A	2122055a	0.15	356.6256	2.172835	0.0035098	0.0002201	0.0216841	0.0091636	0.0121308	0.0003572	57.49499	0.3724692	56.44872	0.3790412	98.18016	0.1956846	3.30E-15	1.90E-13	PPLLLL
8642-01B	2122055a	0.2	363.093	1.97476	0.0001753	0.0001405	0.0170837	0.0073128	0.0121389	0.0003981	57.63014	0.3430725	57.57894	0.3457252	99.91139	0.1556937	4.80E-15	2.76E-13	PPLLLL
8642-01C	2122055a	0.25	360.6378	1.896634	0.0008395	0.0001524	0.0239236	0.0067279	0.0128554	0.0003483	57.39804	0.3278635	57.14941	0.3315959	99.5666	0.1606452	4.73E-15	2.72E-13	PPLLLL
8642-01D	2122055a	0.3	364.6743	2.058444	0.0009179	0.0001842	0.0276331	0.0090101	0.0135724	0.0003963	58.12743	0.356076	57.8559	0.3606919	99.53236	0.173658	3.30E-15	1.92E-13	PPLLLL
8642-01E	2122055a	0.35	362.9194	2.142995	0.0010424	0.0003062	0.0148908	0.0154773	0.0118256	0.0005904	57.85894	0.3634619	57.54856	0.3751424	99.46392	0.2349504	1.93E-15	1.11E-13	PPLLLL
8642-01F	2122055a	0.4	364.8808	2.856846	0.0015989	0.0004094	0.0417445	0.0184195	0.0122897	0.0008346	58.36544	0.48671	57.89209	0.5006496	99.18751	0.3025945	1.40E-15	8.17E-14	PPLLLL
8642-01G	2122055a	0.45	364.4005	2.735608	0.0019899	0.0004265	0.0840625	0.0221976	0.0141538	0.0007678	58.3929	0.4631545	57.80794	0.4792756	98.99385	0.2884423	1.41E-15	8.25E-14	PPLLLL
8642-01H	2122055a	0.5	357.1799	2.67229	0.0017989	0.0003624	0.0409744	0.0208517	0.0126146	0.0007375	57.07859	0.4546148	56.54543	0.4663123	99.06451	0.2847683	1.53E-15	8.73E-14	PPLLLL
8642-01I	2122055a	0.6	363.4568	2.047965	0.0008283	0.0002706	0.022407	0.01287	0.012079	0.0005571	57.88818	0.3489695	57.64265	0.3586137	99.57571	0.2114088	2.22E-15	1.28E-13	PPLLLL
8642-01J	2122055a	0.7	364.0818	2.387285	0.0005911	0.0004117	0.0261649	0.0214387	0.0119077	0.0007867	57.9264	0.3996805	57.7521	0.418176	99.69869	0.3108973	1.41E-15	8.19E-14	PPLLLL
8642-01K	2122055a	1	372.8185	5.037562	-0.0009294	0.0009514	0.0946041	0.0519748	0.0131611	0.0016797	58.99831	0.8367596	59.28621	0.8867033	100.4828	0.5611232	5.15E-16	3.04E-14	PPLLLL
8642-01L	2122055a	2.5	366.8371	3.734891	0.0056212	0.0007115	0.1689585	0.0343797	0.0138003	0.0011359	59.89439	0.6289727	58.23512	0.6552332	97.21964	0.4945128	8.39E-16	5.03E-14	PPLLLL
8642-02A	2122055a	0.15	188.1798	36.95177	-0.0042875	0.0146324	-0.6316422	0.629787	0.0244856	0.0254478	27.17439	3.766554	28.3942	5.871447	104.5375	16.52775	3.50E-17	9.52E-16	PPLLLL
8642-02B	2122055a	0.2	306.382	10.46987	0.0087227	0.0030833	0.0598437	0.1569302	0.0097997	0.0050833	50.40382	1.597643	47.80487	1.776258	94.84134	1.925497	1.57E-16	7.94E-15	PPLLLL

8642-02C	2122055a	0.25	360.9039	2.456235	0.0012863	0.0003705	-0.0047333	0.0170055	0.0148981	0.0005972	57.58109	0.415254	57.19593	0.4294965	99.33282	0.2814355	1.72E-15	9.88E-14	PPLLLL
8642-02D	2122055a	0.3	362.4314	2.208286	-0.0003691	0.0002928	0.0091065	0.0135818	0.0139678	0.0006071	57.35251	0.3764995	57.46315	0.3864673	100.1937	0.2603763	1.75E-15	1.00E-13	PPLLLL
8642-02E	2122055a	0.35	364.6588	1.976302	-0.0004678	0.0002992	-0.0410115	0.0135793	0.0131356	0.0005238	57.71902	0.334885	57.8532	0.3462955	100.2367	0.251338	1.96E-15	1.13E-13	PPLLLL
8642-02F	2122055a	0.4	366.2334	2.353369	0.0001476	0.0002271	0.0016461	0.0124768	0.0119903	0.0005719	58.17395	0.4071173	58.12922	0.4127269	99.92437	0.2837582	2.19E-15	1.28E-13	PPLLLL
8642-02G	2122055a	0.45	369.2766	2.199239	-0.0009069	0.0003037	0.0173168	0.0124134	0.0133326	0.0005907	58.39126	0.3757451	58.66338	0.3863471	100.4662	0.2413507	2.04E-15	1.19E-13	PPLLLL
8642-02H	2122055a	0.5	362.8456	2.386727	0.0007075	0.0003941	-0.0356364	0.0168192	0.0130765	0.0007782	57.75176	0.4009234	57.53564	0.4177918	99.62964	0.2898827	1.74E-15	1.00E-13	PPLLLL
8642-02I	2122055a	0.6	371.4065	2.077751	-0.0008363	0.0002672	-0.0235027	0.0113672	0.0123818	0.0006752	58.79164	0.3569995	59.03777	0.3654361	100.4217	0.2171024	2.08E-15	1.23E-13	PPLLLL
8642-02J	2122055a	0.7	368.803	2.228586	0.0006321	0.0002805	-0.0140865	0.0138245	0.0133435	0.000554	58.77128	0.3822104	58.58019	0.3913998	99.6772	0.2238791	2.04E-15	1.20E-13	PPLLLL
8642-02K	2122055a	1	369.7165	2.230536	0.0005017	0.0002986	0.0269953	0.0145292	0.0130103	0.0006491	58.88805	0.3815312	58.74067	0.3919408	99.74924	0.2600329	1.87E-15	1.10E-13	PPLLLL
8642-02L	2122055a	2.5	367.9122	2.257331	-0.0004179	0.0001403	-0.0101318	0.0074188	0.0129965	0.0003974	58.30094	0.3940281	58.42378	0.3962526	100.2128	0.1415268	4.30E-15	2.51E-13	PPLLLL
8643-01A	MLRG01	0.1	325.7732	7.660983	0.135531	0.0032275	0.2598181	0.0783366	0.0379556	0.0025117	91.54822	1.553152	51.11241	1.313764	55.8216	0.7793171	3.61E-16	3.31E-14	LPLLLL
8643-01B	MLRG01	0.2	360.6082	2.961704	0.0099942	0.0005216	0.5673623	0.0301365	0.0124654	0.0007572	60.06315	0.5005809	57.14423	0.5177978	95.10422	0.3257643	1.12E-15	6.74E-14	PPLLLL
8643-01C	MLRG01	0.3	358.5184	2.130792	0.0051601	0.0003013	0.2833413	0.0149863	0.0125102	0.0005508	58.28771	0.3582627	56.77909	0.3720973	97.39404	0.2708409	2.12E-15	1.24E-13	PPLLLL
8643-01D	MLRG01	0.4	350.9328	2.000486	0.0053581	0.0001861	0.057201	0.0051898	0.0125083	0.0003002	57.05122	0.3404414	55.4572	0.3478764	97.20352	0.1288848	6.15E-15	3.51E-13	PPLLLL
8643-01E	MLRG01	0.5	356.9177	1.682025	0.0048228	0.0001519	0.0496634	0.0073118	0.0132576	0.0002939	57.93463	0.2833415	56.49967	0.2934692	97.52115	0.1256966	6.13E-15	3.55E-13	PPLLLL
8643-01F	MLRG01	0.6	354.7413	2.178185	0.0048473	0.0002531	0.0678005	0.0128605	0.0128751	0.0004616	57.56041	0.3705445	56.12018	0.379578	97.49468	0.2216963	2.68E-15	1.54E-13	PPLLLL
8643-01G	MLRG01	0.7	362.8873	2.186941	0.0052035	0.0003761	0.8792861	0.0218867	0.0139143	0.0005743	58.99481	0.3629276	57.54295	0.3828285	97.48108	0.2952517	1.88E-15	1.11E-13	PPLLLL
8643-01H	MLRG01	0.8	347.1018	3.461586	0.0052384	0.0006283	0.5320156	0.0341505	0.0133034	0.0011591	56.29552	0.5785916	54.79171	0.6006787	97.29433	0.4168694	1.00E-15	5.65E-14	PPLLLL
8643-01I	MLRG01	0.9	180.9296	72.12998	0.0243607	0.0305077	-0.3344535	1.288571	-0.007445	0.0372334	34.55301	8.959023	27.24449	11.41512	78.86844	26.45384	2.01E-17	6.93E-16	PPLLLL
8643-01J	MLRG01	1	359.8095	3.389542	0.0030964	0.0006198	0.2938165	0.0363361	0.012763	0.0010153	57.8958	0.5668146	57.00463	0.5923349	98.44212	0.4010807	8.28E-16	4.79E-14	PPLLLL
8643-01K	MLRG01	1.2	349.8446	4.334923	0.0059869	0.0010184	0.2742366	0.0511882	0.0131853	0.001459	57.02478	0.7036408	55.26802	0.7533708	96.90231	0.6109361	5.48E-16	3.13E-14	PPLLLL
8643-01L	MLRG01	1.6	-958.0386	1346.037	0.4420808	0.4629195	-0.6076056	6.435277	0.409109	0.4497663	25.54957	26.50369	-106.4069	113.3022	-416.6602	164.1998	4.54E-18	1.16E-16	PPLLLL
8643-01M	MLRG01	2	354.9315	3.202365	0.0036103	0.0005925	0.2403725	0.0292338	0.012167	0.0009385	57.20436	0.533294	56.15333	0.5581139	98.14776	0.4404961	1.10E-15	6.29E-14	PPLLLL
8643-01N	MLRG01	2.5	365.825	4.524539	0.0017433	0.0011727	0.1948073	0.0607938	0.0126275	0.0019488	58.55612	0.7157542	58.05761	0.7933205	99.13667	0.6714706	4.67E-16	2.73E-14	PPLLLL
8643-01O	MLRG01	3	345.2406	6.227132	0.002286	0.0017121	0.043763	0.0879181	0.0150274	0.0025388	55.14699	0.9603736	54.46891	1.079462	98.76888	1.017404	3.20E-16	1.77E-14	PPLLLL
8643-02A	MLRG01	0.1	273.5771	14.07382	0.4354416	0.0082415	0.2556581	0.0671484	0.0937257	0.0031598	172.2689	2.933309	42.28968	2.344658	24.54442	0.701082	4.32E-16	7.43E-14	PPLLLL
8643-02B	MLRG01	0.2	340.7996	2.44304	0.0207094	0.000496	0.3899058	0.0245287	0.0156389	0.0007189	59.83951	0.3852896	53.70002	0.4224552	89.71709	0.3162502	1.89E-15	1.13E-13	PPLLLL
8643-02C	MLRG01	0.3	349.41	2.939028	0.0095577	0.0004937	0.5068388	0.0310019	0.0134534	0.0008498	57.98869	0.4957321	55.19249	0.5106537	95.14602	0.3838469	1.30E-15	7.53E-14	PPLLLL
8643-02D	MLRG01	0.4	347.6451	3.776022	0.0115859	0.0006248	0.3933874	0.0352643	0.016613	0.0009671	58.30057	0.6508365	54.886	0.6554392	94.11888	0.4148294	8.69E-16	5.07E-14	PPLLLL
8643-02E	MLRG01	0.5	338.62	3.633785	0.0180116	0.0006582	0.3999703	0.0334454	0.0171225	0.0011004	58.65612	0.6273259	53.32335	0.6276024	90.88454	0.4090557	8.67E-16	5.09E-14	PPLLLL
8643-02F	MLRG01	0.6	346.8848	3.060475	0.016774	0.0005814	0.1855092	0.0265759	0.0152028	0.0009069	59.7417	0.5157368	54.75406	0.5310113	91.64083	0.331099	1.19E-15	7.08E-14	PPLLLL
8643-02G	MLRG01	0.7	341.1943	2.567496	0.0176442	0.0004776	0.0682549	0.0174116	0.0164852	0.0006184	59.02907	0.4200425	53.76827	0.4440734	91.08474	0.3038539	1.76E-15	1.04E-13	PPLLLL
8643-02H	MLRG01	0.8	343.1001	1.9712	0.0144538	0.0003853	0.0529431	0.0140938	0.0151474	0.0005084	58.40815	0.3032387	54.09808	0.3412987	92.61866	0.2303376	2.51E-15	1.46E-13	PPLLLL
8643-02I	MLRG01	0.9	346.1977	2.054334	0.0111736	0.0002499	0.0726046	0.0078059	0.014587	0.000337	57.96333	0.3405348	54.63486	0.3563039	94.25423	0.174485	4.92E-15	2.85E-13	PPLLLL
8643-02J	MLRG01	1	343.8058	1.811892	0.010892	0.0001913	0.052213	0.0061053	0.0141607	0.0003193	57.46708	0.2948751	54.22029	0.3138384	94.3481	0.1564646	6.62E-15	3.81E-13	PPLLLL
8643-02K	MLRG01	1.2	346.8354	2.081223	0.0110032	0.0002443	0.3543221	0.0088156	0.0140402	0.0002892	57.99086	0.3465724	54.74549	0.3610952	94.38186	0.1783265	6.23E-15	3.61E-13	PPLLLL
8643-02L	MLRG01	1.6	346.2823	2.983217	0.013001	0.0006131	0.2250793	0.0250632	0.017234	0.0009169	58.50589	0.4934671	54.64954	0.5174337	93.39538	0.3692573	1.31E-15	7.68E-14	PPLLLL
8643-02M	MLRG01	2	347.1208	3.151754	0.0093765	0.000609	0.411448	0.0315522	0.0140809	0.001009	57.54811	0.5258659	54.795	0.5469204	95.19025	0.3806764	1.03E-15	5.95E-14	PPLLLL
8643-02N	MLRG01	2.5	350.2065	5.791831	0.0061365	0.0012559	-0.0153898	0.0686668	0.0176243	0.002445	57.16518	0.9597627	55.33093	1.00677	96.79371	0.7314043	4.23E-16	2.42E-14	PPLLLL
8643-02O	MLRG01	3	338.9521	2.132888	0.0083038	0.0002712	0.110027	0.0097418	0.0140628	0.0004407	55.84818	0.3566107	53.3807	0.3684456	95.57591	0.1944077	3.73E-15	2.08E-13	PPLLLL
8644-01A	2152164b	0.1	1993.229	53.08997	1.990495	0.078722	0.8892845	0.2403658	0.3857318	0.0182714	1115.269	43.41685	521.3744	22.94303	46.72007	0.4335409	1.45E-16	1.61E-13	PPLLLL
8644-01B	2152164b	0.2	875.4604	13.74658	0.2707783	0.0054357	0.8079287	0.069011	0.0744254	0.0029366	242.0057	3.91999	161.3145	3.197078	66.62035	0.4378029	4.72E-16	1.14E-13	PPLLLL
8644-01C	2152164b	0.3	590.2537	5.404136	0.026651	0.0008881	0.3949517	0.0377083	0.0189927	0.0011821	107.8607	1.078706	99.96071	1.073068	92.65117	0.3272973	9.11E-16	9.83E-14	PPLLLL
8644-01D	2152164b	0.4	589.0265	4.185499	0.0125939	0.0004981	0.2568112	0.0208152	0.0160709	0.0007056	103.4404	0.8242863	99.71711	0.8305251	96.38419	0.2021132	1.62E-15	1.68E-13	PPLLLL
8644-01E	2152164b	0.5	570.6516	6.313937	0.0143947	0.0008697	0.3553981	0.0417749	0.0172134	0.0013577	100.3369	1.248958	96.08949	1.240173	95.74412	0.3263547	6.97E-16	6.99E-14	PPLLLL
8644-01F	2152164b	0.7	756.2783	6.89014	0.0426939	0.0009499	0.8395526	0.0338684	0.0238582	0.0010927	147.0965	1.544835	134.4918	1.500016	91.37847	0.2541156	9.74E-16	1.43E-13	PPLLLL
8644-01G	2152164b	1	918.8801	11.74197	0.0656829	0.0017202	1.654102	0.0792916	0.0301886	0.0022626	190.8228	2.996265	171.5353	2.797382	89.79008	0.2859069	4.49E-16	8.57E-14	PPLLLL
8644-01H	2152164b	1.5	914.4211	17.85721	0.0740084	0.0028207	1.967647	0.1324775	0.0334747	0.0037506	192.1875	4.660299	170.4743	4.243763	88.58184	0.4120915	2.64E-16	5.07E-14	PPLLLL
8644-01I	2152164b	2	924.3692	10.45122	0.0513055	0.0014456	1.286261	0.0483927	0.0267137	0.0017132	187.9107	2.617541	172.845	2.497465	91.90114	0.2710576	6.39E-16	1.20E-13	PPLLLL
8644-01J	2152164b	2.5	790.0015	20.07644	0.0475034	0.0027399	1.345708	0.1248234	0.0279258	0.0045693	155.85	4.796602	141.9025	4.453207	90.9665	0.5550048	2.22E-16	3.46E-14	PPLLLL
8644-02A	2152164b	0.1	1104.684	18.42373	0.0221648	0.0020896	-0.1124027	0.0982229	0.0186467	0.0027179	224.8043	4.958073	218.1606	4.865384	97.05257	0.4392147	3.08E-16	6.93E-14	PPLLLL
8644-02B	2152164b	0.2	416.0473	3.016776	0.0017714	0.0003933	-0.0163263	0.0229681	0.0102718	0.0006964	67.51911	0.5320984	66.98717	0.5438854	99.21446	0.2418504	1.43E-15	9.68E-14	PPLLLL
8644-02C	2152164b	0.3	376.8214	3.273515	0.0013151	0.0004711	-0.0064566	0.0260024	0.0104528	0.0007933	60.38602	0.5617264	59.99158	0.5774785	99.34857	0.3192366	1.16E-15	7.00E-14	PPLLLL
8644-02D	2152164b	0.4	372.9977	3.215253	0.0015076	0.0004746	-0.023878	0.0221053	0.0126482	0.0007391	59.7715	0.5497363	59.31776	0.5659989	99.24386	0.3615013	1.24E-15	7.43E-14	PPLLLL
8644-02E	2152164b	0.5	381.8713	3.072851	0.0024511	0.0004438	0.0802455	0.0247993	0.0120117	0.0007143	61.60683	0.5292996	60.88367	0.543599	98.82199	0.3213594	1.26E-15	7.74E-14	PPLLLL
8644-02F	2152164b	0.7	401.357	2.83422	0.0018386	0.0003972	0.0408488	0.0166018	0.0122441	0.0006158	64.8943	0.4935018	64.34946	0.5068291	99.15886	0.2625644	1.60E-15	1.04E-13	PPLLLL
8644-02G	2152164b	1	425.8836	3.261806	0.0007028	0.0003752	0.0344292	0.0190758	0.0123329	0.0007087	68.97175	0.5811291	68.76536	0.5912761	99.69957	0.2447052	1.31E-15	9.06E-14	PPLLLL
8644-02H	2152164b	1.5	428.4966	3.198237	0.0016519	0.0004411	0.064753	0.0204063	0.0118656	0.0007641	69.72539	0.5665683	69.23938	0.5805932	99.29968	0.2544466	1.39E-15	9.71E-14	PPLLLL
8644-02I	2152164b	2	434.6505	4.246928	0.000608	0.0007589	-0.012062	0.0294819	0.0130896	0.0010732	70.54222	0.7406599	70.35843	0.773602	99.74144	0.3981556	8.08E-16	5.70E-14	PPLLLL
8644-02J	2152164b	2.5	429.3098	4.666793	-0.0009927	0.0008679	-0.2137379	0.0440168	0.0090143	0.0014344	69.11847	0.8052449	69.38704	0.8475701	100.4046	0.4923834	5.86E-16	4.05E-14	PPLLLL
8645-01A	2152164c	0.1	537.5014	13.57549	0.0759574	0.0036338	1.753323	0.1598352	0.0266268	0.0046875	112.0732	2.983842	89.63765	2.617927	79.88505	0.8450389	2.05E-16	2.30E-14	PPLLLL
8645-01B	2152164c	0.2	459.7742	10.72807	0.0857509	0.003499	7.688096	0.2631118	0.0400571	0.0040092	99.58	2.205328	74.96687	1.981584	74.88373	0.9488157	2.20E-16	2.19E-14	PPLLLL
8645-01C	2152164c	0.3	385.2408	9.377025	0.0224826	0.0024296	12.24665	0.3807898	0.0131766	0.0032993	66.73388	1.591428	61.48031	1.661933	91.34906	1.181311	2.36E-16	1.58E-14	PPLLLL
8645-01D	2152164c	0.4	399.8145	11.37388	0.0093488	0.0026526	3.932396	0.1975087	0.0127195	0.0041477	66.39	1.789652	64.07373	2.032194	96.25003	1.269089	2.01E-16	1.34E-14	PPLLLL
8645-01E	2152164c	0.5	406.6075	18.14143	0.023206	0.0052	1.86483	0.2664118	0.0078987	0.0083701	71.99268	3.151128	65.28974	3.253594	90.57357	2.195714	1.07E-16	7.68E-15	PPLLLL
8645-01F	2152164c	0.7	598.3235	15.30707	0.0445729	0.0034995	2.984268	0.2128255	0.018705	0.0050581	114.437	3.215209	101.5667	3.053063	88.57098	0.9153966	1.70E-16	1.95E-14	PPLLLL
8645-01G	2152164c	1	861.2674	31.23816	0.0587768	0.0059351	3.83139	0.3339504	0.0247786	0.0065282	174.8633	7.727464	158.0266	7.208209	90.13268	0.9747344	1.15E-16	2.02E-14	PPLLLL
8645-01H	2152164c	1.5	1048.813	33.98474	0.0633105	0.0054711	4.654953	0.352346	0.0301946	0.0078279	221.522	9.275548	203.6321	8.701087	91.62873	0.6902728	1.13E-16	2.50E-14	PPLLLL
8645-01I	2152164c	2	1026.938	39.03603	0.0430475	0.0058968	4.17708	0.3601395	0.0212086	0.0069531	210.0261	10.27696	198.0653	9.873915	94.03327	0.8125232	1.12E-16	2.34E-14	LPLLLL

8645-01J	2152164c	2.5	1051.096	120.1735	0.0462923	0.0185025	4.611647	1.28207	-0.0394397	0.029111	217.0408	32.16867	204.217	30.80689	93.79203	2.482532	2.81E-17	6.10E-15	PPLLLL
8645-02A	2152164c	0.1	506.3787	14.23741	0.1246787	0.004995	10.95395	0.4088767	0.036146	0.0049837	119.4382	3.314489	83.68734	2.698614	69.5376	0.9355663	1.68E-16	2.01E-14	PPLLLL
8645-02B	2152164c	0.2	298.0749	6.407546	0.0732279	0.0022057	21.1751	0.4452595	0.0295955	0.0027244	65.95836	1.113616	46.39877	1.082073	69.31709	0.9057872	3.22E-16	2.13E-14	PPLLLL
8645-02C	2152164c	0.3	411.5939	6.561658	0.0150839	0.0013855	1.838391	0.0965551	0.013315	0.0023418	70.46459	1.16047	66.18526	1.180065	93.80874	0.6319356	3.59E-16	2.53E-14	PPLLLL
8645-02D	2152164c	0.4	422.2065	8.788732	0.0094857	0.0019925	0.977353	0.1125057	0.0178421	0.0035216	70.81096	1.525001	68.09949	1.589913	96.10697	0.9112856	2.63E-16	1.86E-14	PPLLLL
8645-02E	2152164c	0.5	490.7724	17.14466	0.0192698	0.0040697	1.328216	0.2138347	0.0270123	0.0067157	86.3188	3.183483	80.74202	3.221675	93.45436	1.441207	1.34E-16	1.16E-14	PPLLLL
8645-02F	2152164c	0.7	566.0584	13.66253	0.0364637	0.0028093	1.725128	0.1540598	0.0279407	0.0040197	105.8291	2.810523	95.18845	2.67675	89.83895	0.7981332	2.15E-16	2.28E-14	PPLLLL
8645-02G	2152164c	1	604.6121	13.03259	0.0420283	0.002788	1.799981	0.1440616	0.0169519	0.004416	115.1063	2.744586	102.8231	2.608484	89.2184	0.7328148	2.43E-16	2.79E-14	PPLLLL
8645-02H	2152164c	1.5	676.4298	12.9072	0.0541965	0.0026862	1.927276	0.1254803	0.0220659	0.0035256	133.3649	2.879258	117.4875	2.688302	87.97797	0.5799313	2.54E-16	3.39E-14	PPLLLL
8645-02I	2152164c	2	808.1696	73.91772	0.0348369	0.0124941	2.738311	0.7107526	0.0219481	0.0214172	155.8679	17.23333	145.9528	16.56183	93.46209	2.368296	4.42E-17	6.88E-15	PPLLLL
8645-02J	2152164c	2.5	1185.542	557.0271	-0.0935764	0.0829375	1.816143	3.198522	0.0721361	0.1215678	211.6131	134.6249	239.9995	153.844	113.2724	8.326726	8.36E-18	1.77E-15	PPLLLL
8646-01A	2122054a	0.15	394.5553	2.178774	0.0021952	0.0001672	0.0401838	0.0077267	0.0125768	0.0003603	63.78684	0.3832119	63.13544	0.3881529	98.97729	0.164838	3.56E-15	2.27E-13	PPLLLL
8646-01B	2122054a	0.2	399.8711	2.817645	0.0011724	0.0002918	0.0336483	0.014703	0.0136802	0.0005363	64.43049	0.496154	64.08384	0.5034502	99.46092	0.2226448	1.76E-15	1.14E-13	PPLLLL
8646-01C	2122054a	0.25	391.887	2.911411	0.0249038	0.0005695	0.0569675	0.0169945	0.0175558	0.0006916	70.08959	0.476998	62.66041	0.517907	89.39797	0.2884793	1.44E-15	1.01E-13	PPLLLL
8646-01D	2122054a	0.3	400.9922	3.139861	0.0009229	0.0004289	0.0323478	0.0226952	0.011182	0.0008207	64.55681	0.5471826	64.28422	0.5613717	99.57678	0.2622883	1.27E-15	8.18E-14	PPLLLL
8646-01E	2122054a	0.35	399.7889	3.789479	0.0007776	0.0006346	0.1063655	0.0371322	0.0094768	0.0013135	64.28957	0.6509534	64.06915	0.6770643	99.65107	0.4267064	7.59E-16	4.88E-14	PPLLLL
8646-01F	2122054a	0.4	402.491	5.258229	-0.0004977	0.0012532	0.0683013	0.068492	0.009564	0.0021738	64.39651	0.8616973	64.5523	0.9408934	100.2384	0.6315393	3.96E-16	2.55E-14	PPLLLL
8646-01G	2122054a	0.45	413.8203	12.06355	0.0034354	0.0029557	0.2475704	0.1542828	0.0092702	0.004569	67.58244	2.012091	66.58592	2.172218	98.5098	1.390657	1.63E-16	1.10E-14	PPLLLL
8646-01H	2122054a	0.5	392.2217	21.62163	0.0033131	0.0060943	-0.1832588	0.2987451	-0.0036681	0.0098369	63.73378	3.443548	62.71996	3.846957	98.42302	2.915537	8.37E-17	5.33E-15	PPLLLL
8646-01I	2122054a	0.6	339.5126	20.81556	0.0162343	0.0068435	0.6271464	0.3180891	-0.0092131	0.0117849	58.25666	3.226658	53.47754	3.596899	91.75793	3.563384	7.28E-17	4.24E-15	LPLLLL
8646-01J	2122054a	0.8	370.2405	17.51618	0.0122977	0.0051284	0.5662264	0.2410699	0.0191658	0.009002	62.43822	2.831504	58.83276	3.078767	94.18991	2.532887	9.37E-17	5.85E-15	PPLLLL
8646-01K	2122054a	1	372.2075	19.64307	0.0146194	0.0057485	1.079621	0.2759108	0.0200358	0.0106658	63.41672	3.212285	59.17868	3.456369	93.24873	2.783212	8.11E-17	5.14E-15	PPLLLL
8646-01L	2122054a	2.5	394.0454	12.92031	0.0024981	0.0033808	0.8499713	0.1739269	-0.0027779	0.0059166	63.69071	2.086159	63.04459	2.301127	98.92867	1.682555	1.41E-16	8.98E-15	PPLLLL
8646-02A	2122054a	0.15	399.4648	2.375491	0.0025918	0.0001585	0.0028561	0.0065888	0.0132146	0.0003505	64.7855	0.4205964	64.01125	0.4243517	98.80595	0.1302405	4.34E-15	2.81E-13	PPLLLL
8646-02B	2122054a	0.2	407.5622	2.051579	0.000944	0.0001361	0.0189994	0.0060843	0.0127161	0.0002734	65.74132	0.3648677	65.461	0.3681374	99.57352	0.1098253	5.54E-15	3.64E-13	PPLLLL
8646-02C	2122054a	0.25	407.7243	2.637736	0.0009002	0.0001719	0.0177857	0.0083028	0.0134652	0.0004343	65.7574	0.4705362	65.4901	0.4733607	99.59351	0.1794239	3.83E-15	2.52E-13	PPLLLL
8646-02D	2122054a	0.3	405.3448	2.436602	0.0005489	0.0002385	0.0123022	0.010926	0.012549	0.0004702	65.22654	0.4306342	65.06335	0.4366893	99.7502	0.1996152	2.57E-15	1.68E-13	PPLLLL
8646-02E	2122054a	0.35	406.5011	2.193577	0.0003953	0.0002568	0.0032401	0.0147213	0.0131566	0.000624	65.389	0.3855009	65.27066	0.3933862	99.82002	0.1923927	2.28E-15	1.49E-13	PPLLLL
8646-02F	2122054a	0.4	407.641	2.592522	0.0007811	0.0002877	0.0105656	0.0154073	0.0127448	0.0004498	65.70786	0.457093	65.47515	0.4652252	99.64635	0.2251164	1.99E-15	1.31E-13	PPLLLL
8646-02G	2122054a	0.45	405.8531	2.331626	0.0007075	0.0002976	-0.0181859	0.0175445	0.0123131	0.0005272	65.36874	0.4080137	65.15448	0.4179932	99.67472	0.1995327	1.98E-15	1.30E-13	PPLLLL
8646-02H	2122054a	0.5	406.7272	2.673879	0.0010121	0.0004111	0.009246	0.0188404	0.0138339	0.0007097	65.61292	0.4634998	65.3112	0.4795816	99.54076	0.2605932	1.59E-15	1.04E-13	PPLLLL
8646-02I	2122054a	0.6	409.1629	2.512124	0.0005179	0.0003461	0.0361844	0.0179319	0.0145567	0.0009731	65.89914	0.4389929	65.74836	0.4511782	99.76993	0.2168672	1.89E-15	1.25E-13	PPPLLL
8646-02J	2122054a	0.8	405.2115	2.86939	0.0015167	0.0004256	0.061709	0.0224782	0.0088997	0.0009915	65.486	0.4985231	65.03947	0.5142158	99.31512	0.2880176	1.30E-15	8.53E-14	PPLLLL
8646-02K	2122054a	1	400.6941	7.475172	0.0074124	0.0016566	0.4115421	0.0910595	0.0137175	0.0029698	66.39493	1.276488	64.23093	1.336256	96.71438	0.8112363	3.29E-16	2.18E-14	PPLLLL
8646-02L	2122054a	2.5	412.394	4.877475	0.0016288	0.0009121	0.458241	0.0548303	0.0113559	0.0015213	66.76028	0.8373464	66.32919	0.8775663	99.32401	0.5176387	5.83E-16	3.89E-14	PPLLLL
8763-02A	MLLJ06	0.1	420.2422	0.9785194	0.0010183	0.0001157	0.0108025	0.0118573	0.0121312	0.0001657	69.33145	0.176184	69.0279	0.1801754	99.5626	0.0784061	2.99E-14	2.07E-12	PPLLLL
8763-02B	MLLJ06	0.2	491.5374	1.045447	0.0012083	0.0001114	0.0480645	0.0109494	0.0114105	0.0001606	82.77366	0.1965347	82.41838	0.2002584	99.56845	0.0688116	3.06E-14	2.53E-12	PPLLLL
8763-02C	MLLJ06	0.3	457.1	1.482897	0.0021563	0.0002196	0.0221716	0.0235412	0.0106046	0.0002422	76.52637	0.2708994	75.88436	0.2786825	99.16059	0.1282612	1.44E-14	1.10E-12	PPLLLL
8763-02D	MLLJ06	0.4	436.5912	2.254114	0.0037108	0.0006867	0.0704737	0.0645823	0.0120431	0.0007296	73.15187	0.3679349	72.05195	0.4188298	98.49267	0.2975834	4.95E-15	3.62E-13	PPLLLL
8763-02E	MLLJ06	0.5	379.5084	8.601973	0.0206682	0.004015	0.5167322	0.3844224	0.0072651	0.0037943	67.72261	1.072839	61.61161	1.548525	90.94504	1.785132	8.45E-16	5.72E-14	PPLLLL
8763-02F	MLLJ06	0.7	346.3024	13.75145	0.0213016	0.0070666	0.3494194	0.7489567	0.0060698	0.0068534	62.01021	1.339818	55.68856	2.430385	89.78496	3.414863	4.77E-16	2.96E-14	PPLLLL
8763-02G	MLLJ06	1	33.74469	58.86611	0.1576454	0.0320679	-1.012832	2.923201	0.0533868	0.0298554	52.11579	4.436362	4.968608	8.74883	9.540606	16.76801	1.06E-16	5.54E-15	PPLLLL
8763-02H	MLLJ06	1.5	-147.2886	166.0861	0.2372728	0.0867374	-5.595403	7.375496	0.0663134	0.0718097	50.55826	9.825588	-20.63112	22.32738	-40.96506	43.63941	4.35E-17	2.20E-15	PPLLLL
8763-02I	MLLJ06	2	318.7908	150.8449	-0.0219297	0.0797668	6.62418	8.006091	0.192485	0.0868999	43.5521	9.288047	50.86313	26.25634	116.2544	54.83156	3.94E-17	1.72E-15	PPLLLL
8763-02J	MLLJ06	3.5	-1766.549	2835.25	0.9157839	0.7659708	34.2973	38.9362	0.9240843	0.7761059	110.2731	86.57869	-164.3126	155.3432	-145.4748	73.01	1.03E-17	1.14E-15	PPLLLL
8764-01A	MLHR02a	0.15	437.8419	1.780975	0.0060072	0.0008005	0.011423	0.0379181	0.0130882	0.0003936	74.07734	0.2273135	72.28442	0.3311467	97.57996	0.3422221	8.53E-15	6.32E-13	PLLLPL
8764-01B	MLHR02a	0.165	440.1806	2.780079	0.0046405	0.000953	-0.0372386	0.0843307	0.0146605	0.0010072	74.11036	0.4374327	72.71955	0.5175864	98.12693	0.408679	3.52E-15	2.61E-13	PPLLLL
8764-01C	MLHR02a	0.185	436.2659	2.323622	0.0054961	0.0005254	-0.0673983	0.0528227	0.0113776	0.0004969	73.64201	0.4076252	71.9915	0.4316669	97.76437	0.2300449	5.59E-15	4.12E-13	PPLLLL
8764-01D	MLHR02a	0.2	441.283	1.948688	0.0037335	0.0004355	0.0234864	0.0436664	0.012999	0.0004706	74.03735	0.3409582	72.92484	0.3630224	98.49684	0.2171095	7.67E-15	5.68E-13	PPLLLL
8764-01E	MLHR02a	0.25	443.6141	1.407559	0.0028118	0.0003075	0.0077208	0.0263106	0.0118039	0.000291	74.19886	0.2456275	73.35939	0.2625541	98.86918	0.157821	1.17E-14	8.64E-13	PPLLLL
8764-01F	MLHR02a	0.3	439.848	2.44061	0.0049892	0.0005739	-0.0653108	0.0640016	0.012255	0.000746	74.15645	0.4261708	72.65763	0.4543014	97.98434	0.2424309	5.20E-15	3.86E-13	PPLLLL
8764-01G	MLHR02a	0.5	443.602	1.955218	0.0030042	0.0005668	-0.0243338	0.0543474	0.011956	0.0005833	74.25809	0.3243989	73.35713	0.3647073	98.78946	0.249904	5.85E-15	4.35E-13	PPLLLL
8764-01H	MLHR02a	1	442.6615	1.7054	0.0019552	0.0003689	-0.0793754	0.0287657	0.012486	0.0004082	73.77643	0.2988771	73.18175	0.317943	99.20048	0.1777223	9.66E-15	7.13E-13	PPLLLL
8764-01I	MLHR02a	2	443.0977	1.692995	0.0020726	0.0003853	0.0748542	0.0345965	0.0135642	0.0004327	73.87303	0.2944827	73.26307	0.3157065	99.17027	0.1903501	8.00E-15	5.91E-13	PPLLLL
8764-01J	MLHR02a	3	440.5484	15.4854	0.0096411	0.0077227	-0.5579047	0.7169355	0.0163022	0.0081507	75.73789	1.800227	72.78803	2.883611	96.14326	3.058554	4.60E-16	3.48E-14	PPLLLL
8764-02A	MLHR02a	0.15	407.8942	1.34344	0.0123852	0.0002474	-0.0257901	0.0269853	0.0144158	0.0002499	70.46376	0.2322458	66.76203	0.2456811	94.7494	0.1369908	1.50E-14	1.06E-12	PPLLLL
8764-02B	MLHR02a	0.165	501.2781	3.877556	0.0067968	0.0010116	-0.2476848	0.1145942	0.0086845	0.0011336	86.35343	0.6959259	84.28929	0.7467784	97.62729	0.419198	3.11E-15	2.68E-13	PPLLLL
8764-02C	MLHR02a	0.185	534.8773	5.377168	0.0045918	0.0013269	-0.332298	0.1431496	0.008062	0.0012692	92.23955	0.9909466	90.8208	1.055056	98.48536	0.5389046	2.57E-15	2.37E-13	PPLLLL
8764-02D	MLHR02a	0.2	549.1031	6.202907	0.0033642	0.0013785	-0.3280506	0.1404369	0.0091559	0.0013447	94.67517	1.166997	93.62307	1.22671	98.91199	0.5982183	2.54E-15	2.40E-13	PPLLLL
8764-02E	MLHR02a	0.25	483.1506	2.01824	0.0007712	0.0004123	-0.1274961	0.0356167	0.010649	0.0004054	81.06378	0.3649793	80.81559	0.3848067	99.70362	0.2324787	9.70E-15	7.86E-13	PPLLLL
8764-02F	MLHR02a	0.3	482.0031	2.170991	0.0002952	0.0003145	-0.0282196	0.0297736	0.0102544	0.0003532	80.68984	0.4030721	80.59688	0.4136678	99.88775	0.201959	1.20E-14	9.67E-13	PPLLLL
8764-02G	MLHR02a	0.5	476.9854	1.779916	0.0005603	0.0002305	-0.0802616	0.0204285	0.0104719	0.0002732	79.82102	0.3313398	79.64211	0.338209	99.78241	0.1672052	1.75E-14	1.40E-12	PPLLLL
8764-02H	MLHR02a	1	490.8926	2.278068	-0.0015831	0.0002615	-0.0671118	0.0286932	0.0104278	0.0003446	81.83223	0.4279218	82.2949	0.4362146	100.5711	0.207595	1.33E-14	1.09E-12	PPLLLL
8764-02I	MLHR02a	2	1014.021	38.43856	-0.0377987	0.0041516	-0.7542958	0.3848175	-0.0099291	0.0040533	187.3799	9.245323	198.5009	9.836331	105.9907	1.297669	9.33E-16	1.75E-13	PPLLLL
8764-02J	MLHR02a	3	62.79696	6.424452	0.0221387	0.0018898	0.7295501	0.1835954	0.0295652	0.0020042	15.86957	0.8544901	9.321383	0.9703188	58.71083	6.604813	1.96E-15	3.11E-14	PPLLLL
8766-01A	MLPD02	0.07	380.5381	2.181984	0.0068168	0.0007536	-0.1863778	0.0705016	0.0139747	0.0006937	63.85528	0.3276829	61.79703	0.3930245	96.79038	0.3716852	5.22E-15	3.33E-13	PPLLLL
8766-01B	MLPD02	0.1	458.151	2.004595	0.0005633	0.0005454	0.0183149	0.0618498	0.0116365	0.0006465	76.24865	0.3401479	76.08193	0.3769454	99.78115	0.2305723	5.89E-15	4.49E-13	PPLLLL
8766-01C	MLPD02	0.15	464.1542	1.426422	0.0016738	0.0002501	-0.0396011	0.026428	0.0115621	0.0002817	77.71849	0.2583681	77.21265	0.2691193	99.3529	0.1382047	1.47E-14	1.14E-12	PPLLLL
8766-01D	MLPD02	0.2	470.2115	1.161057	-0.0001093	0.0001373	0.0260944	0.0121256	0.0122634	0.00018	78.32216	0.215974	78.35739	0.2197904	100.0442	0.0823716	2.85E-14	2.23E-12	PPLLLL

8766-01E	MLPD02	0.25	469.3486	1.113347	0.0010629	0.0001198	0.0341768	0.0116129	0.0115486	0.0001683	78.50788	0.2070129	78.19408	0.2106579	99.59897	0.0681344	3.05E-14	2.39E-12	PPLLLL
8766-01F	MLPD02	0.3	467.9617	1.15492	0.0010929	0.0001333	0.0439731	0.0133011	0.0113125	0.0001876	78.25328	0.2141734	77.93176	0.2183561	99.58715	0.0761405	2.74E-14	2.14E-12	PPLLLL
8766-01G	MLPD02	0.4	465.8784	1.433572	0.0007958	0.0001926	0.088977	0.0195168	0.0112706	0.0002851	77.7651	0.2644723	77.53812	0.2707269	99.70303	0.1198068	1.71E-14	1.33E-12	PPLLLL
8766-01H	MLPD02	0.7	469.1184	1.555414	0.0013778	0.0002578	0.0628089	0.029576	0.0112622	0.0003223	78.55466	0.2840712	78.15053	0.2942645	99.48225	0.1391007	1.30E-14	1.02E-12	PPLLLL
8766-01I	MLPD02	1.5	470.6602	2.143857	0.0018351	0.000408	0.1633604	0.0410604	0.0119778	0.0005087	78.96972	0.388408	78.44234	0.4059372	99.32198	0.1833323	8.28E-15	6.54E-13	PPLLLL
8766-01J	MLPD02	3	-2643.699	5033.322	0.9183204	0.6633943	116.1185	81.71097	-0.8580038	0.6227642	79.26317	52.48812	-202.3723	169.5899	-234.8331	102.0496	1.35E-17	1.07E-15	PPLLLL
8766-02A	MLPD02	0.07	337.3131	2.521323	0.0087804	0.0008801	-0.0865026	0.0866319	0.0164141	0.0010512	56.73561	0.3691221	54.10377	0.4433952	95.36829	0.4768671	3.99E-15	2.27E-13	PPLLLL
8766-02B	MLPD02	0.1	429.3465	1.980834	0.0003836	0.0006072	-0.1631531	0.0582011	0.0146826	0.0006235	70.84409	0.3188095	70.70854	0.3665774	99.82106	0.2735819	5.93E-15	4.20E-13	PPLLLL
8766-02C	MLPD02	0.15	459.1991	1.410937	-0.000254	0.0002762	-0.0678047	0.0204299	0.0120757	0.000271	76.21285	0.2523567	76.27907	0.2654677	100.0926	0.1317998	1.56E-14	1.19E-12	PPLLLL
8766-02D	MLPD02	0.2	465.6001	1.272861	0.00152	0.0001421	0.0140438	0.0128497	0.0120096	0.0001872	77.93843	0.2361593	77.48557	0.2403398	99.41901	0.0755954	2.67E-14	2.08E-12	PPLLLL
8766-02E	MLPD02	0.25	468.6776	1.104178	0.0010234	0.0000982	0.0229612	0.0080337	0.0117699	0.0001482	78.37062	0.2062063	78.06716	0.2088454	99.61223	0.0679268	4.09E-14	3.21E-12	PPLLLL
8766-02F	MLPD02	0.3	468.0897	1.108122	0.0003286	0.0001116	0.0129604	0.0055101	0.0116968	0.0001088	78.05329	0.2066779	77.95597	0.209523	99.87546	0.0691692	6.19E-14	4.83E-12	PPLLPL
8766-02G	MLPD02	0.4	470.3031	1.032184	0.0007244	0.0000607	0.0294944	0.004987	0.0120284	0.0001026	78.58801	0.1940628	78.37474	0.1954044	99.72762	0.0596363	7.39E-14	5.81E-12	PPLLLL
8766-02H	MLPD02	0.7	472.7728	0.8989919	0.0007072	0.0000698	0.0227999	0.0067373	0.0118236	0.0001398	79.05165	0.1684296	78.8426	0.1704227	99.735	0.0617668	5.68E-14	4.49E-12	PPLLLL
8766-02I	MLPD02	1.5	473.2253	1.525019	0.0014789	0.0002284	0.0378455	0.0209089	0.0127466	0.0002621	79.36576	0.2810559	78.9284	0.2891717	99.44734	0.1165841	1.62E-14	1.28E-12	PPLLLL
8766-02J	MLPD02	3	418.4474	16.01016	0.0229169	0.0072902	0.4637391	0.6943591	0.0152229	0.0061566	75.48306	2.179531	68.69759	2.945028	90.98243	2.91332	5.06E-16	3.82E-14	PPLLLL
8767-01A	MLPD01	0.07	378.0926	80.55902	-0.0859774	0.0432214	3.590697	4.365006	-0.0284585	0.0370424	35.26362	4.143737	61.35683	14.49084	173.567	35.85561	1.01E-18	3.55E-17	PPLLLL
8767-01A*	MLPD01	0.07	334.4374	3.192719	0.0028707	0.0013481	-0.0303378	0.1175961	0.0180126	0.0012332	54.45914	0.3946382	53.59846	0.5605714	98.42311	0.7573134	2.98E-15	1.62E-13	PPLLLL
8767-01B	MLPD01	0.1	477.2906	2.90751	0.000495	0.0009146	0.2471088	0.0865541	0.0119765	0.0008511	79.81619	0.4805483	79.70011	0.5525613	99.83853	0.3629833	3.86E-15	3.08E-13	PPLLLL
8767-01C	MLPD01	0.15	478.6175	1.956033	-0.0008541	0.0004438	0.0876909	0.0417651	0.0108979	0.0003876	79.68679	0.3471249	79.95237	0.3720101	100.3282	0.2110867	9.02E-15	7.19E-13	PPLLLL
8767-01D	MLPD01	0.2	472.0876	1.480018	-0.0001991	0.0002369	0.0118998	0.0190539	0.0119697	0.0002609	78.65258	0.2713798	78.71273	0.2804617	100.0767	0.1280101	1.58E-14	1.25E-12	PPLLLL
8767-01E	MLPD01	0.25	471.9218	1.25898	0.0002564	0.0002793	0.0386656	0.0119411	0.0119003	0.0001626	78.75367	0.2233874	78.68131	0.2385533	99.90647	0.1278717	2.87E-14	2.26E-12	PPLLPL
8767-01F	MLPD01	0.3	467.8348	1.138622	0.0005457	0.0001235	0.0236343	0.0126326	0.0116049	0.0001559	78.06854	0.2117963	77.90777	0.2152596	99.79348	0.0859012	2.82E-14	2.20E-12	PPLLLL
8767-01G	MLPD01	0.4	468.7704	0.9711611	0.0005696	0.0000816	0.0292624	0.0070827	0.0117106	0.0001236	78.25185	0.1816055	78.08469	0.1836959	99.78541	0.0651225	3.98E-14	3.11E-12	PPLLLL
8767-01H	MLPD01	0.7	470.0136	0.9640894	0.0003489	0.0000862	0.027397	0.0079375	0.0120496	0.0001403	78.42136	0.1803655	78.31993	0.182484	99.8698	0.0638823	4.05E-14	3.18E-12	PPLLLL
8767-01I	MLPD01	1.5	467.828	1.904496	0.0020073	0.0005358	0.1236761	0.0481214	0.0128183	0.000547	78.49042	0.3231577	77.90648	0.3600487	99.24858	0.2139485	6.95E-15	5.46E-13	PPLLLL
8767-01J	MLPD01	3	400.7192	231.7993	0.0277686	0.1159392	3.816602	10.27592	0.2925536	0.1458341	73.24308	26.9898	65.4525	42.22195	89.12871	47.24852	3.58E-17	2.62E-15	PPLLLL
8767-02A	MLPD01	0.07	277.7696	2.321818	0.0030009	0.000986	-0.1089627	0.0972949	0.0178275	0.0009721	44.71125	0.266713	43.80347	0.3950543	97.97882	0.6774054	3.67E-15	1.64E-13	PPLLLL
8767-02B	MLPD01	0.1	403.5312	3.528338	0.0065887	0.0012517	0.4892449	0.1274948	0.0197607	0.001225	67.87239	0.5340275	65.96511	0.6436849	97.15821	0.664245	2.70E-15	1.83E-13	PPLLLL
8767-02C	MLPD01	0.15	471.7014	2.132719	0.0021289	0.000477	-0.1389341	0.0541839	0.0127684	0.0005026	79.29417	0.3795768	78.63955	0.4040613	99.18497	0.2021614	6.64E-15	5.27E-13	PPLLLL
8767-02D	MLPD01	0.2	475.1222	1.473827	0.000885	0.000241	-0.0525855	0.020287	0.0114896	0.000267	79.56037	0.2703181	79.28827	0.2797588	99.66264	0.1191541	1.51E-14	1.20E-12	PPLLLL
8767-02E	MLPD01	0.25	472.1289	1.234628	0.0007101	0.0001061	-0.0083082	0.0113613	0.0118015	0.0001666	78.93454	0.2315719	78.72055	0.233966	99.73049	0.0751601	3.07E-14	2.42E-12	PPLLLL
8767-02F	MLPD01	0.3	470.4173	1.217121	0.001019	0.0001171	0.0189044	0.0107788	0.0118529	0.0001887	78.69902	0.2273932	78.39635	0.2304296	99.61514	0.0677097	3.12E-14	2.45E-12	PPLLLL
8767-02G	MLPD01	0.4	468.5076	1.24409	0.0007601	0.0001333	0.0219654	0.0119805	0.0121596	0.0001561	78.25992	0.2316412	78.035	0.2352863	99.71212	0.0942295	2.93E-14	2.29E-12	PPLLLL
8767-02H	MLPD01	0.7	468.4725	1.028525	0.000723	0.000089	0.0067612	0.0095158	0.0120894	0.0001303	78.24418	0.1921758	78.02835	0.1945143	99.72473	0.0738063	3.71E-14	2.90E-12	PPLLLL
8767-02I	MLPD01	1.5	465.7431	2.084703	0.0038677	0.000582	0.0821501	0.0657441	0.0127524	0.0006592	78.65746	0.3551484	77.51256	0.393662	98.53987	0.2430517	5.60E-15	4.41E-13	PPLLLL
8767-02J	MLPD01	3	375.3272	25.57724	0.0682412	0.0132416	-2.361515	1.515481	0.0384733	0.0122122	81.51351	3.306668	60.85978	4.593748	74.78479	4.768288	2.54E-16	2.07E-14	PPLLLL
8769-01A	AOM03	0.07	295.451	1.085202	0.0023149	0.0002758	-0.0226154	0.033487	0.012412	0.0003623	47.52119	0.1673068	46.82672	0.1864643	98.54184	0.1942345	1.16E-14	5.53E-13	PPLLLL
8769-01B	AOM03	0.1	312.5533	1.621868	0.0006749	0.0006261	0.0268977	0.042599	0.0116393	0.0004672	49.97871	0.2104284	49.7793	0.2813309	99.60076	0.3886274	1.00E-14	5.02E-13	PPLLPL
8769-01C	AOM03	0.15	314.1207	1.074189	0.0005922	0.0001699	-0.0143568	0.0235272	0.0125784	0.0002601	50.2305	0.1794575	50.05129	0.1864919	99.64582	0.1599169	1.82E-14	9.14E-13	PPLLLL
8769-01D	AOM03	0.2	313.2726	0.9697074	0.0004483	0.0001727	0.0172166	0.019778	0.0123549	0.0002254	50.03686	0.1600764	49.9041	0.1682736	99.73511	0.1437733	2.10E-14	1.05E-12	PPLLLL
8769-01E	AOM03	0.25	310.554	1.193804	0.0006195	0.000204	-0.0040079	0.0246732	0.0119774	0.000335	49.61895	0.1978335	49.43269	0.2068492	99.6265	0.1583425	1.63E-14	8.10E-13	PPLLLL
8769-01F	AOM03	0.3	305.267	1.414973	0.0017858	0.0003834	-0.0078299	0.0423801	0.0123729	0.0003934	49.05282	0.2168365	48.51795	0.2444534	98.91177	0.2501443	1.01E-14	4.96E-13	PPLLLL
8769-01G	AOM03	0.4	299.6366	1.356765	0.0020193	0.0003953	0.030207	0.0501951	0.0112849	0.0004632	48.14732	0.2023617	47.54675	0.2336669	98.75225	0.2615555	8.55E-15	4.12E-13	PPLLLL
8769-01H	AOM03	0.7	281.833	2.38976	0.0075213	0.0009949	0.0208251	0.114098	0.0125224	0.0009439	46.73991	0.2874172	44.49563	0.4075313	95.19862	0.6658699	3.65E-15	1.71E-13	PPLLLL
8769-01I	AOM03	1.5	265.6791	5.624055	0.0315905	0.0026496	-0.0149567	0.2919402	0.0198037	0.0024906	51.18702	0.6416436	41.75317	0.950534	81.57197	1.547584	1.38E-15	7.08E-14	PPLLLL
8769-01J	AOM03	3	306.0729	21.14892	0.0866091	0.0112124	0.5734161	1.321688	0.017597	0.0111483	74.45419	2.571278	48.65722	3.65536	65.3267	4.351743	3.06E-16	2.28E-14	PPLLLL
8769-02A	AOM03	0.07	292.1822	0.8114459	-0.0000665	0.0002112	-0.0033181	0.0155559	0.0122319	0.0001916	46.2469	0.1240941	46.26557	0.1391739	100.0424	0.163193	2.35E-14	1.09E-12	PPLLLL
8769-02B	AOM03	0.1	316.267	0.7833784	0.0006317	0.0001189	0.0317824	0.0115002	0.0118805	0.0001695	50.61009	0.1310649	50.42414	0.1361657	99.63199	0.1083145	3.10E-14	1.57E-12	PPLLLL
8769-02C	AOM03	0.15	315.7716	0.7077145	0.0005561	0.0000757	0.0121509	0.0074393	0.0117513	0.0001319	50.50361	0.1204518	50.33805	0.1229801	99.67293	0.0823076	5.22E-14	2.63E-12	PPLLLL
8769-02D	AOM03	0.2	313.4525	0.8165273	0.0001725	0.0001644	0.0074997	0.0080912	0.0120349	0.0001235	49.98683	0.1328325	49.93531	0.1417063	99.89802	0.1247636	4.53E-14	2.26E-12	PPLLPL
8769-02E	AOM03	0.225	306.4392	0.9479912	0.0011386	0.0001905	-0.0120578	0.0216518	0.0115677	0.0002688	49.06275	0.153412	48.72054	0.1638832	99.30497	0.1523534	1.84E-14	9.01E-13	PPLLLL
8769-02F	AOM03	0.25	302.8868	1.511426	0.0008027	0.0004478	-0.0265446	0.0498119	0.0115509	0.0005217	48.35051	0.2243041	48.10702	0.2607725	99.4999	0.2955571	8.93E-15	4.32E-13	PPLLLL
8769-02G	AOM03	0.3	299.7353	1.684971	0.001198	0.0005944	0.0900274	0.0662076	0.0105023	0.0005824	47.91265	0.2302344	47.56376	0.2902076	99.26731	0.3903574	6.34E-15	3.04E-13	PPLLLL
8769-02H	AOM03	0.7	288.1539	1.533864	0.004498	0.0005281	-0.0588879	0.0572535	0.0120479	0.0005782	46.92569	0.2121741	45.57544	0.2624916	97.1282	0.3502449	7.18E-15	3.37E-13	PPLLLL
8769-02I	AOM03	3	145.6146	4.954501	0.0386358	0.0023528	4.228306	0.30687	0.0273575	0.0028991	33.26713	0.5580261	22.12132	0.7834566	66.30335	2.047576	1.79E-15	5.94E-14	PPLLLL
8770-01A	NQ37	0.1	432.9178	5.263196	0.0157491	0.0022459	-0.090168	0.2265451	0.0078141	0.0021002	76.08529	0.7496718	71.3701	0.9759485	93.80961	0.8916147	1.62E-15	1.23E-13	LPLLLL
8770-01B	NQ37	0.15	456.6952	4.878988	0.0046664	0.0021234	0.0196451	0.20117	0.0060176	0.0018561	77.20069	0.6715785	75.80829	0.916708	98.19609	0.8406431	1.83E-15	1.41E-13	PPLLLL
8770-01C	NQ37	0.17	446.6315	4.595536	0.0043394	0.0018554	0.0920715	0.2005964	0.0107714	0.0018597	75.20763	0.6648383	73.9227	0.8586473	98.2863	0.7646992	1.69E-15	1.27E-13	PPLLLL
8770-01D	NQ37	0.21	445.1367	2.441956	0.0017516	0.0005206	-0.1076417	0.0577961	0.0114911	0.0004772	74.18118	0.4305312	73.64352	0.4558864	99.28368	0.2300439	6.37E-15	4.72E-13	PPLLLL
8770-01E	NQ37	0.25	445.4504	1.535019	0.0002709	0.0002179	-0.0130236	0.0231822	0.0116395	0.0002863	73.78553	0.279175	73.70208	0.2866211	99.88891	0.1281113	1.65E-14	1.22E-12	PPLLLL
8770-01F	NQ37	0.3	447.3975	1.536019	0.0002335	0.0002524	0.0061476	0.0269213	0.0115024	0.0002747	74.13571	0.2770566	74.06585	0.2871174	99.90644	0.1424108	1.43E-14	1.06E-12	PPLLLL
8770-01G	NQ37	0.5	449.7135	2.550865	0.0020158	0.0007755	0.0341642	0.0927955	0.0125818	0.0005823	75.09734	0.4193445	74.49905	0.4774283	99.20205	0.3278323	4.31E-15	3.23E-13	PPLLLL
8770-01H	NQ37	1	448.6562	1.219065	0.0004989	0.0001932	0.0339375	0.0198775	0.0117627	0.0002071	74.44671	0.2204315	74.30121	0.2280304	99.80331	0.1150234	1.86E-14	1.38E-12	PPLLLL
8770-01I	NQ37	3	449.3764	1.884002	0.0012533	0.0004523	-0.1240311	0.0461727	0.0112129	0.0005128	74.82702	0.3262713	74.43596	0.35255	99.48698	0.1951225	7.35E-15	5.50E-13	PPLLLL
8770-02A	NQ37	0.1	339.3436	2.385146	0.0235896	0.0008575	-0.1091513	0.0719071	0.0145735	0.0007511	61.51755	0.358087	54.46105	0.4199198	88.53713	0.4255368	4.56E-15	2.81E-13	PPLLLL
8770-02B	NQ37	0.15	423.4167	2.889221	0.0123358	0.0008528	-0.1114696	0.0877508	0.0126107	0.0008934	73.31092	0.4855982	69.61295	0.5329308	94.96413	0.3676435	3.76E-15	2.76E-13	PPLLLL
8770-02C	NQ37	0.17	443.4272	2.339416	0.0056937	0.0005833	-0.0523796	0.0615688	0.011122	0.0006547	75.03221	0.4053288	73.32452	0.4363297	97.72865	0.2533278	5.84E-15	4.38E-13	PPLLLL
8770-02D	NQ37	0.21	447.8504	1.039136	0.0010478	0.0001094	0.0014718	0.0116313	0.0116547	0.0001822	74.46409	0.19087	74.15052	0.1942872	99.57988	0.0781934	3.11E-14	2.31E-12	PPLLLL

8770-02E	NQ37	0.25	448.2441	0.9357114	0.0007675	0.0000793	0.0033886	0.0087624	0.0117976	0.0001265	74.45375	0.1727484	74.22414	0.1749882	99.69247	0.0575367	4.31E-14	3.21E-12	PPLLLL
8770-02F	NQ37	0.3	447.5427	0.994913	0.0007812	0.0000675	0.0124184	0.0059841	0.0116475	0.0001084	74.32555	0.1843629	74.093	0.1859872	99.68734	0.058699	5.85E-14	4.35E-12	PPLLLL
8770-02G	NQ37	0.5	444.6505	1.380828	0.0016945	0.0001946	0.0078341	0.0199181	0.0120073	0.0002683	74.05858	0.2509875	73.55277	0.2577159	99.31756	0.110077	1.91E-14	1.42E-12	PPLLLL
8770-02H	NQ37	1	448.0251	0.981458	0.0004847	0.0000825	0.0010291	0.0081143	0.011576	0.0001266	74.3287	0.1815159	74.18319	0.183521	99.80525	0.0594013	4.53E-14	3.37E-12	PPLLLL
8770-02H	NQ37	1	448.0251	0.981458	0.0004847	0.0000825	0.0010291	0.0081143	0.011576	0.0001266	74.3287	0.1815159	74.18319	0.183521	99.80525	0.0594013	4.53E-14	3.37E-12	PPLLLL
8771-01A	MLHR02b	0.05	230.578	3.267462	0.0408226	0.0015773	-0.1776097	0.1502021	0.0196394	0.0014081	48.08489	0.3239839	35.878	0.5416001	74.62429	0.9813773	2.80E-15	1.35E-13	PPLLLL
8771-01B	MLHR02b	0.07	370.7227	3.827326	0.0222807	0.0014435	-0.2227505	0.1881878	0.0166519	0.0016322	66.71309	0.5818026	60.03385	0.685647	90.00305	0.6684073	2.09E-15	1.39E-13	PPLLLL
8771-01C	MLHR02b	0.1	436.0892	3.74207	0.0201941	0.001489	-0.0989503	0.1465822	0.0138252	0.0014128	78.00146	0.567454	71.95868	0.6951086	92.26026	0.5886269	2.42E-15	1.88E-13	PPLLLL
8771-01D	MLHR02b	0.15	460.1193	3.531578	0.00908	0.0011944	-0.2769946	0.1423721	0.0147682	0.0011744	79.19979	0.5762546	76.45226	0.6648052	96.55035	0.4659105	3.01E-15	2.38E-13	PPLLLL
8771-01E	MLHR02b	0.17	441.7365	3.476185	0.0116771	0.0014703	-0.159177	0.1760978	0.0105387	0.0015053	76.51724	0.4913389	73.00934	0.6477436	95.42705	0.591474	2.44E-15	1.87E-13	PPLLLL
8771-01F	MLHR02b	0.21	444.6675	1.51475	0.0038013	0.0003086	0.0106811	0.0368158	0.0123735	0.0004508	74.6904	0.2674785	73.55594	0.2827137	98.48145	0.1410296	9.51E-15	7.10E-13	PPLLLL
8771-01G	MLHR02b	0.25	445.9438	1.504234	0.0040308	0.0005291	0.0676183	0.0537944	0.0128092	0.000554	74.98989	0.2311141	73.79423	0.2809496	98.40204	0.2316821	7.28E-15	5.46E-13	PLLLLL
8771-01H	MLHR02b	0.3	452.2251	3.045066	0.0055236	0.000963	0.0111851	0.1214422	0.0107187	0.0011523	76.61828	0.5003748	74.96944	0.5707184	97.84826	0.3941822	3.48E-15	2.67E-13	PPLLLL
8771-01I	MLHR02b	0.5	450.8044	2.218902	0.0040512	0.000648	0.1363528	0.0690531	0.0114554	0.0005934	75.89633	0.3704671	74.70328	0.415548	98.41983	0.2653709	5.56E-15	4.22E-13	PPLLLL
8771-01J	MLHR02b	1	446.6952	1.82996	0.002593	0.0005811	0.0922024	0.0794024	0.0108296	0.0007307	74.69804	0.2950759	73.9346	0.3419287	98.97273	0.2529005	5.04E-15	3.76E-13	PLLLLL
8771-01K	MLHR02b	3	446.413	4.161213	0.0021636	0.0012906	0.3794895	0.1599296	0.0105345	0.0013823	74.48045	0.6792078	73.88187	0.7774026	99.1714	0.540303	2.60E-15	1.94E-13	PPLLLL
8771-02A	MLHR02b	0.05	267.2628	2.743624	0.0431105	0.0012833	-0.2577979	0.1159125	0.0204421	0.001207	54.9201	0.2950174	42.02095	0.4641131	76.52764	0.7010744	3.04E-15	1.67E-13	PPLLLL
8771-02B	MLHR02b	0.07	419.2046	3.818785	0.0154888	0.001647	-0.3444	0.1702867	0.0130884	0.0016494	73.50516	0.5264616	68.83691	0.7027509	93.6724	0.6940872	2.18E-15	1.61E-13	PPLLLL
8771-02C	MLHR02b	0.1	445.1503	4.368494	0.0146765	0.0014592	0.2213672	0.1648843	0.0116724	0.0014199	78.00086	0.7239244	73.64605	0.8155561	94.40351	0.5742597	2.47E-15	1.93E-13	PPLLLL
8771-02D	MLHR02b	0.15	448.5968	2.983819	0.0066004	0.0008259	-0.1326801	0.0959465	0.0145973	0.0008755	76.27838	0.5094418	74.2901	0.5581156	97.40335	0.4082125	3.79E-15	2.89E-13	PPLLLL
8771-02E	MLHR02b	0.17	441.5991	2.678514	0.0059044	0.0011133	-0.0298764	0.12816	0.0132399	0.0010793	74.75119	0.3760417	72.98373	0.4990695	97.63862	0.4811922	3.23E-15	2.41E-13	PLLLLL
8771-02F	MLHR02b	0.21	449.9245	2.756976	0.0052875	0.0008315	0.0496973	0.1117495	0.0131983	0.0009604	76.11162	0.4583614	74.53853	0.516065	97.93087	0.3499464	4.03E-15	3.07E-13	PPLLLL
8771-02G	MLHR02b	0.25	449.4275	3.13724	0.0089899	0.0014195	0.0577415	0.1673118	0.0165943	0.0012383	77.12263	0.4134029	74.44552	0.5870829	96.52593	0.5713282	2.33E-15	1.79E-13	PLLLLL
8771-02H	MLHR02b	0.3	453.5614	4.219666	0.0113126	0.0015992	-0.1983011	0.1871442	0.0135387	0.0017226	78.62395	0.6537422	75.22	0.7914527	95.68469	0.6379258	2.10E-15	1.65E-13	PPLLLL
8771-02I	MLHR02b	0.5	449.6003	2.244369	0.0076123	0.0007182	-0.1841393	0.0956386	0.0138539	0.0008388	76.775	0.3660343	74.47787	0.420037	97.02134	0.2939783	4.31E-15	3.31E-13	PPLLLL
8771-02J	MLHR02b	1	426.6065	3.401296	0.0041793	0.0013417	0.2387328	0.1545089	0.0163393	0.0012264	71.42011	0.4898241	70.20184	0.628496	98.27912	0.5786032	2.69E-15	1.92E-13	PPLLLL
8771-02K	MLHR02b	3	405.7957	17.3196	0.0385414	0.0087254	0.6260385	1.14887	0.0036458	0.0091256	77.81155	2.113169	66.37849	3.163634	85.27072	3.350279	3.52E-16	2.74E-14	PPLLLL
8774-01A	MLH505	0.05	305.1047	2.798047	0.007582	0.0012029	0.4796308	0.1351958	0.0109348	0.0010967	50.70189	0.3330495	48.48991	0.4833525	95.6071	0.7230383	3.03E-15	1.53E-13	PPLLLL
8774-01B	MLH505	0.07	389.1664	3.08811	0.0025765	0.0011644	0.585429	0.1357466	0.0089956	0.0011346	64.0549	0.440454	63.35491	0.5589048	98.86844	0.5614561	2.91E-15	1.86E-13	PPLLLL
8774-01C	MLH505	0.1	445.4519	2.530339	0.0010811	0.0006282	0.1879953	0.0708222	0.0119506	0.000615	74.00203	0.4345929	73.70238	0.4724691	99.58323	0.2703592	5.78E-15	4.28E-13	PPLLLL
8774-01D	MLH505	0.15	468.1157	1.768037	0.0008876	0.0003037	0.1712362	0.0412055	0.0117723	0.0003447	78.20442	0.3219415	77.96089	0.3343043	99.67784	0.1551623	1.11E-14	8.65E-13	PPLLLL
8774-01E	MLH505	0.17	486.144	2.468408	-0.0006726	0.0005227	0.2767119	0.0499925	0.0114089	0.0004381	81.1501	0.4438841	81.38679	0.4714193	100.2735	0.2236243	7.92E-15	6.42E-13	PPLLLL
8774-01F	MLH505	0.21	487.5631	1.672377	-0.0001504	0.0002953	0.1051606	0.0345949	0.0110311	0.00042	81.6	0.3071315	81.65792	0.3196438	100.0647	0.1360849	1.14E-14	9.34E-13	PPLLLL
8774-01G	MLH505	0.25	490.8662	1.707489	0.0015919	0.000317	0.1723326	0.0346477	0.0114839	0.0003067	82.74305	0.3131082	82.28983	0.3269529	99.44139	0.1508806	1.14E-14	9.46E-13	PPLLLL
8774-01H	MLH505	0.3	497.4563	1.801163	0.0002665	0.0003362	0.0887777	0.0367848	0.0117686	0.0004474	83.62256	0.3312667	83.55403	0.3461519	99.9129	0.1556375	1.08E-14	9.01E-13	PPLLLL
8774-01I	MLH505	0.5	508.4347	1.552125	0.0004226	0.000256	0.0841539	0.0252952	0.0112971	0.0003535	85.78601	0.290148	85.67032	0.3001118	99.86027	0.1184538	1.51E-14	1.30E-12	PPLLLL
8774-01J	MLH505	0.9	533.8695	3.375802	0.0020992	0.0009843	0.5033987	0.1042214	0.0157869	0.0009324	91.18011	0.5952645	90.62311	0.6619975	99.35544	0.3410092	3.68E-15	3.35E-13	PPLLLL
8774-01K	MLH505	1	395.8686	60.00176	0.0315577	0.0325104	4.129576	3.461607	0.0572956	0.0280382	73.4866	5.592439	64.57016	10.8999	87.61681	13.21682	1.19E-16	8.77E-15	PPLLLL
8774-01L	MLH505	3	237.6107	56.61337	0.1554684	0.032072	4.296305	3.313462	0.0885878	0.0291531	83.01761	6.081022	37.04597	9.420634	44.49219	10.83002	1.20E-16	1.00E-14	PPLLLL
8774-02A	MLH505	0.05	294.1614	2.52409	0.0058379	0.001256	0.1884235	0.1089923	0.0136073	0.0009639	48.32847	0.2196289	46.60523	0.4333906	96.42338	0.7896051	3.29E-15	1.59E-13	PLLLLL
8774-02B	MLH505	0.07	384.3219	2.696234	0.0018228	0.0010495	0.0000659	0.1086941	0.0117986	0.0010588	63.02444	0.3742127	62.4793	0.4866721	99.1363	0.5137461	3.19E-15	2.01E-13	PPLLLL
8774-02C	MLH505	0.1	446.8828	2.288893	0.0015504	0.0006385	0.0877814	0.062912	0.0116746	0.0006291	74.42227	0.3840317	73.96966	0.4277251	99.3869	0.2746837	6.06E-15	4.51E-13	PPLLLL
8774-02D	MLH505	0.15	468.61	1.674859	0.0002114	0.0002675	0.0311269	0.0293227	0.0109383	0.0003038	78.11441	0.3065483	78.05436	0.3167727	99.92202	0.1541064	1.26E-14	9.84E-13	PPLLLL
8774-02E	MLH505	0.17	481.1896	2.005454	-0.0000336	0.0003688	0.0070862	0.0460735	0.011727	0.0004438	80.43183	0.3656581	80.4419	0.3819535	100.013	0.183091	9.13E-15	7.34E-13	PPLLLL
8774-02F	MLH505	0.21	489.3911	1.749565	0.0000745	0.0002442	0.1131749	0.0313747	0.0111092	0.0003312	82.01562	0.3266361	82.0075	0.3347357	99.98328	0.119607	1.30E-14	1.06E-12	PPLLLL
8774-02G	MLH505	0.25	492.9856	1.596545	-0.0007142	0.0002905	0.0909712	0.0278167	0.011703	0.0003026	82.47135	0.2934222	82.6959	0.3060684	100.267	0.1408167	1.42E-14	1.17E-12	PPLLLL
8774-02H	MLH505	0.3	493.9163	1.454767	-0.0008333	0.000275	0.0692782	0.0291782	0.0115905	0.0002708	82.61719	0.2667515	82.87437	0.2790326	100.3075	0.1391488	1.31E-14	1.08E-12	PPLLLL
8774-02I	MLH505	0.5	516.5364	1.544386	0.0005626	0.0001928	0.0614229	0.0239177	0.0114459	0.00025	87.40083	0.2943149	87.24035	0.2999596	99.81307	0.0994961	1.62E-14	1.41E-12	PPLLLL
8774-02J	MLH505	0.9	523.649	3.104547	0.0108283	0.001115	0.4193818	0.1251922	0.0131275	0.0010279	91.80055	0.5157771	88.62453	0.605365	96.51318	0.38108	3.24E-15	2.97E-13	PPLLLL
8774-02K	MLH505	1	368.4009	72.16535	0.0699313	0.0375677	12.89467	5.544945	-0.0191145	0.0390512	78.98285	8.621583	59.61819	12.91145	74.81065	13.9732	8.20E-17	6.47E-15	PPLLLL
8774-02L	MLH505	3	232.8286	45.33944	0.1564287	0.0257713	5.630092	2.90794	0.0371495	0.0251191	82.38299	5.296517	36.25128	7.524647	43.8326	8.641645	1.33E-16	1.09E-14	PPLLLL
8775-01A	MLH503	0.05	312.8474	4.37785	0.0106353	0.0019963	0.3615293	0.2308277	0.0224477	0.001615	52.96513	0.4944978	49.83031	0.7595104	94.0593	1.147007	1.82E-15	9.65E-14	PPLLLL
8775-01B	MLH503	0.07	296.3269	2.862844	0.0018453	0.0012596	-0.0226216	0.1658985	0.0173585	0.0012311	47.53086	0.3195815	46.97727	0.4921456	98.83853	0.8062129	2.45E-15	1.16E-13	LPLLLL
8775-01C	MLH503	0.1	465.0287	2.674998	0.00037	0.0009092	0.0657838	0.1131623	0.0135735	0.0007979	77.48024	0.4257744	77.37769	0.5049297	99.86415	0.3779687	3.74E-15	2.90E-13	PPLLLL
8775-01D	MLH503	0.15	476.6992	1.77977	0.0000457	0.0003773	-0.0276653	0.0470146	0.0129098	0.0004365	79.60577	0.3187669	79.58774	0.3381276	99.98028	0.1711165	9.04E-15	7.19E-13	PPLLLL
8775-01E	MLH503	0.17	493.1434	1.646686	0.0003186	0.0004606	0.1741932	0.0594708	0.0124402	0.0005008	82.79875	0.2840012	82.72615	0.3157084	99.90127	0.1809143	6.65E-15	5.51E-13	PLLLLL
8775-01F	MLH503	0.21	498.9743	1.369218	-0.0007572	0.0003659	0.0362089	0.0411841	0.0121929	0.0004031	83.61574	0.2398713	83.84589	0.2633611	100.2737	0.1741353	9.29E-15	7.77E-13	PLLLLL
8775-01G	MLH503	0.25	497.6588	1.931651	0.0002463	0.0003349	0.1613939	0.0408757	0.0112073	0.000389	83.64572	0.3575198	83.59294	0.3712711	99.92672	0.1437725	9.75E-15	8.16E-13	PPLLLL
8775-01H	MLH503	0.3	494.2637	1.752819	-0.0007365	0.0003331	0.0992795	0.0454004	0.0108005	0.0003784	82.70881	0.3209458	82.941	0.3362653	100.2748	0.1622693	9.48E-15	7.84E-13	PPLLLL
8775-01I	MLH503	0.5	505.8572	1.928069	0.0006191	0.00034	0.1373075	0.0413483	0.0117461	0.0003564	85.33943	0.358278	85.1723	0.3722704	99.79564	0.1610188	1.01E-14	8.60E-13	PPLLLL
8775-01J	MLH503	1	495.7774	3.599657	0.0031669	0.0011035	0.0387113	0.1160112	0.0133612	0.0010699	84.1726	0.612531	83.23153	0.6911472	98.88028	0.4173818	3.35E-15	2.82E-13	PPLLLL
8775-01K	MLH503	3	500.0374	26.54682	0.0172665	0.0130914	2.06891	1.538385	0.0133778	0.0128061	88.92771	3.46496	84.05043	5.109136	94.3812	4.415527	2.54E-16	2.26E-14	PPLLLL
8775-02A	MLH503	0.05	265.6647	4.309587	0.011383	0.0020482	-0.2423308	0.2032175	0.0166311	0.0018743	45.17534	0.4225812	41.75073	0.7283669	92.43642	1.370499	2.00E-15	9.02E-14	PPLLLL
8775-02B	MLH503	0.07	408.4315	4.430552	-0.0013669	0.0019128	0.2879171	0.2411742	0.0089859	0.0017444	66.41802	0.5709034	66.86029	0.8104769	100.6471	0.8776706	1.74E-15	1.16E-13	LPLLLL
8775-02C	MLH503	0.1	469.1781	3.178221	0.0013233	0.0009169	-0.0306571	0.1211766	0.0127155	0.0009593	78.56172	0.5371258	78.16183	0.6012988	99.49412	0.3731313	3.45E-15	2.71E-13	PPLLLL
8775-02D	MLH503	0.15	474.7929	2.089551	-0.000267	0.0004278	0.0503003	0.0582783	0.01198	0.0005513	79.14028	0.375141	79.22577	0.3965619	100.1056	0.1997213	7.43E-15	5.88E-13	PPLLLL
8775-02E	MLH503	0.17	498.8513	2.609199	0.000026	0.0006808	-0.0249898	0.0844209	0.0117081	0.000625	83.83423	0.4587097	83.82222	0.50183	99.98837	0.2658283	4.94E-15	4.14E-13	PPLLLL
8775-02F	MLH503	0.21	496.0499	1.787485	0.0006447	0.0003708	0.0540484	0.0512547	0.0113839	0.0004454	83.47002	0.3249501	83.28386	0.3432555	99.77421	0.1818304	7.82E-15	6.52E-13	PPLLLL
8775-02G	MLH503	0.25	500.7054	2.226187	-0.000319	0.000429	0.141681	0.054595	0.0117216	0.0005391	84.06554	0.4086211	84.17902	0.4286052	100.1262	0.2034875	7.88E-15	6.63E-13	PPLLLL

8775-02H	MLH503	0.3	494.5674	1.731996	0.0009441	0.0004483	0.0208968	0.0642968	0.0108064	0.0004289	83.27939	0.3041374	82.99927	0.3323265	99.66317	0.1886475	6.93E-15	5.77E-13	PPLLLL
8775-02I	MLH503	0.5	504.2089	1.787001	0.0005575	0.0003555	0.0937249	0.0430977	0.0116902	0.0004112	85.00886	0.3279826	84.8542	0.3447181	99.81255	0.166149	9.58E-15	8.14E-13	PPLLLL
8775-02J	MLH503	1	515.7999	6.749258	0.0050851	0.002335	0.2999956	0.2767492	0.0167624	0.0022598	88.57482	1.125714	87.09733	1.310345	98.31245	0.8175801	1.43E-15	1.27E-13	PPLLLL
8775-02K	MLH503	3	461.1216	70.98089	0.0308263	0.0362303	-7.242582	4.706175	-0.0317281	0.0268546	86.79121	9.053144	76.64099	13.36929	88.74779	12.47319	8.84E-17	7.68E-15	PPLLLL
8776-01A	MLH502	0.05	245.3357	7.690299	0.0260846	0.0039727	-0.3343342	0.4183852	0.0225972	0.0030048	46.15662	0.5901846	38.3342	1.28518	83.07307	2.577111	9.75E-16	4.50E-14	PPLLLL
8776-01B	MLH502	0.07	325.7177	6.998041	-0.0027527	0.0030315	-0.1869377	0.3656545	0.007703	0.0028208	51.27174	0.8096737	52.07116	1.222778	101.5739	1.805137	1.19E-15	6.12E-14	PPLLLL
8776-01C	MLH502	0.1	403.3968	3.421372	0.0024488	0.0013018	0.0042369	0.1721097	0.0125796	0.0013125	66.67204	0.491913	65.94059	0.6241243	98.90383	0.6133986	2.43E-15	1.62E-13	PPLLLL
8776-01D	MLH502	0.15	474.0317	2.327448	-0.0001046	0.0006696	0.0375348	0.079578	0.0129671	0.0007238	79.0459	0.3934031	79.08133	0.4415244	100.0433	0.2738592	5.43E-15	4.29E-13	PPLLLL
8776-01E	MLH502	0.17	489.0096	2.464978	0.0002038	0.0008553	-0.0423678	0.0935313	0.0128991	0.0008639	82.00174	0.3963403	81.93451	0.4715125	99.92194	0.3275035	4.26E-15	3.49E-13	PPLLLL
8776-01F	MLH502	0.21	488.7263	2.289939	0.001327	0.0004983	0.1166938	0.0649521	0.0107252	0.0004611	82.26202	0.4127684	81.88033	0.4379615	99.52896	0.1976961	6.84E-15	5.63E-13	PPLLLL
8776-01G	MLH502	0.25	494.1969	2.007974	0.000862	0.0003805	0.1314122	0.0470362	0.0122104	0.0003905	83.16879	0.3683374	82.92819	0.3852008	99.70263	0.1906473	8.06E-15	6.70E-13	PPLLLL
8776-01H	MLH502	0.3	487.107	1.816285	0.001116	0.0003491	0.0079045	0.0401693	0.0115989	0.0003811	81.90384	0.3313194	81.57077	0.3470614	99.59377	0.1725557	9.76E-15	7.99E-13	PPLLLL
8776-01I	MLH502	0.5	496.8479	1.640934	0.0015465	0.0002837	0.0544741	0.0312212	0.0114626	0.0002693	83.89248	0.3037308	83.43712	0.3152523	99.45443	0.1396609	1.30E-14	1.09E-12	PPLLLL
8776-01J	MLH502	1	512.4713	3.492918	0.0022701	0.0009407	0.3275927	0.1093506	0.014937	0.0008989	87.08526	0.6188809	86.45168	0.6768877	99.25092	0.3421579	3.54E-15	3.09E-13	PPLLLL
8776-01K	MLH502	3	439.345	66.67325	0.0726533	0.034891	10.7686	4.749739	0.0227971	0.0308952	92.89033	8.745509	72.56401	12.40727	77.53733	11.04514	8.65E-17	8.03E-15	PPLLLL
8776-02A	MLH502	0.05	215.9399	6.323087	0.0361958	0.0031874	-1.313402	0.369359	0.0175139	0.0031852	44.40026	0.5567453	33.46146	1.039617	75.43298	2.137242	1.08E-15	4.80E-14	PPLLLL
8776-02B	MLH502	0.07	282.2403	5.002833	0.0010056	0.0023999	-0.266647	0.2757978	0.0150636	0.0021495	44.89449	0.4656413	44.56511	0.8533376	99.28639	1.618488	1.39E-15	6.25E-14	PPLLLL
8776-02C	MLH502	0.1	453.0866	3.942807	0.0000167	0.0013481	-0.3143792	0.1701397	0.0131008	0.0014316	75.17709	0.620243	75.13096	0.7393295	99.96143	0.5638614	2.53E-15	1.91E-13	PPLLLL
8776-02D	MLH502	0.15	468.0012	2.424958	0.0022018	0.0005728	0.0532496	0.0741896	0.012353	0.0006578	78.59051	0.4273458	77.93923	0.4584872	99.16867	0.235657	5.60E-15	4.40E-13	PPLLLL
8776-02E	MLH502	0.17	490.3588	2.459816	-0.0002943	0.0007272	0.053997	0.0994378	0.0114272	0.0007192	82.09855	0.4173357	82.19269	0.4708773	100.1119	0.2869318	4.51E-15	3.70E-13	PPLLLL
8776-02F	MLH502	0.21	493.3068	2.223268	-0.0019568	0.0005527	0.0183924	0.0602676	0.012528	0.0004963	82.17152	0.3916282	82.75748	0.4262913	100.7128	0.2202058	6.64E-15	5.45E-13	PPLLLL
8776-02G	MLH502	0.25	493.0836	1.879997	-0.002063	0.0004113	-0.0799284	0.0520933	0.0128753	0.0004207	82.11015	0.3380662	82.71469	0.3604276	100.7428	0.1732361	7.99E-15	6.56E-13	PPLLLL
8776-02H	MLH502	0.3	492.1211	2.334256	-0.0007421	0.0003386	-0.0006136	0.0461983	0.0115642	0.0003824	82.30963	0.4349854	82.5302	0.4472782	100.269	0.1586349	9.36E-15	7.70E-13	PPLLLL
8776-02I	MLH502	0.5	541.5779	1.367647	-0.0007387	0.0002031	0.0400042	0.0210268	0.0129216	0.0002478	91.91253	0.2626824	92.13796	0.2693451	100.2434	0.0907018	2.06E-14	1.89E-12	PPLLLL
8776-02J	MLH502	1	564.0339	1.948588	0.0030362	0.0005525	0.1129999	0.0750792	0.0136351	0.0006085	97.47909	0.3517718	96.5881	0.3885625	99.07906	0.2001966	6.22E-15	6.06E-13	PLLLLL
8776-02K	MLH502	3	367.2162	20.95925	0.0255792	0.0106195	1.64069	1.402952	0.0449593	0.0099698	66.84711	2.242327	59.40629	3.747458	88.76923	4.752377	3.09E-16	2.07E-14	PPLLLL
8777-01A	MLH501	0.05	236.9183	4.40047	0.0248108	0.0021259	-0.9494696	0.2566937	0.0183851	0.0016701	44.43601	0.4284172	36.93079	0.7319705	83.16608	1.438281	1.74E-15	7.74E-14	PPLLLL
8777-01B	MLH501	0.07	319.1747	5.156132	0.0059356	0.0022794	-0.3174502	0.2962125	0.0149454	0.0022589	52.73825	0.6030987	50.92996	0.8976768	96.59387	1.319148	1.50E-15	7.91E-14	PPLLLL
8777-01C	MLH501	0.1	418.891	4.083892	0.0049071	0.0016165	-0.0882108	0.1959349	0.0125936	0.0014145	70.25613	0.5853969	68.7792	0.7514064	97.9049	0.7118242	2.26E-15	1.59E-13	PPLLLL
8777-01D	MLH501	0.15	458.0815	2.105333	0.0003972	0.0006749	-0.1161323	0.0755384	0.0119684	0.0005705	76.20332	0.3408779	76.06886	0.3958729	99.83262	0.2838458	5.02E-15	3.82E-13	PLLLLL
8777-01E	MLH501	0.17	473.4914	3.154769	-0.0000757	0.0008639	-0.3114132	0.1229143	0.0124686	0.0008115	78.99793	0.5398168	78.97886	0.5982905	99.9984	0.3512958	3.43E-15	2.71E-13	PPLLLL
8777-01F	MLH501	0.21	485.4911	2.546494	0.0007228	0.0005924	-0.0555242	0.0675219	0.0114509	0.0006306	81.48626	0.4535278	81.26214	0.4861564	99.72978	0.2311361	5.54E-15	4.51E-13	PPLLLL
8777-01G	MLH501	0.25	497.3554	2.319658	0.0007104	0.0004759	-0.0775182	0.0597925	0.011592	0.0005265	83.75808	0.4230564	83.53464	0.4457725	99.73954	0.195255	7.54E-15	6.32E-13	PPLLLL
8777-01H	MLH501	0.3	493.8379	1.672446	0.0005886	0.0002799	0.0285489	0.0351673	0.0110538	0.0003626	83.03224	0.3097282	82.85933	0.3207706	99.79076	0.1377353	1.09E-14	9.06E-13	PPLLLL
8777-01I	MLH501	0.5	504.6315	1.490497	0.0007124	0.0001577	-0.0182912	0.0175841	0.0119836	0.0002001	85.15175	0.2836495	84.93571	0.2875889	99.7485	0.0921039	2.26E-14	1.92E-12	PPLLLL
8777-01J	MLH501	1	522.2456	2.100418	0.0010606	0.000369	0.0645723	0.0505999	0.0124337	0.0004533	88.65958	0.3945601	88.35098	0.4092483	99.6484	0.1715019	8.12E-15	7.20E-13	PPLLLL
8777-01K	MLH501	3	410.1492	20.0904	0.0421639	0.0093362	0.5317257	1.149313	0.0318755	0.0081341	79.69692	2.87732	67.17466	3.67862	84.25754	3.488712	3.56E-16	2.84E-14	PPLLLL
8777-02A	MLH501	0.05	237.2784	2.512912	0.0233884	0.0010638	-0.1907833	0.1162699	0.0184188	0.0010603	43.99363	0.3066469	36.99069	0.4180791	84.09457	0.7390785	3.34E-15	1.47E-13	PPLLLL
8777-02B	MLH501	0.07	426.9961	3.471142	0.000485	0.0010731	-0.3953548	0.14049	0.0104773	0.0012105	70.46924	0.5569323	70.27384	0.6415407	99.75111	0.4839737	2.75E-15	1.94E-13	PPLLLL
8777-02C	MLH501	0.1	451.7017	2.284037	0.0009302	0.0005575	-0.3093216	0.0787794	0.0123104	0.0006168	75.18966	0.3951726	74.87138	0.4279591	99.59905	0.242205	5.54E-15	4.16E-13	PPLLLL
8777-02D	MLH501	0.15	476.7067	1.884416	0.0009511	0.0003024	-0.1054701	0.0364257	0.0115492	0.0004431	79.88796	0.3468642	79.58917	0.3580103	99.63426	0.176231	1.05E-14	8.38E-13	PPLLLL
8777-02E	MLH501	0.17	490.3656	2.376563	-0.0002414	0.0004965	-0.0057518	0.057788	0.0111377	0.0005079	82.12364	0.4298327	82.194	0.4549421	100.0871	0.2116742	7.17E-15	5.89E-13	PPLLLL
8777-02F	MLH501	0.21	488.7966	2.062052	0.0009736	0.0003074	-0.0056379	0.0382061	0.0119647	0.0003855	82.18607	0.3841271	81.89377	0.3943924	99.64571	0.1532585	1.08E-14	8.87E-13	PPLLLL
8777-02G	MLH501	0.25	487.317	1.988293	0.0011636	0.0003575	0.024268	0.0374916	0.0114491	0.0003903	81.95602	0.3652198	81.61089	0.3799734	99.5782	0.1634032	1.00E-14	8.21E-13	PPLLLL
8777-02H	MLH501	0.3	500.0211	2.192506	0.0011377	0.0004191	-0.1247219	0.0396867	0.0124874	0.0004825	84.4046	0.4037835	84.04728	0.4219605	99.58621	0.1792929	8.57E-15	7.24E-13	PPLLLL
8777-02I	MLH501	0.5	508.4308	1.548124	0.0011093	0.0001982	0.0190291	0.0250979	0.0119494	0.0002453	85.99906	0.29337	85.66956	0.2993377	99.6165	0.1059284	1.69E-14	1.46E-12	PPLLLL
8777-02J	MLH501	1	499.3891	2.216064	0.0026294	0.0003555	0.0062038	0.042968	0.0127611	0.0004328	84.71069	0.414727	83.92567	0.4263451	99.07383	0.1710724	9.00E-15	7.63E-13	PPLLLL
8777-02K	MLH501	3	479.8216	14.7102	0.0175028	0.0068583	-1.102438	0.7519975	0.0423069	0.0067861	85.55005	2.037075	80.18146	2.799542	93.79691	2.410572	4.66E-16	3.98E-14	PPLLLL
8649-01A	GA1550 MD2	0.2	80.88559	3.133103	0.0311451	0.0014585	0.0413036	0.06657	0.0253385	0.0020959	21.13794	0.351375	11.84276	0.4690895	56.02661	2.012443	4.05E-16	8.57E-15	PPLLLL
8649-01B	GA1550 MD2	0.3	101.2	0.8174553	0.002028	0.0002718	0.0593654	0.0151021	0.0163847	0.0005531	15.50214	0.0956359	14.90143	0.1237757	96.126	0.5850785	1.99E-15	3.08E-14	PPLLLL
8649-01C	GA1550 MD2	0.35	102.6495	0.7200885	0.0004302	0.0002385	-0.0037769	0.0133096	0.0166806	0.0006243	15.25009	0.082987	15.12099	0.1091205	99.15893	0.545979	2.20E-15	3.35E-14	PPLLLL
8649-01D	GA1550 MD2	0.4	102.813	0.7158886	-0.0000134	0.0002246	-0.0150982	0.0122901	0.0163196	0.0004867	15.14345	0.0852667	15.14577	0.1084938	100.0217	0.5626922	2.40E-15	3.63E-14	PPLLLL
8649-01E	GA1550 MD2	0.45	100.4614	0.6062598	0.0000766	0.0002104	0.0281251	0.0124947	0.015835	0.000469	14.81045	0.0668998	14.78961	0.0917598	99.86281	0.4763868	2.41E-15	3.57E-14	PPLLLL
8649-01F	GA1550 MD2	0.5	99.56978	0.7374686	0.0005652	0.000207	0.0574986	0.0114536	0.0165236	0.0004625	14.81882	0.0935064	14.6547	0.1115636	98.89392	0.4921129	2.45E-15	3.63E-14	PPLLLL
8649-01G	GA1550 MD2	0.6	99.74951	0.4906591	0.0004727	0.0000983	0.1203649	0.0055092	0.0159952	0.0002464	14.81297	0.0683841	14.68189	0.0742339	99.1122	0.272385	5.92E-15	8.77E-14	PPLLLL
8649-01H	GA1550 MD2	0.8	100.2569	0.4215517	0.0006084	0.0000664	0.5428423	0.0088887	0.0161519	0.0002205	14.89352	0.0605459	14.75866	0.0637962	99.06267	0.2078524	9.97E-15	1.48E-13	PPLLLL
8649-01I	GA1550 MD2	1	98.77211	0.5542882	0.0007914	0.000138	1.09506	0.0177374	0.0170473	0.0004065	14.67561	0.0726279	14.53405	0.0838151	98.96592	0.3889977	3.98E-15	5.84E-14	PPLLLL
8649-01J	GA1550 MD2	2.5	95.47095	4.100391	0.0045111	0.0018588	4.997785	0.1836646	0.0168078	0.003424	14.95059	0.2812364	14.03533	0.6188957	93.55893	3.828623	2.78E-16	4.16E-15	PPLLLL
8649-02A	GA1550	0.2	91.5355	2.057911	0.0276073	0.000916	-0.020782	0.0375548	0.0198184	0.0016032	21.68675	0.2342452	13.44198	0.3099356	61.98564	1.232854	6.85E-16	1.49E-14	PPLLLL

	MD2																		
8649-02B	GA1550 MD2	0.3	99.84894	0.6319592	0.0012269	0.0001655	0.0379223	0.0088974	0.0169356	0.0004668	15.06026	0.0828585	14.69693	0.095617	97.59015	0.412333	3.06E-15	4.60E-14	PPLLLL
8649-02C	GA1550 MD2	0.35	99.41318	0.5936328	0.0004191	0.0001678	-0.0072896	0.0100589	0.0151577	0.0004608	14.75727	0.0747483	14.63101	0.0897964	99.15029	0.4469499	3.00E-15	4.43E-14	PPLLLL
8649-02D	GA1550 MD2	0.4	100.6436	0.5921601	0.0001908	0.0001781	0.0065277	0.0102166	0.0164789	0.0004555	14.87394	0.0722017	14.8172	0.0896348	99.62343	0.5168256	3.06E-15	4.55E-14	PPLLLL
8649-02E	GA1550 MD2	0.45	98.58025	0.5083017	0.00043	0.0001513	0.0208417	0.0083221	0.0156314	0.0004646	14.63206	0.0622128	14.50504	0.0768533	99.13592	0.4290542	3.30E-15	4.83E-14	PPLLLL
8649-02F	GA1550 MD2	0.5	99.07929	0.5190344	0.000392	0.0001561	0.0076601	0.0085828	0.0153079	0.0003839	14.69736	0.0632971	14.58051	0.0784977	99.20982	0.3709338	3.38E-15	4.96E-14	PPLLLL
8649-02G	GA1550 MD2	0.6	99.17395	0.5164663	0.0000531	0.0001537	-0.0022594	0.0083355	0.0157329	0.0003574	14.6113	0.0632118	14.59482	0.0781134	99.89291	0.4015153	3.32E-15	4.85E-14	PPLLLL
8649-02H	GA1550 MD2	0.8	98.85857	0.5200011	0.0002454	0.0000797	0.0074265	0.004727	0.0158853	0.0002575	14.62015	0.0751156	14.54713	0.0786343	99.50548	0.2547213	6.37E-15	9.32E-14	PPLLLL
8649-02I	GA1550 MD2	1	97.90951	0.5843422	0.0009395	0.0001607	-0.0100279	0.0085217	0.0153386	0.00039	14.68549	0.0746893	14.40365	0.0883174	98.08685	0.4292654	3.43E-15	5.04E-14	PPLLLL
8649-02J	GA1550 MD2	2.5	103.6892	5.889131	0.0004364	0.0026268	-0.3483871	0.1453805	0.0105175	0.004657	15.4403	0.4311258	15.27859	0.8929389	98.98164	5.203596	1.86E-16	2.88E-15	PPLLLL

Appendix C: $^{40}Ar/^{39}Ar$ geochronology step-heating spectra, ideograms and isochrons.

Granite Springs Granite (2122054b - plagioclase)

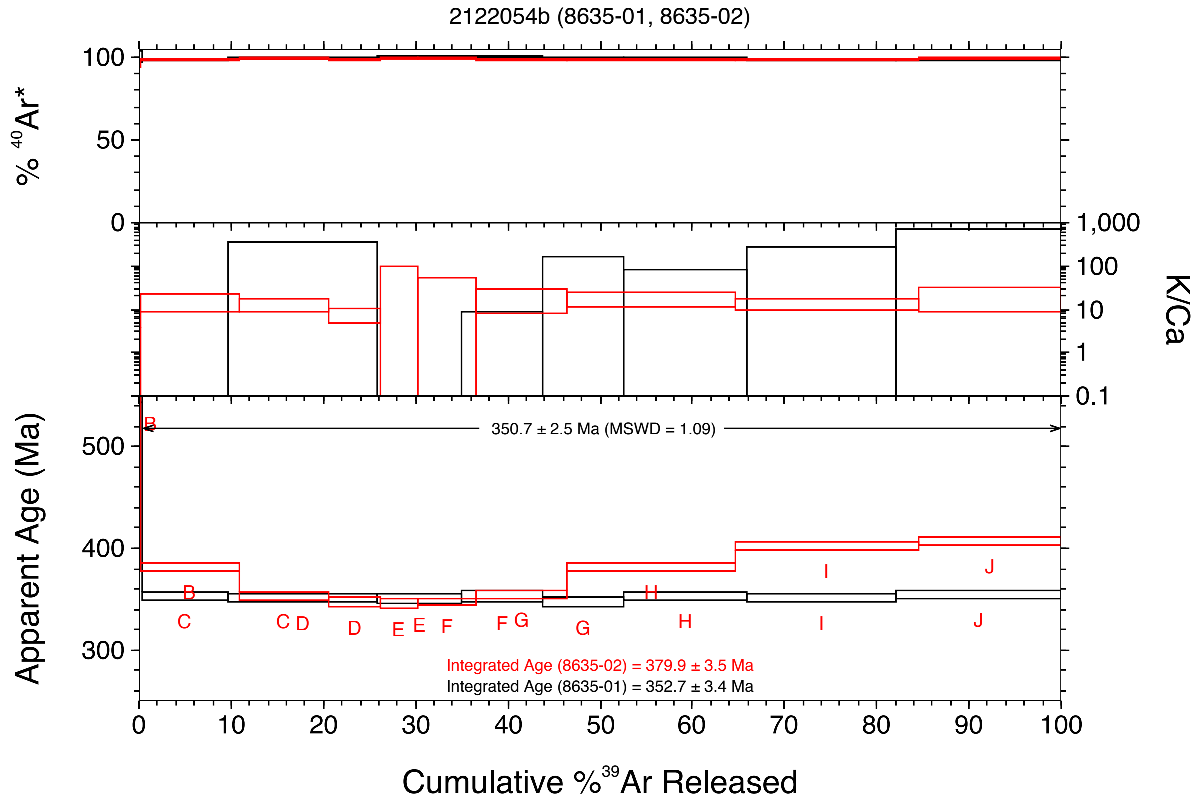

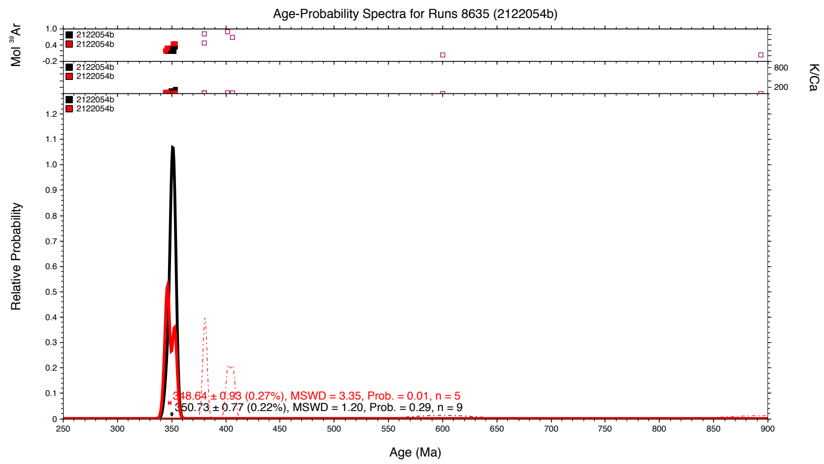

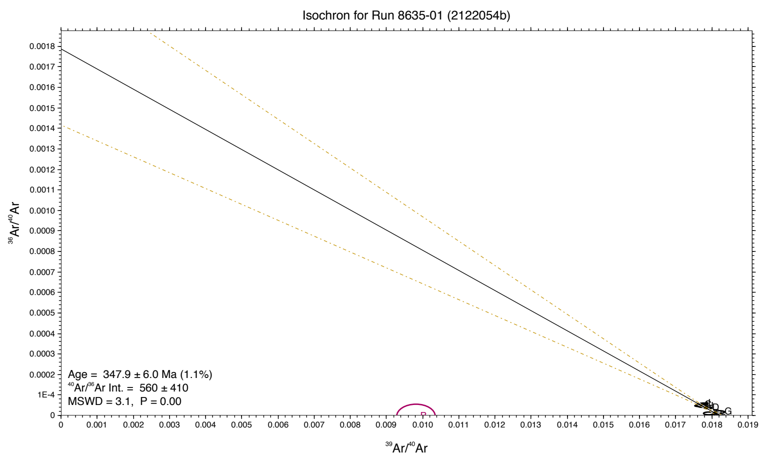

Granite Springs Granite (2122054a - biotite)

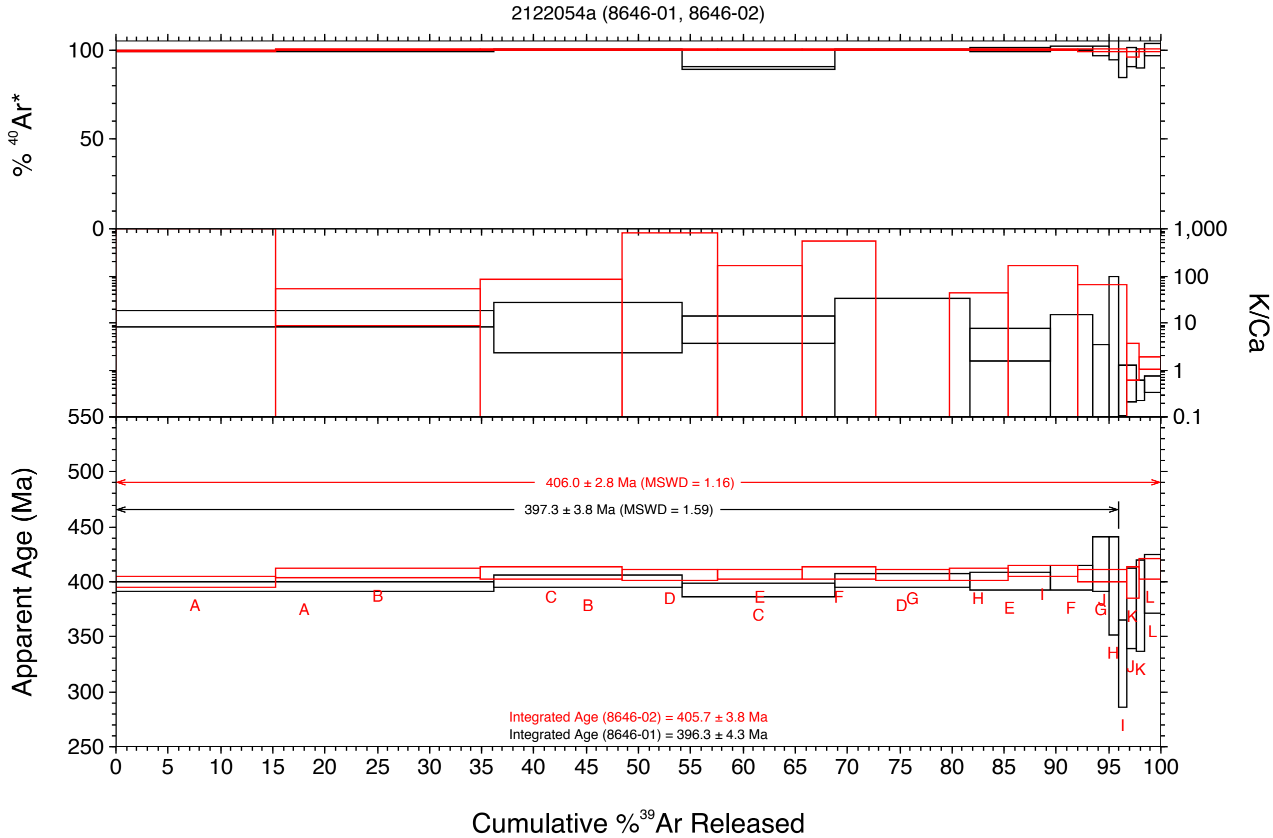

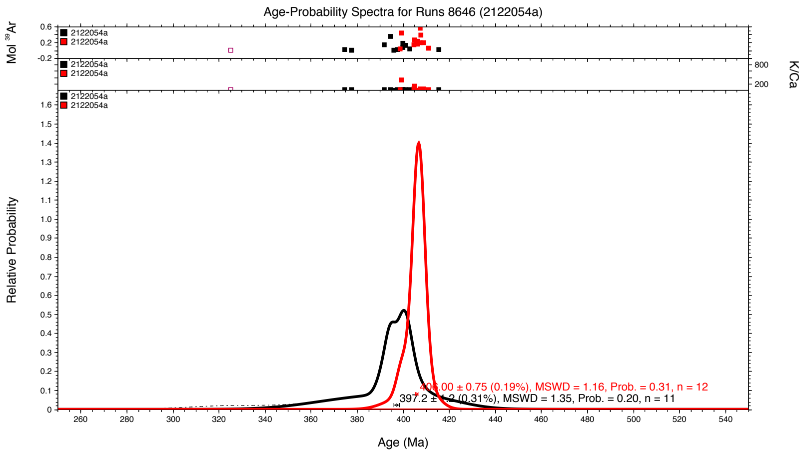

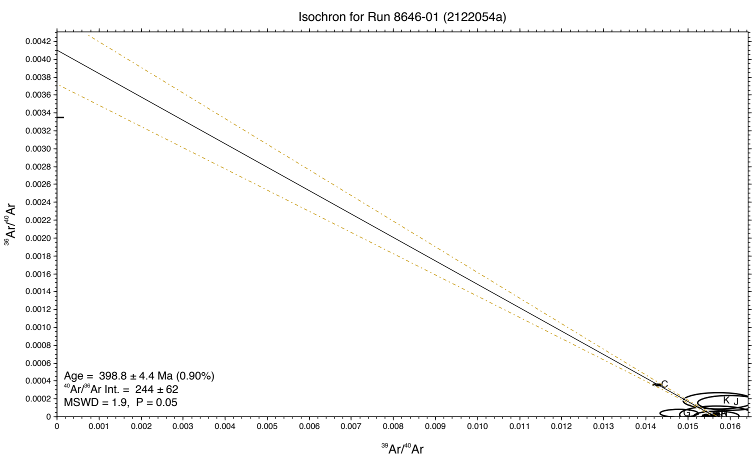

Hungerford Granite (2122055b - plagioclase)

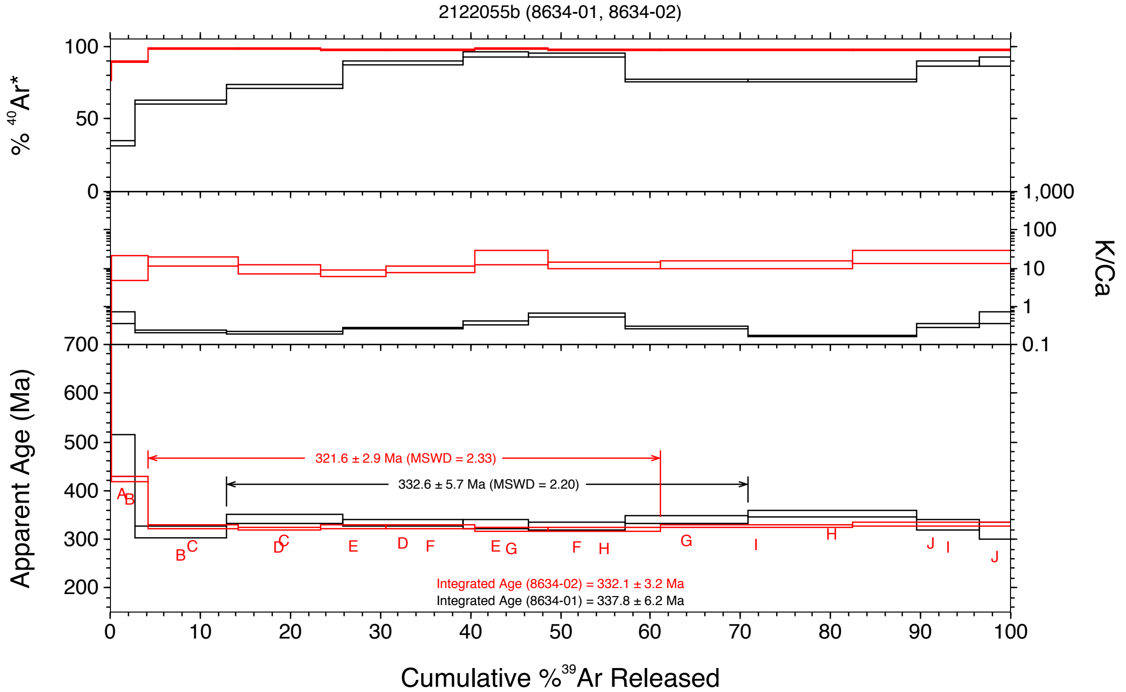

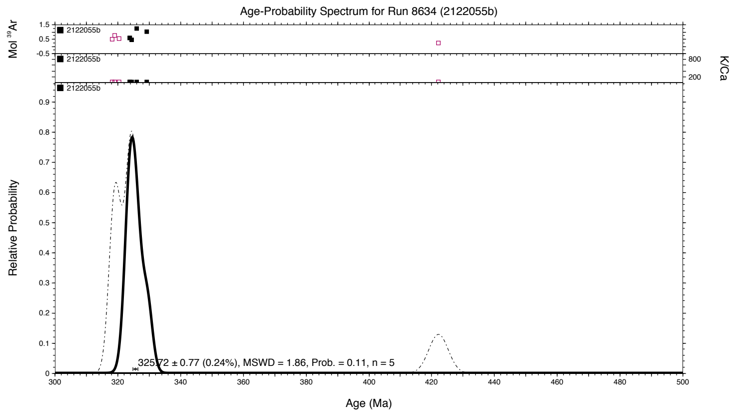

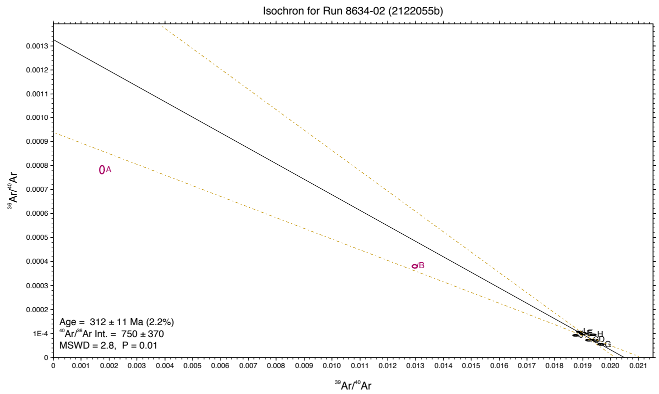

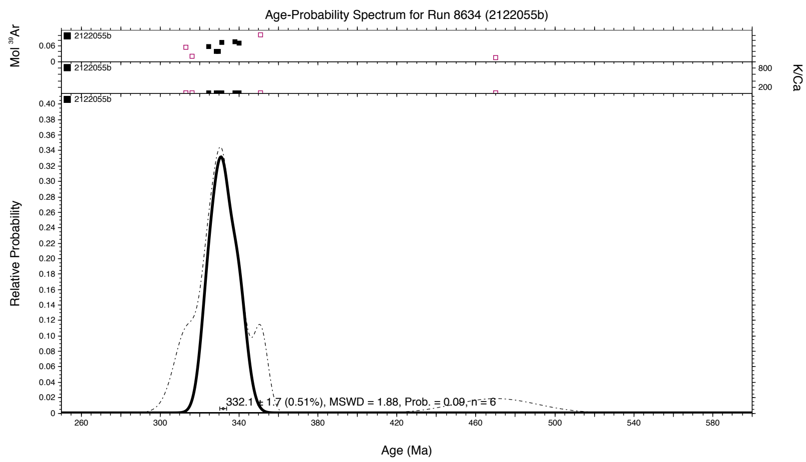

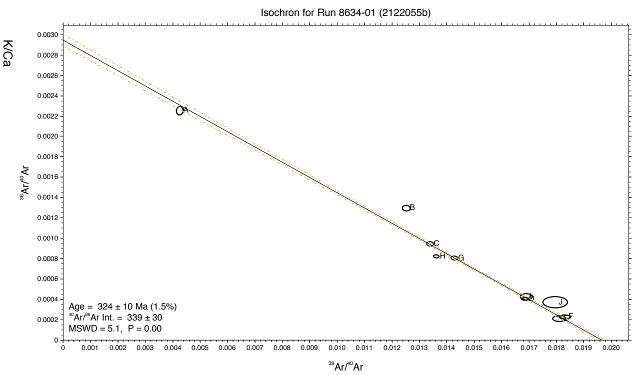

Hungerford Granite (2122055a - biotite)

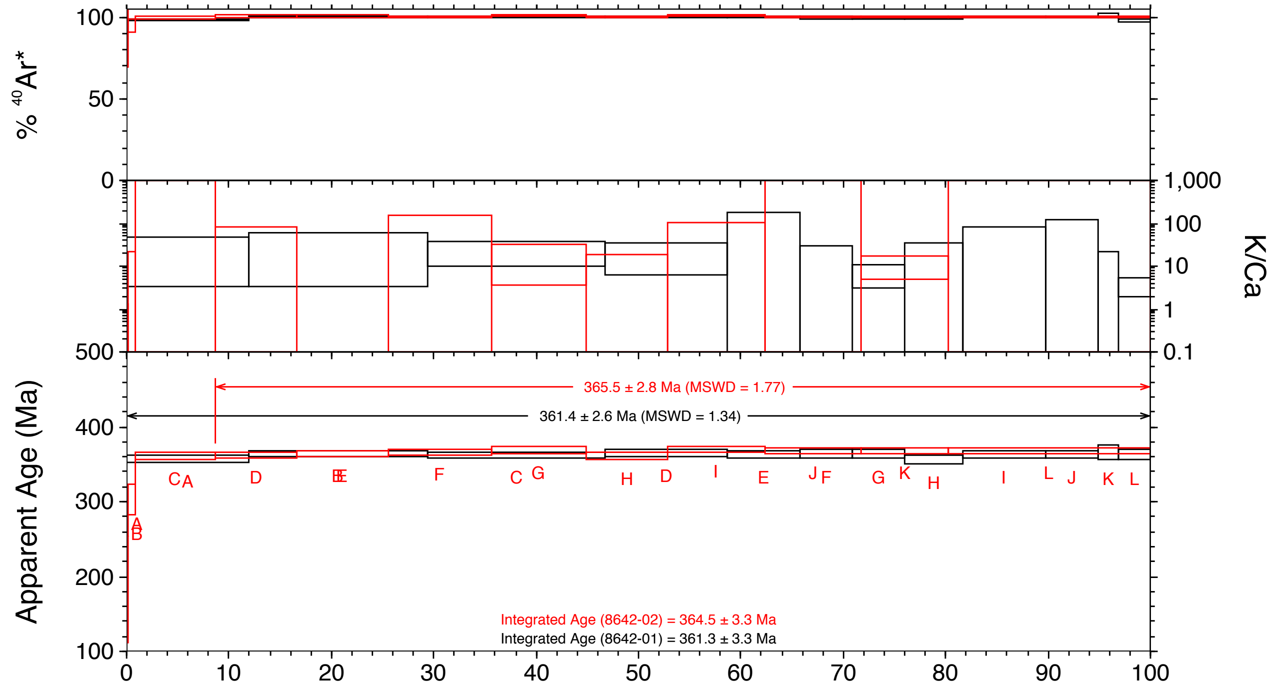

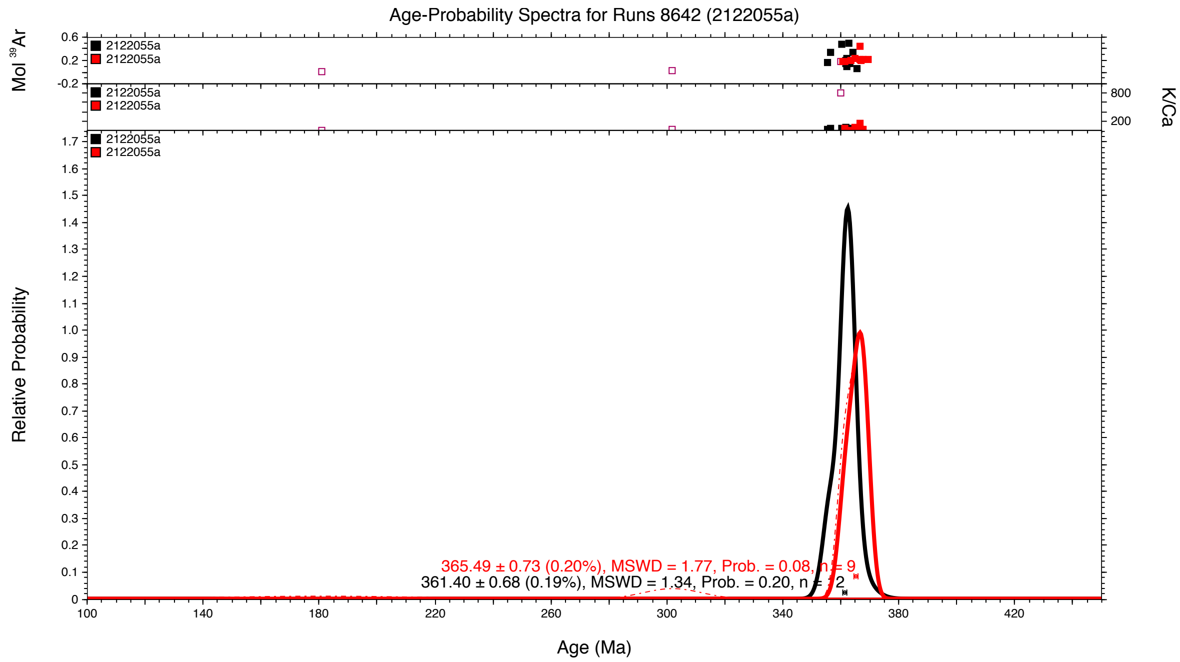

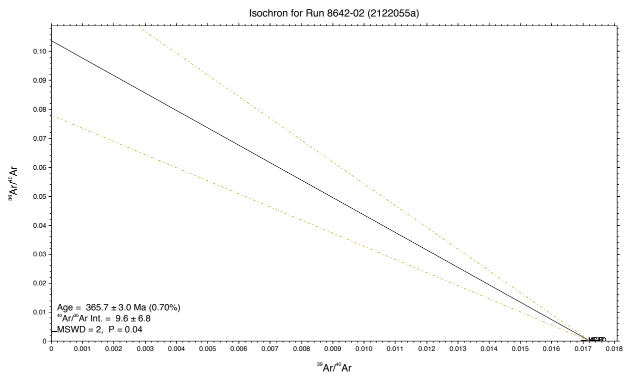

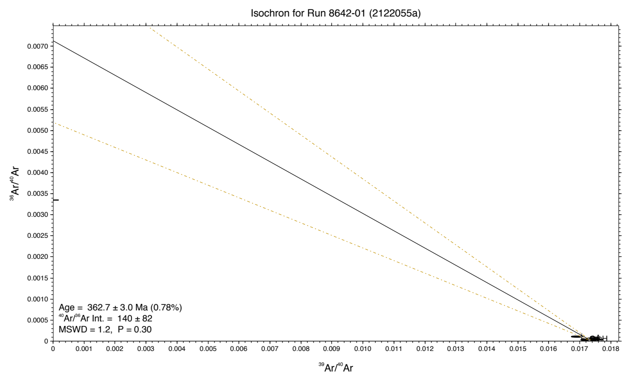

Retreat Granite (MLRG01 - k-feldspar)

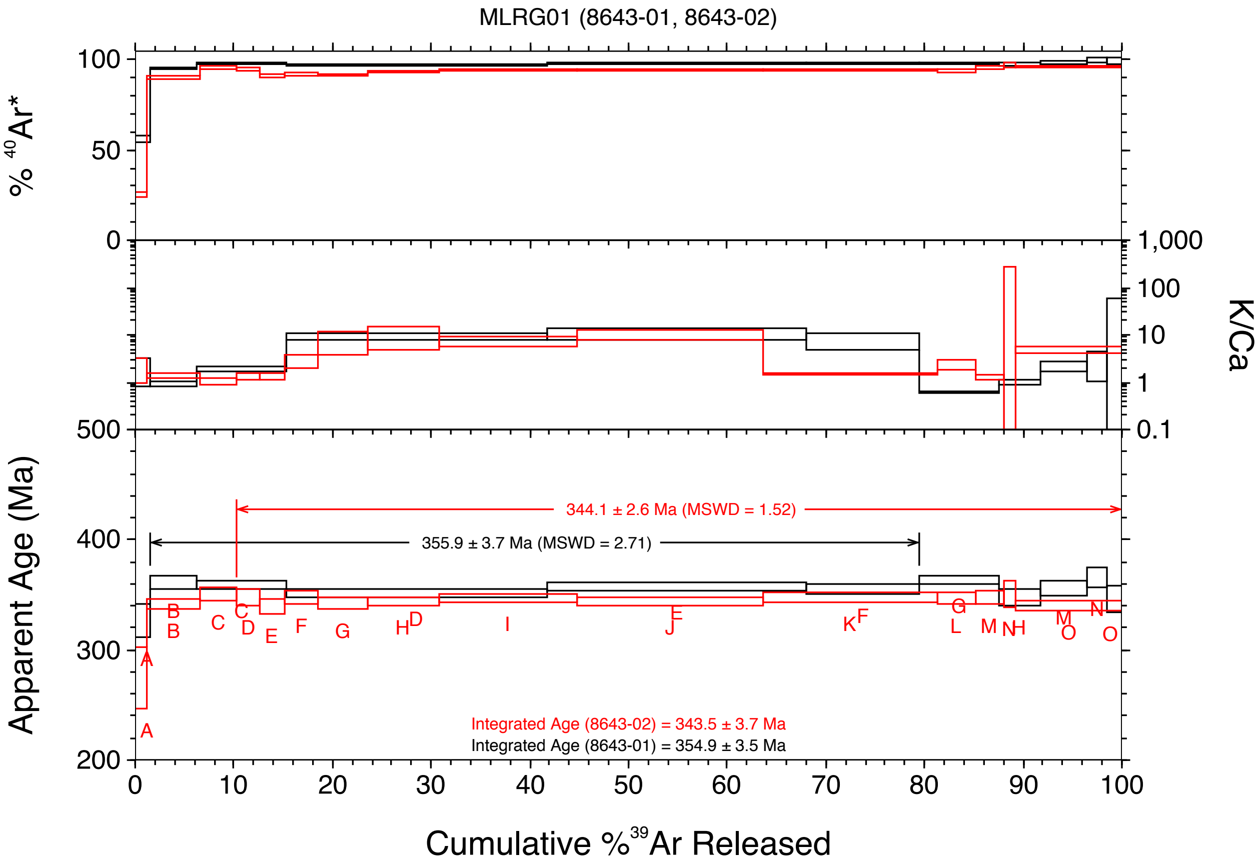

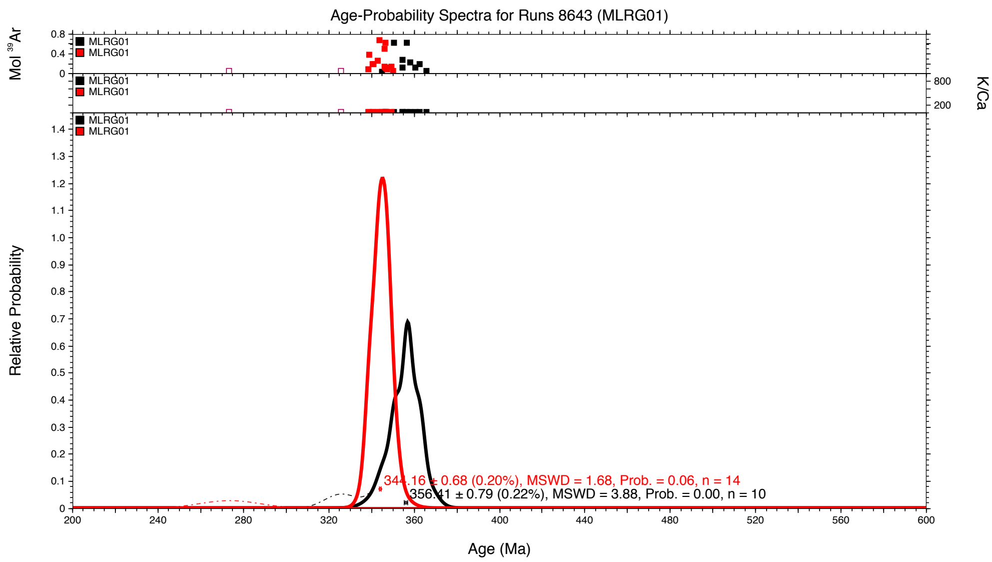

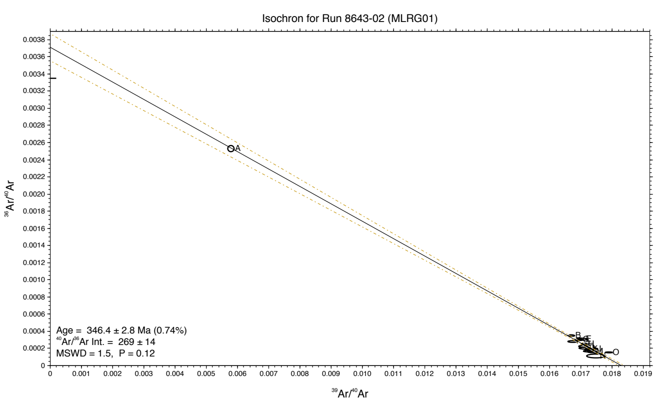

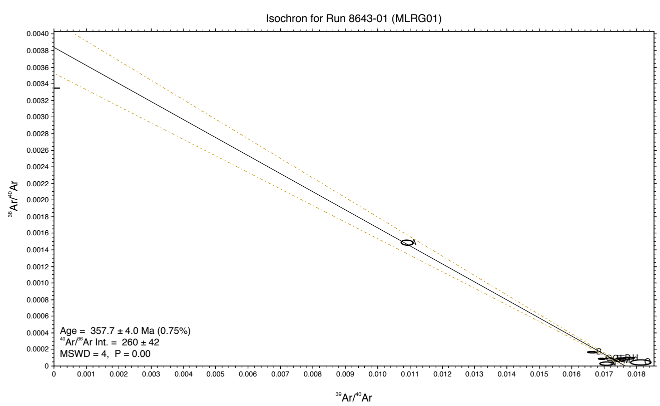

Thunderbolt 1 (2130084 - plagioclase)

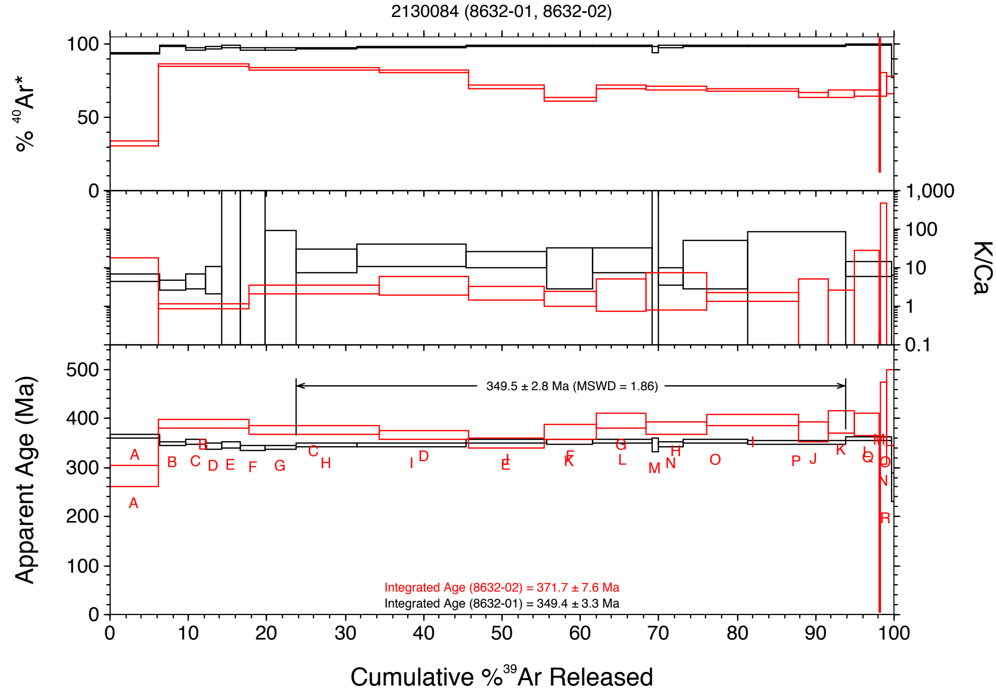

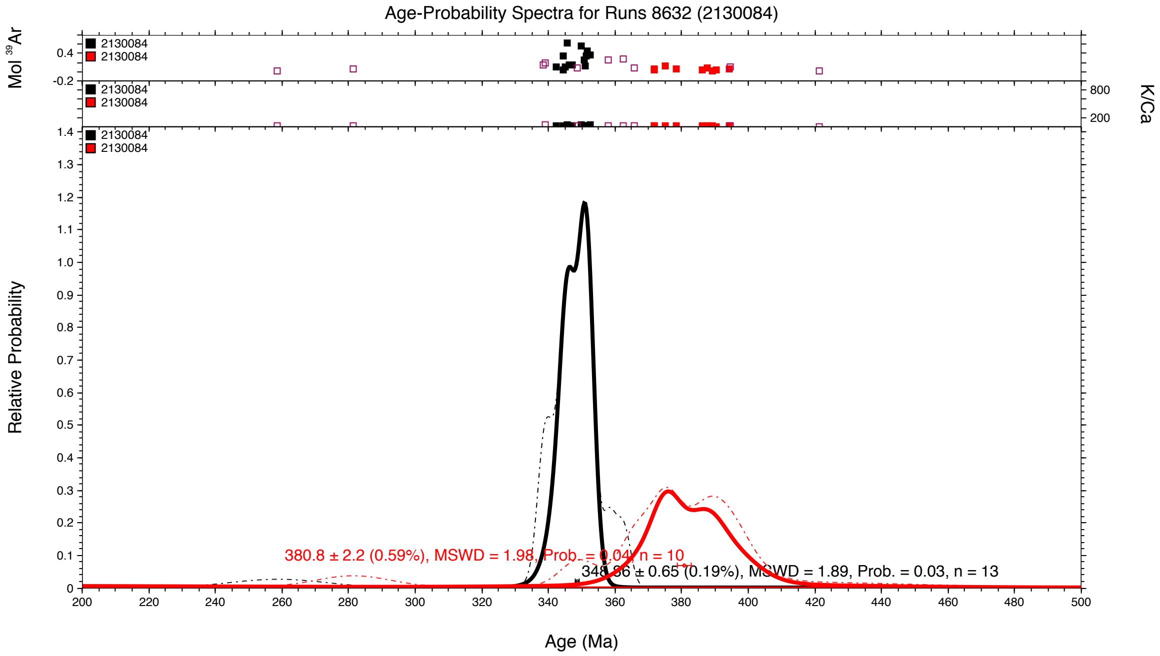

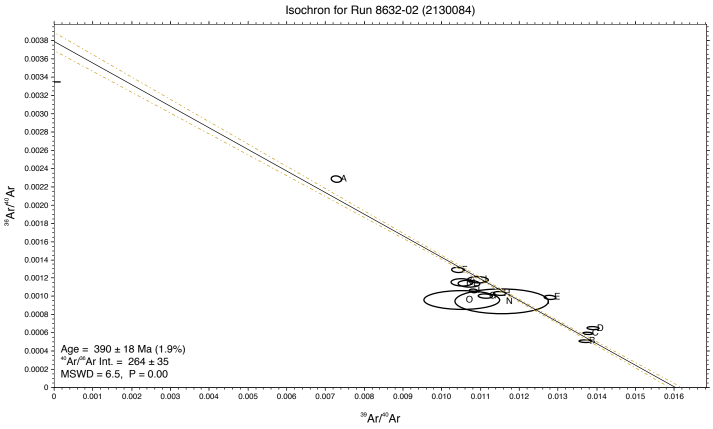

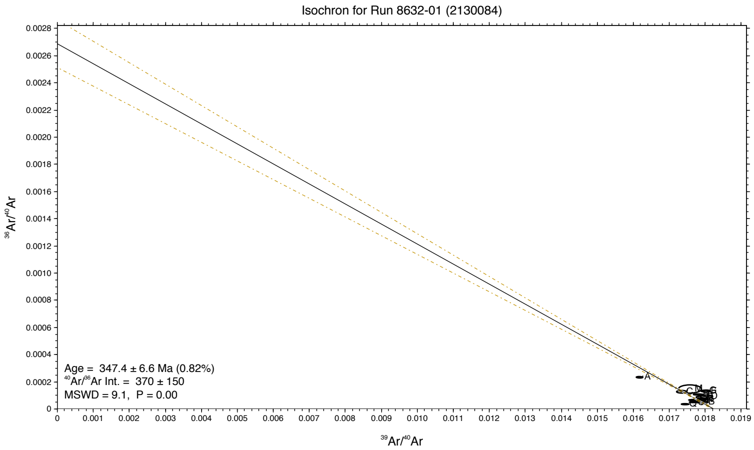

Ooroonoo 1 (2152164a - biotite)

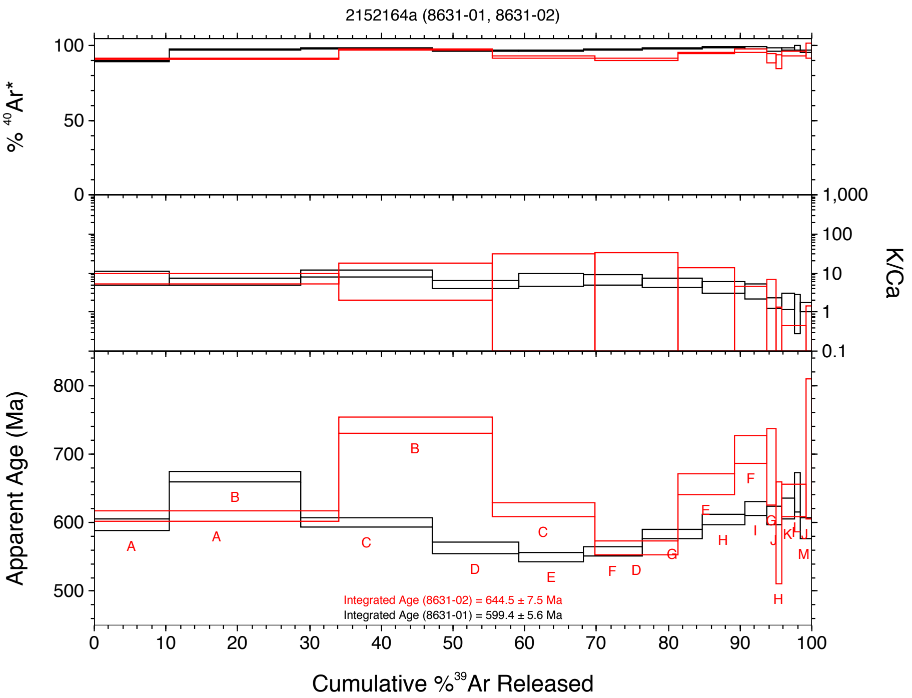

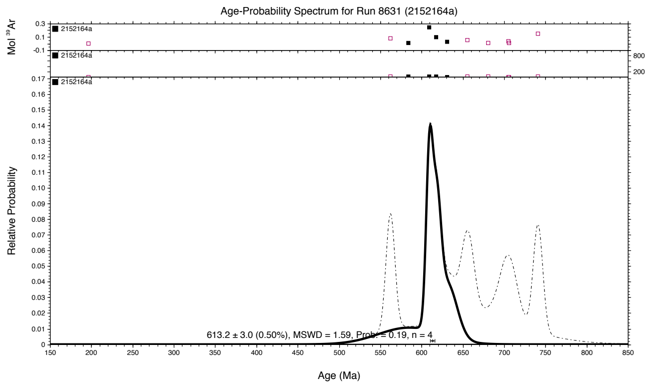

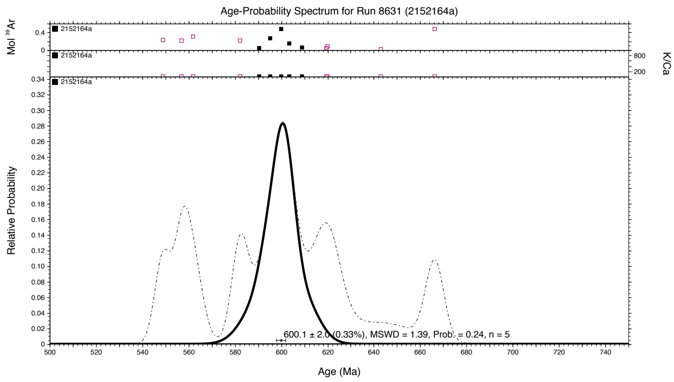

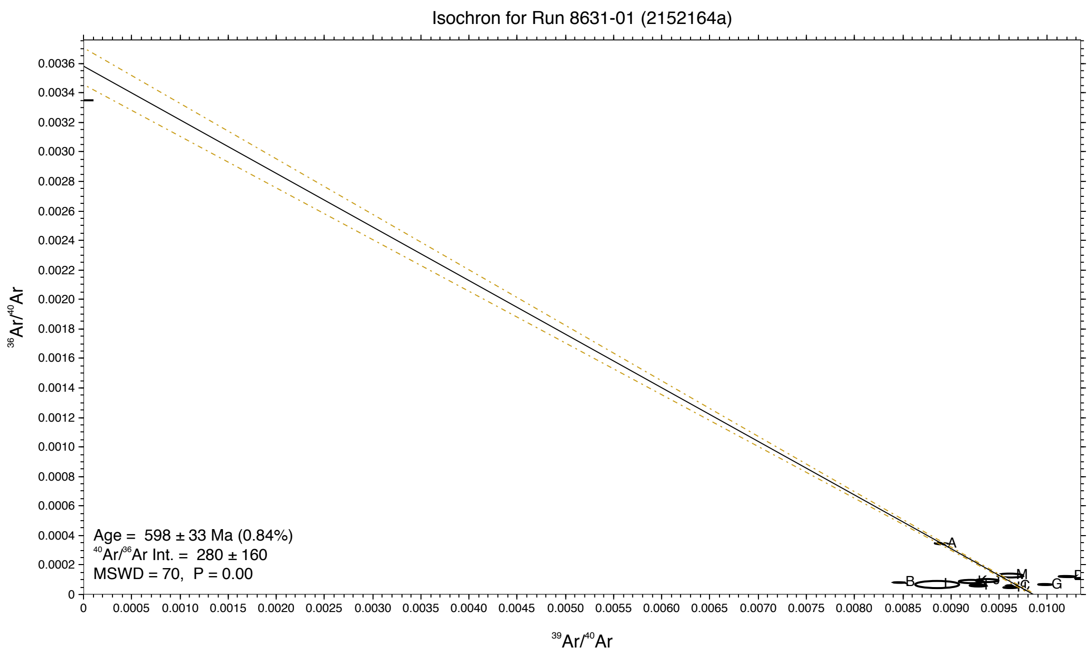

Ooroonoo 1 (2152164b - plagioclase)

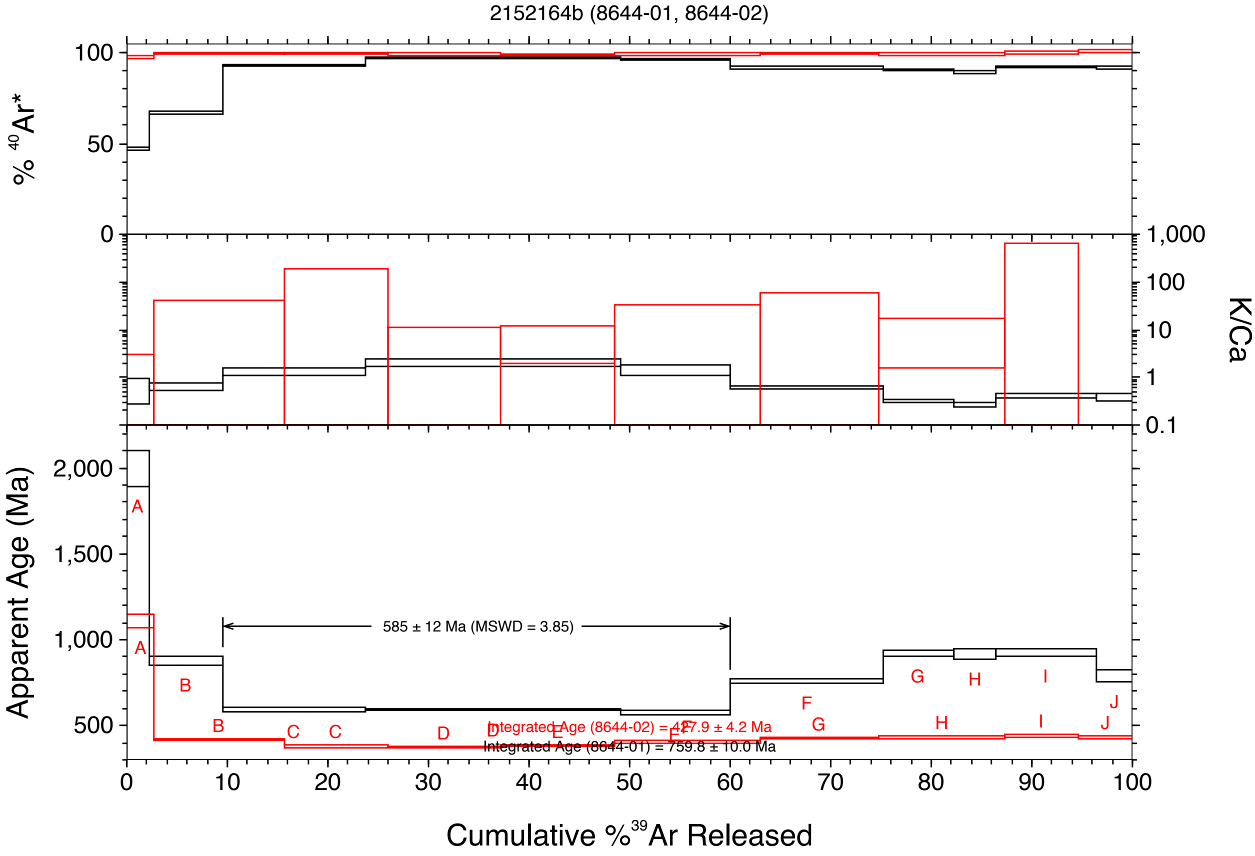

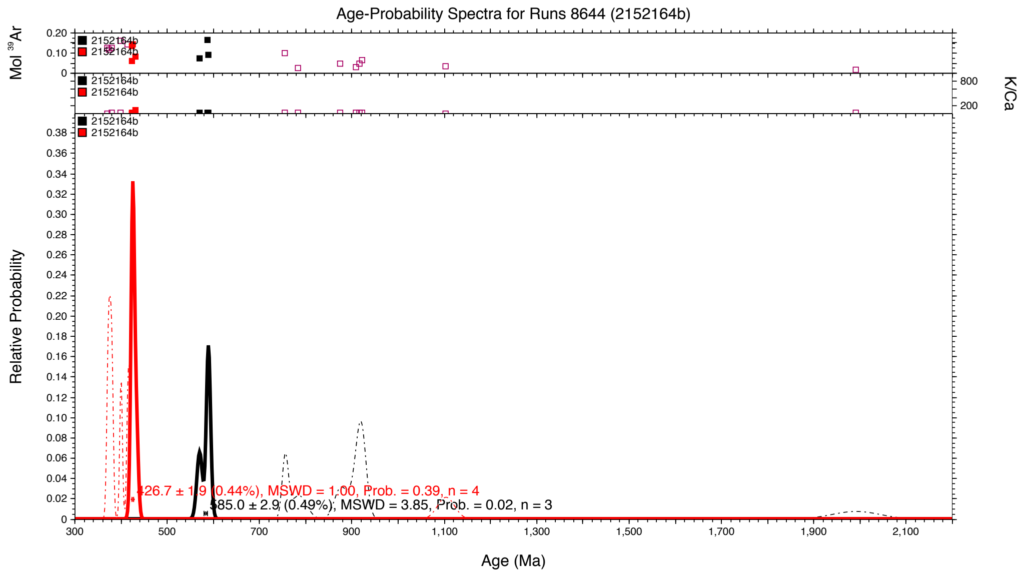

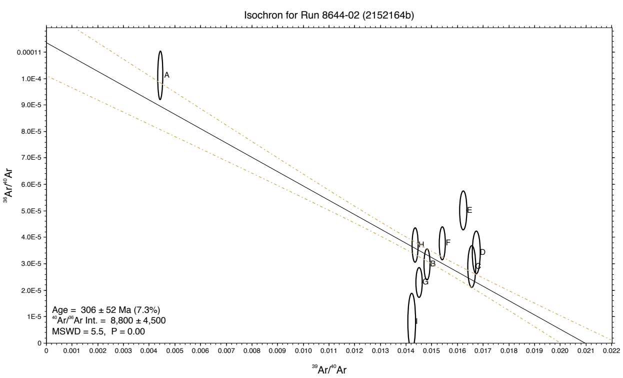

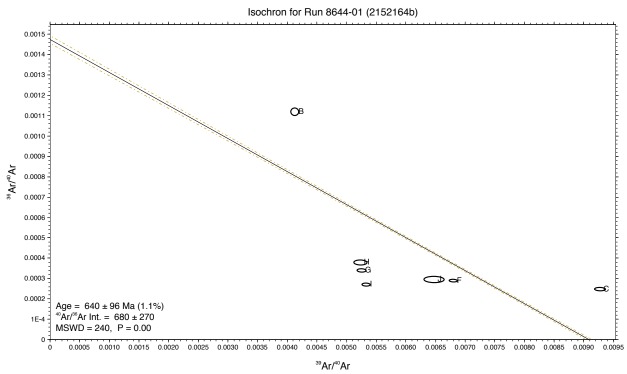

Ooroonoo 1 (2152164c - plagioclase)

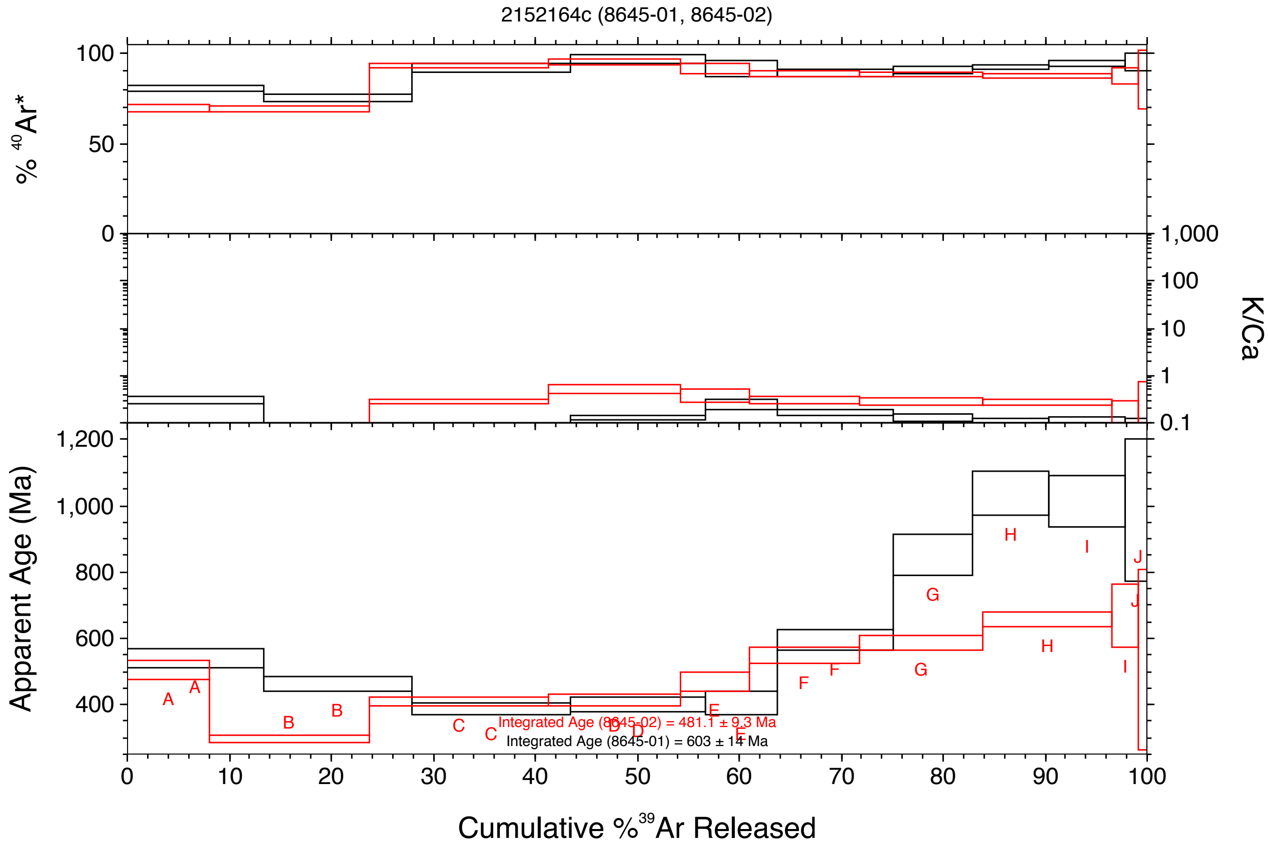

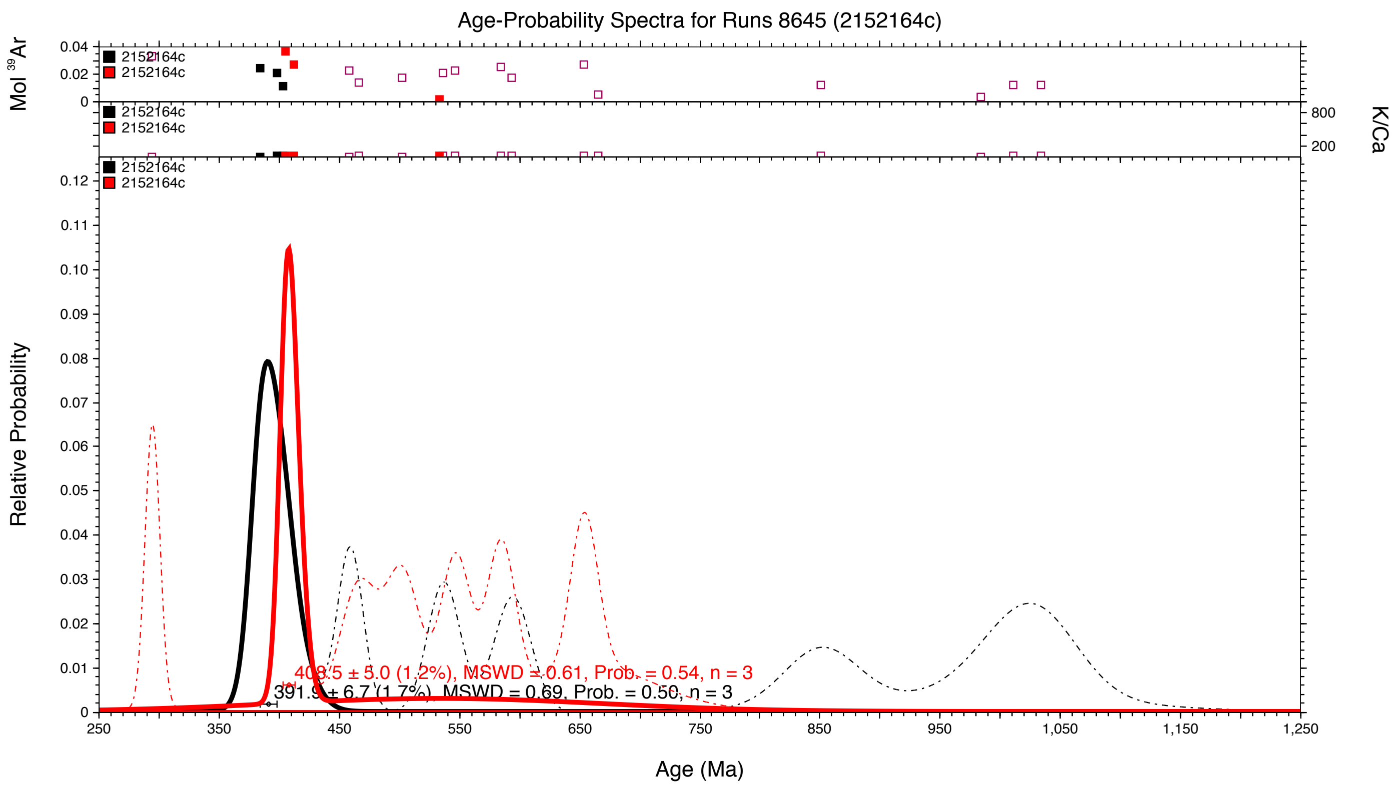

Sefton Metamorphics (2152166 - amphibole)

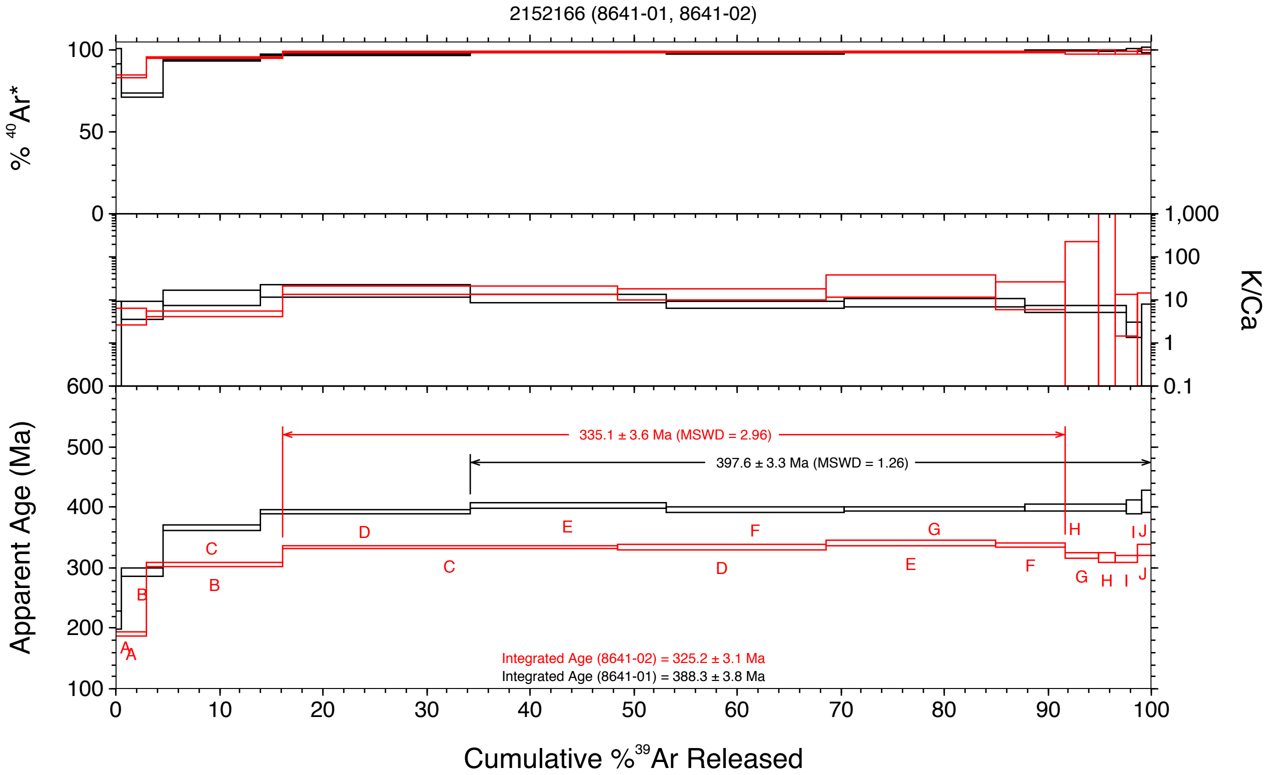

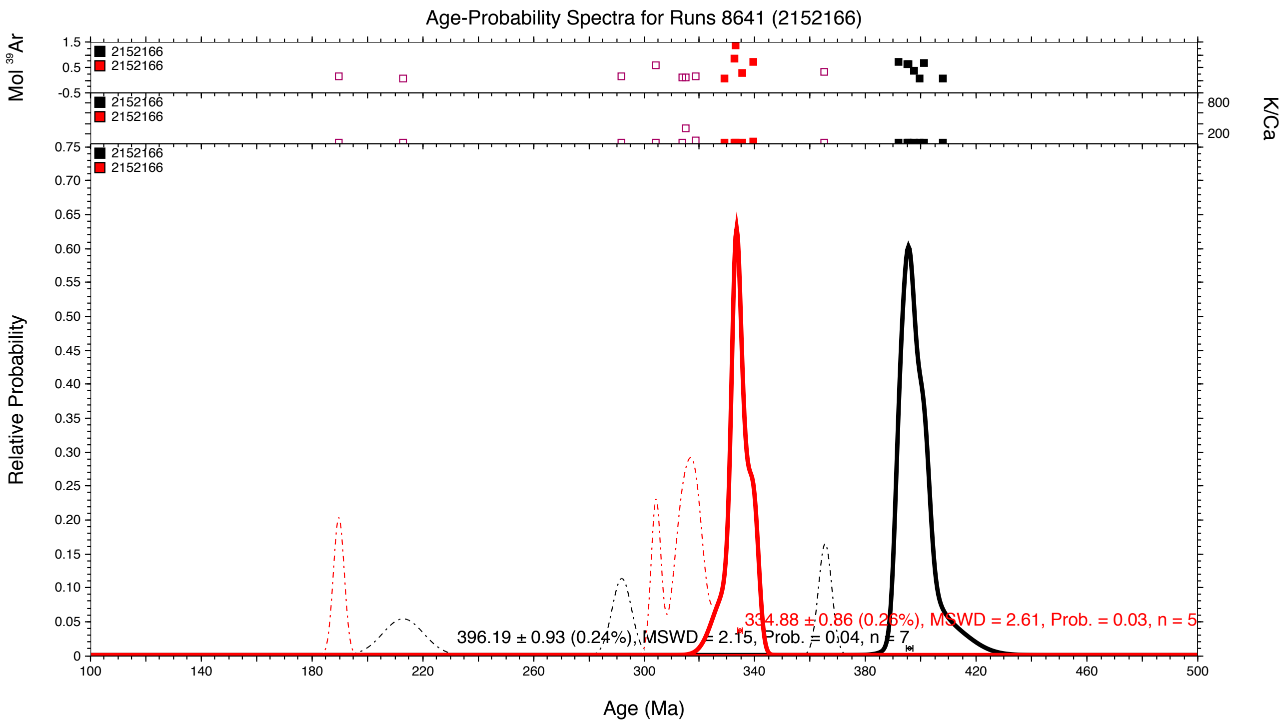

Halls Reward Metamorphics (MLHR02a - muscovite)

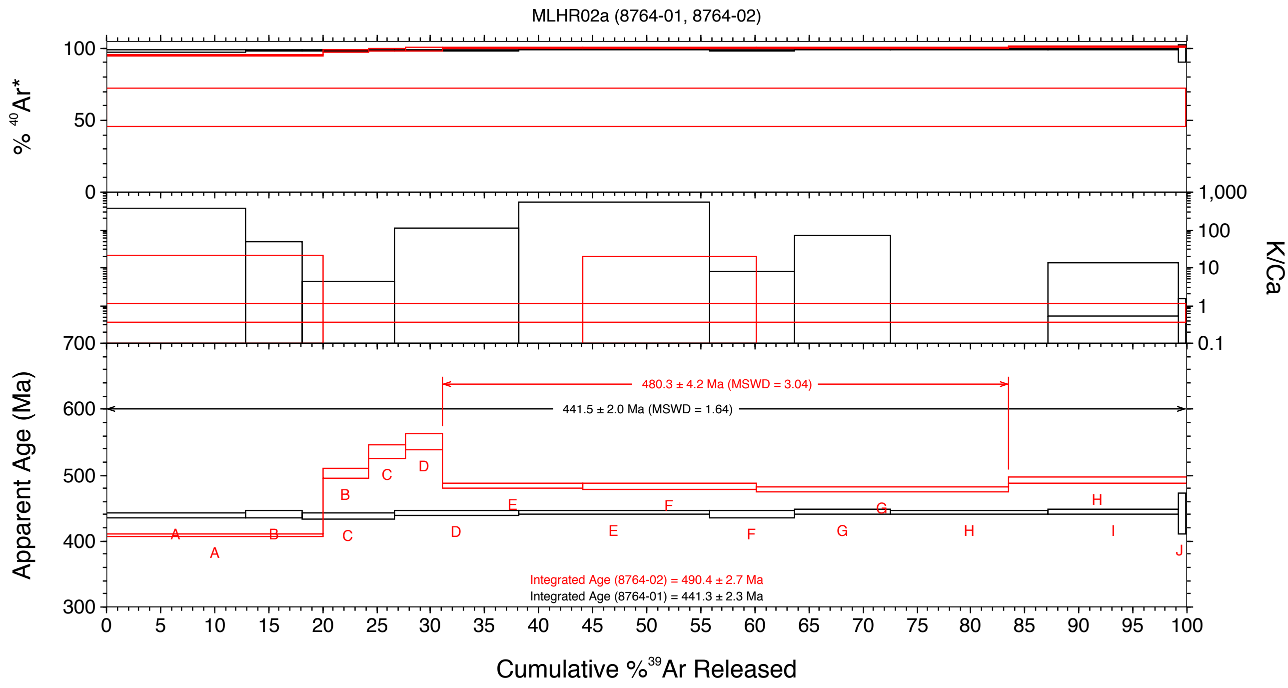

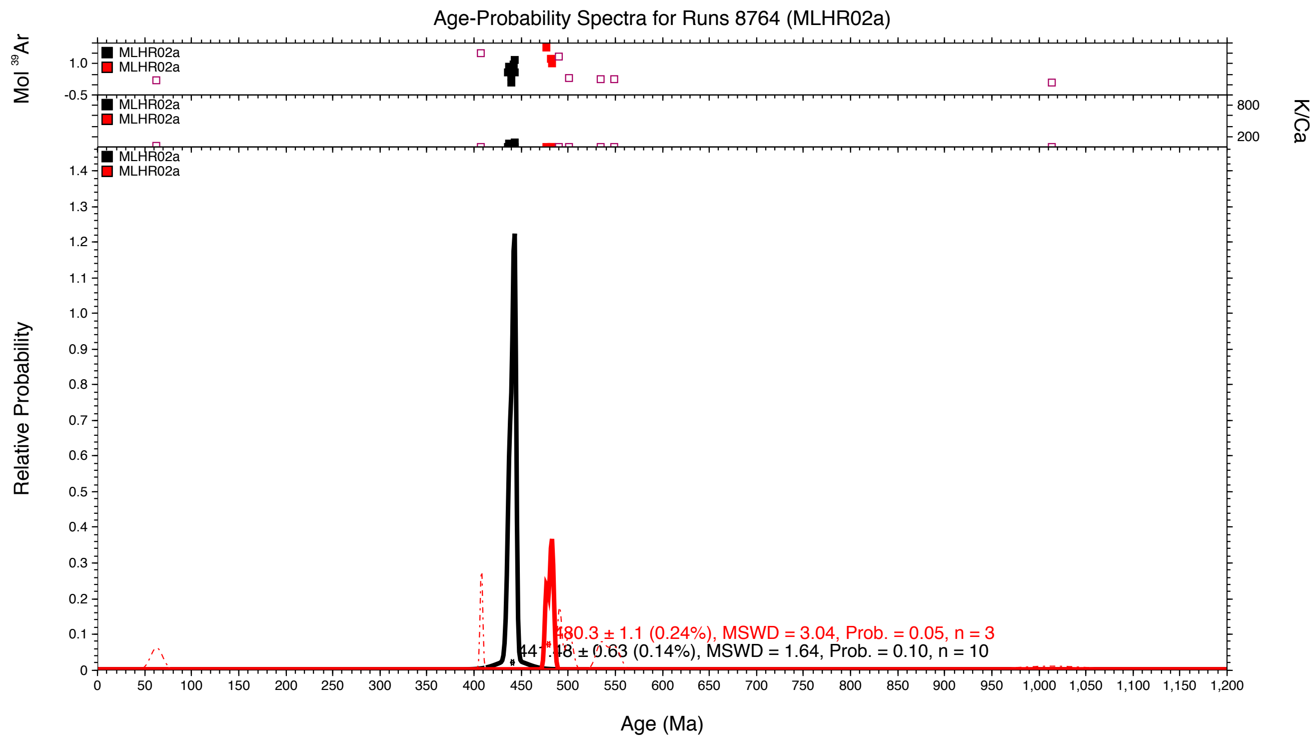

Halls Reward Metamorphics (MLHR02b - biotite)

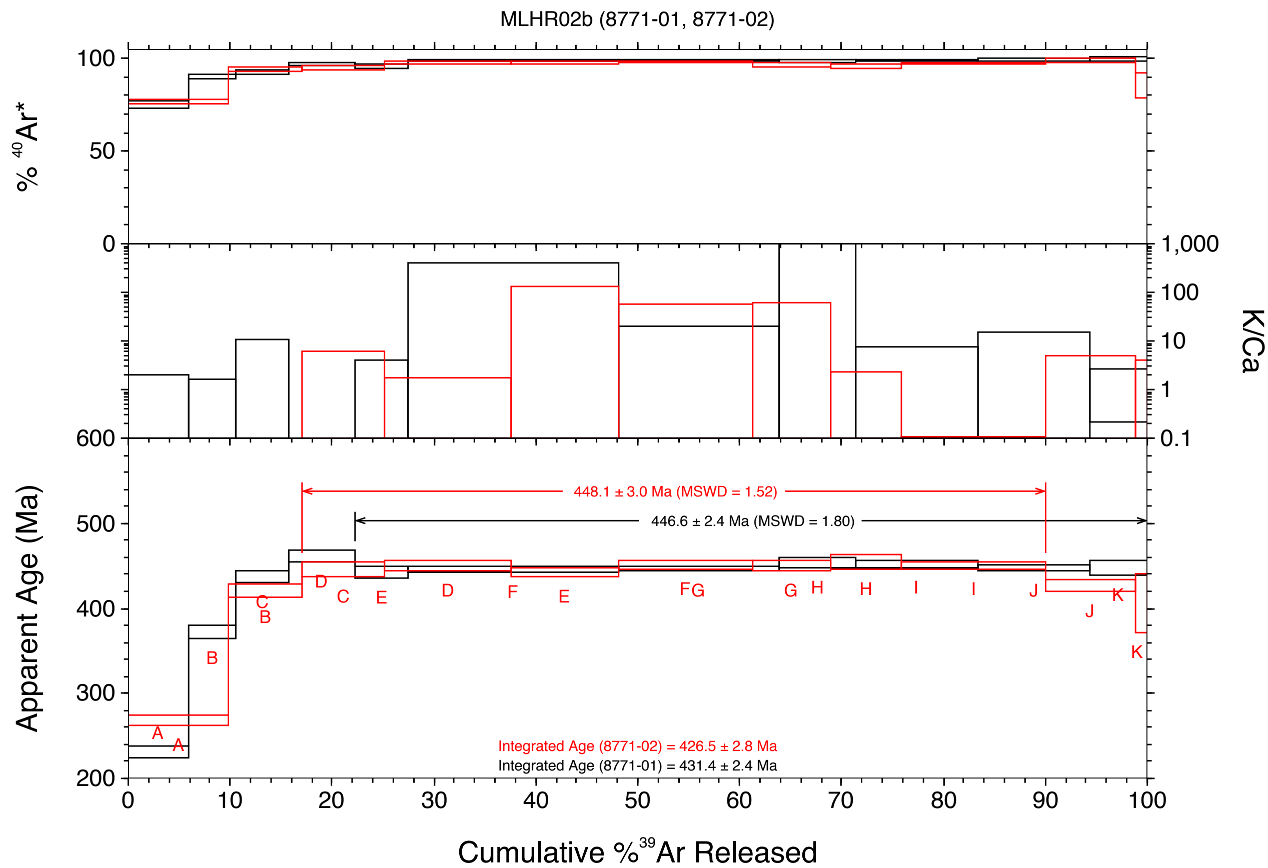

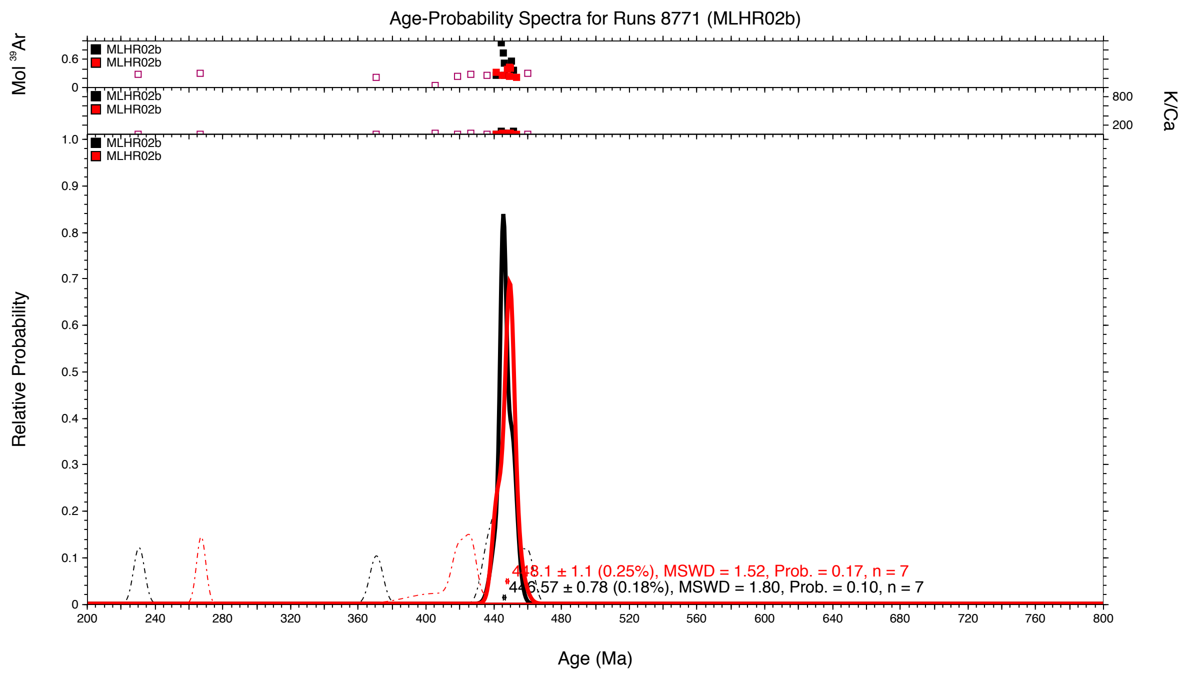

Halls Reward Metamorphics (NQ37 - muscovite)

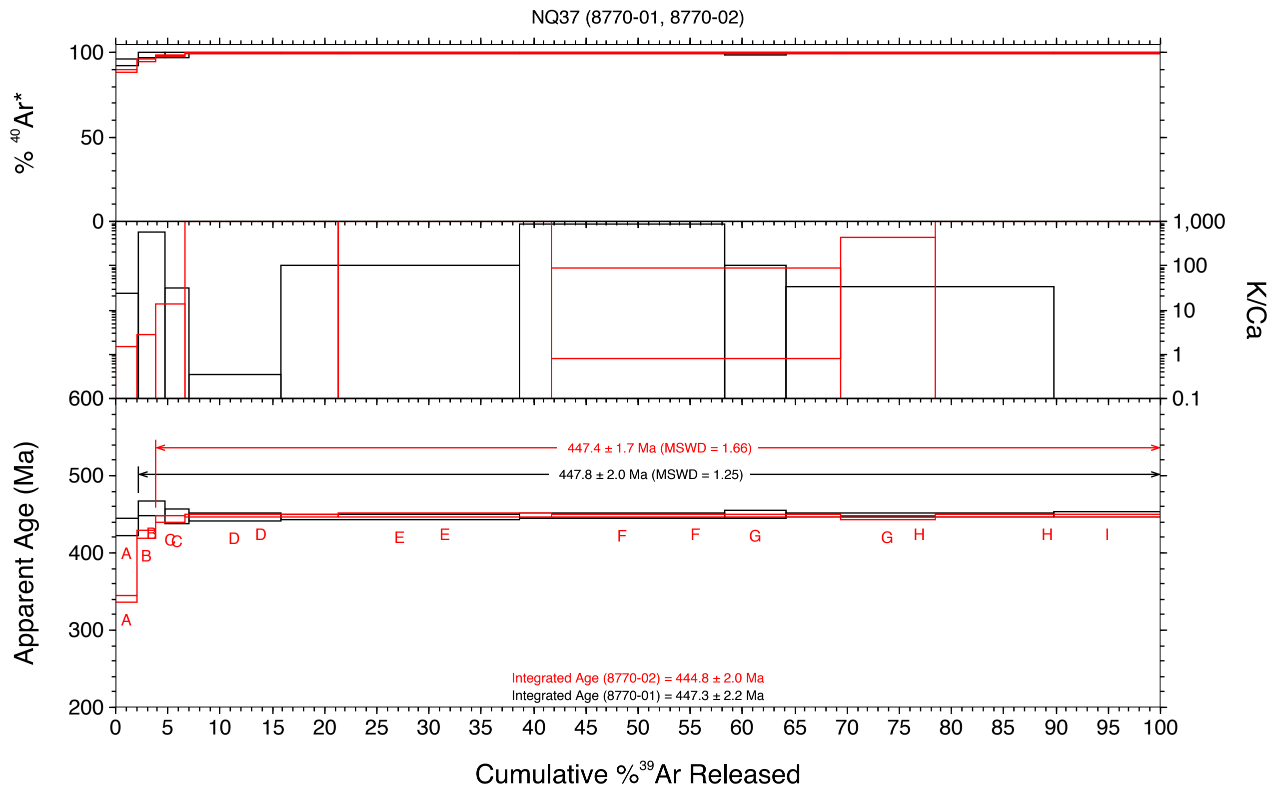

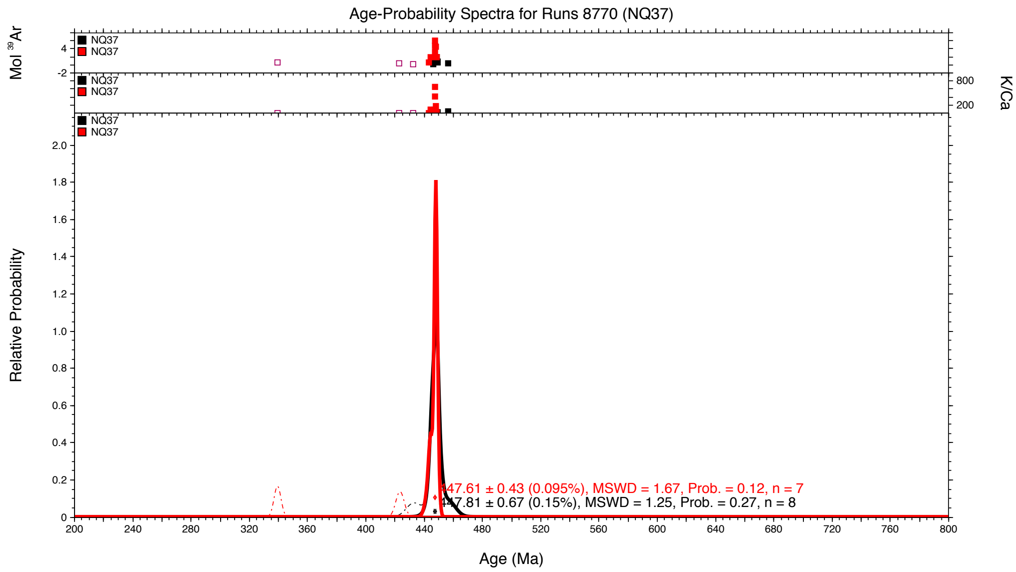

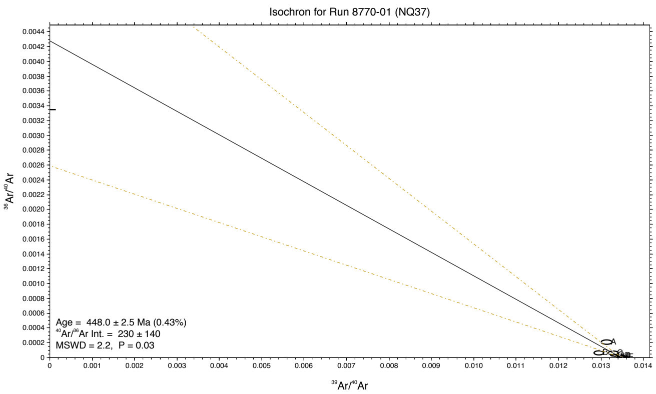

Les Jumelles beds (MLLJ06 - WR)

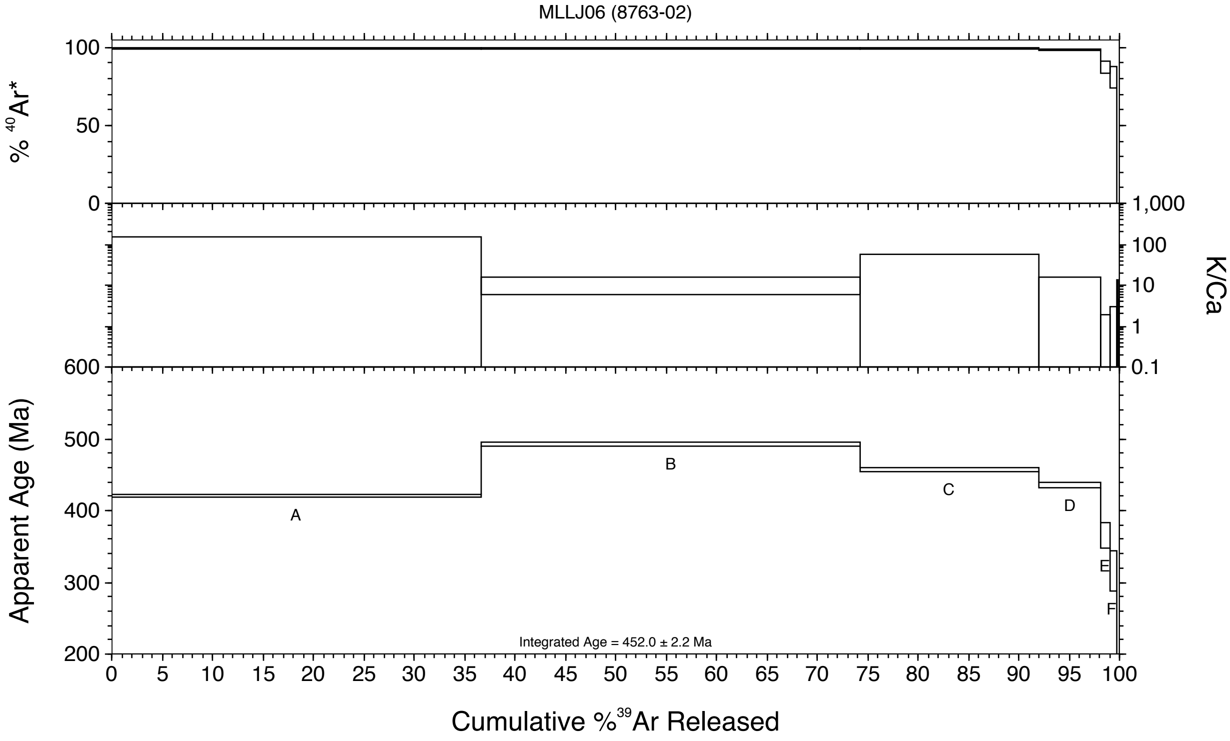

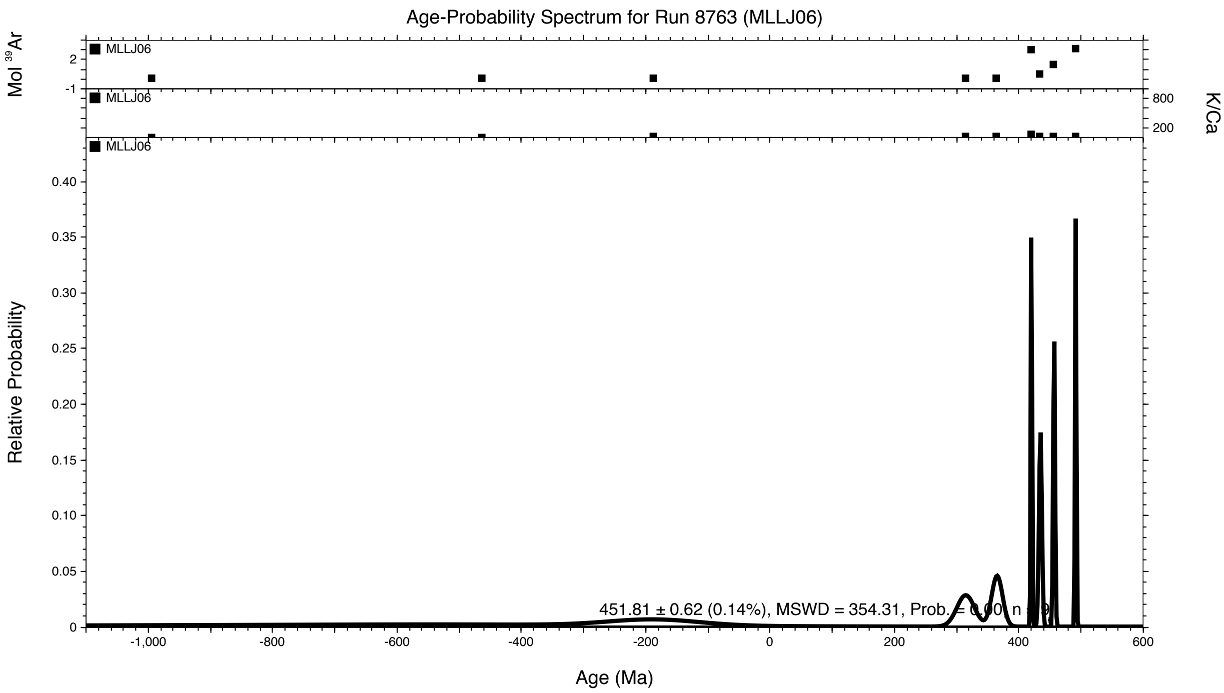

Mt. McLaren beds (AOM03 - WR)

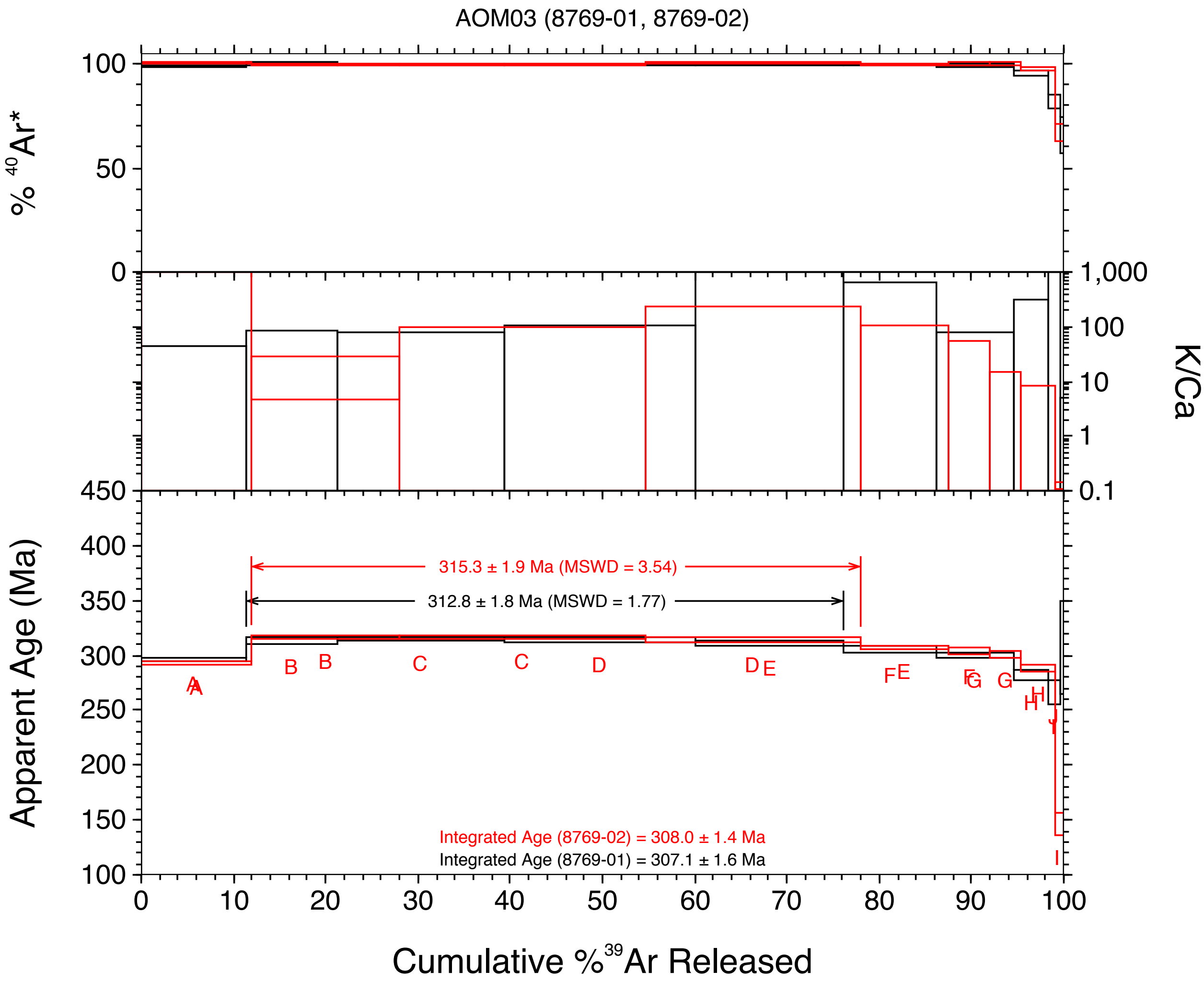

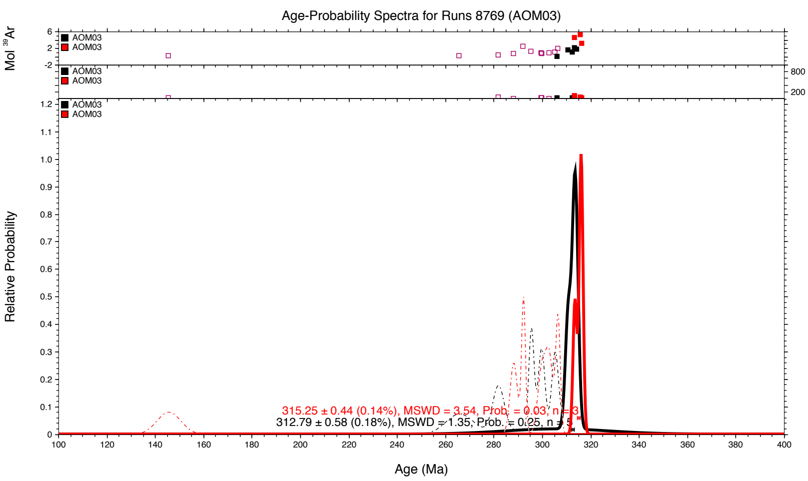

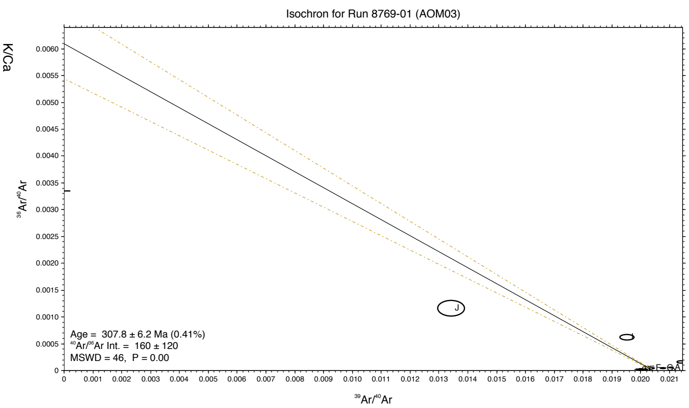

Anakie Metamorphic Group (MLH501 - WR)

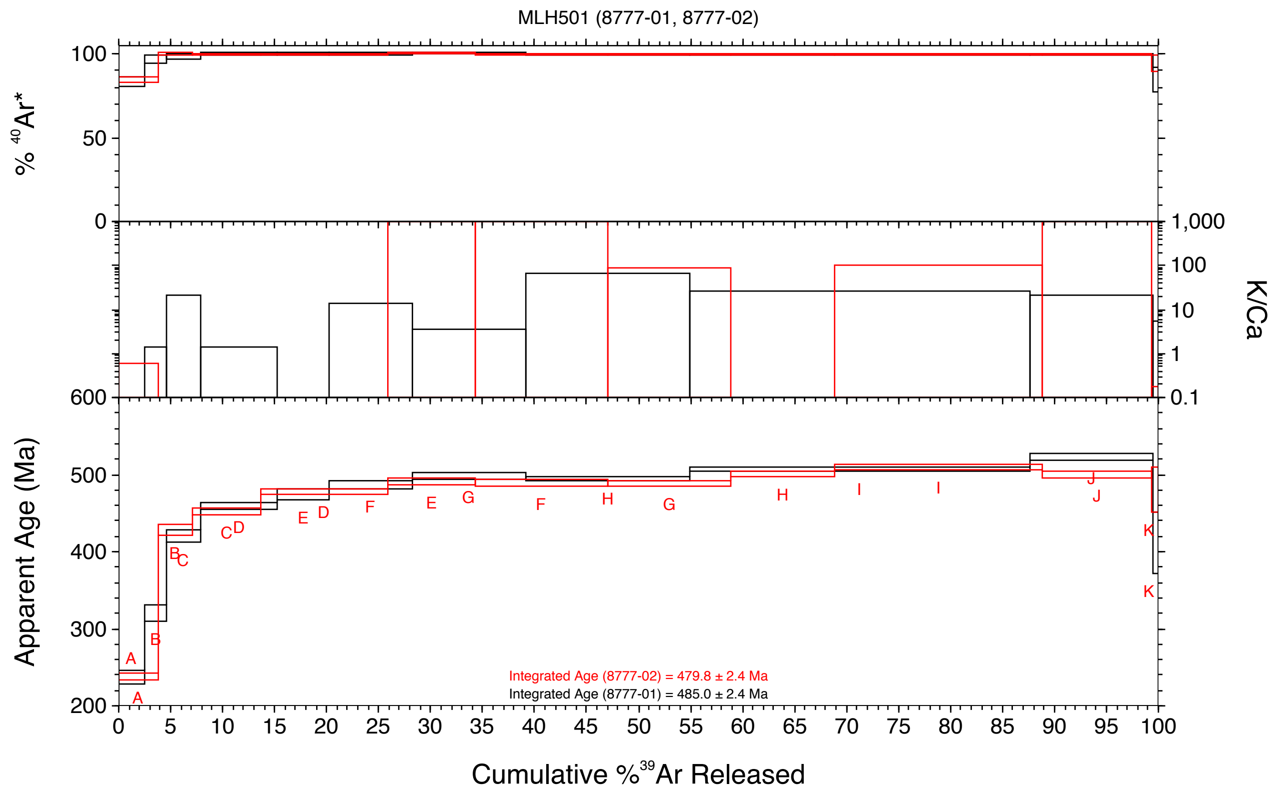

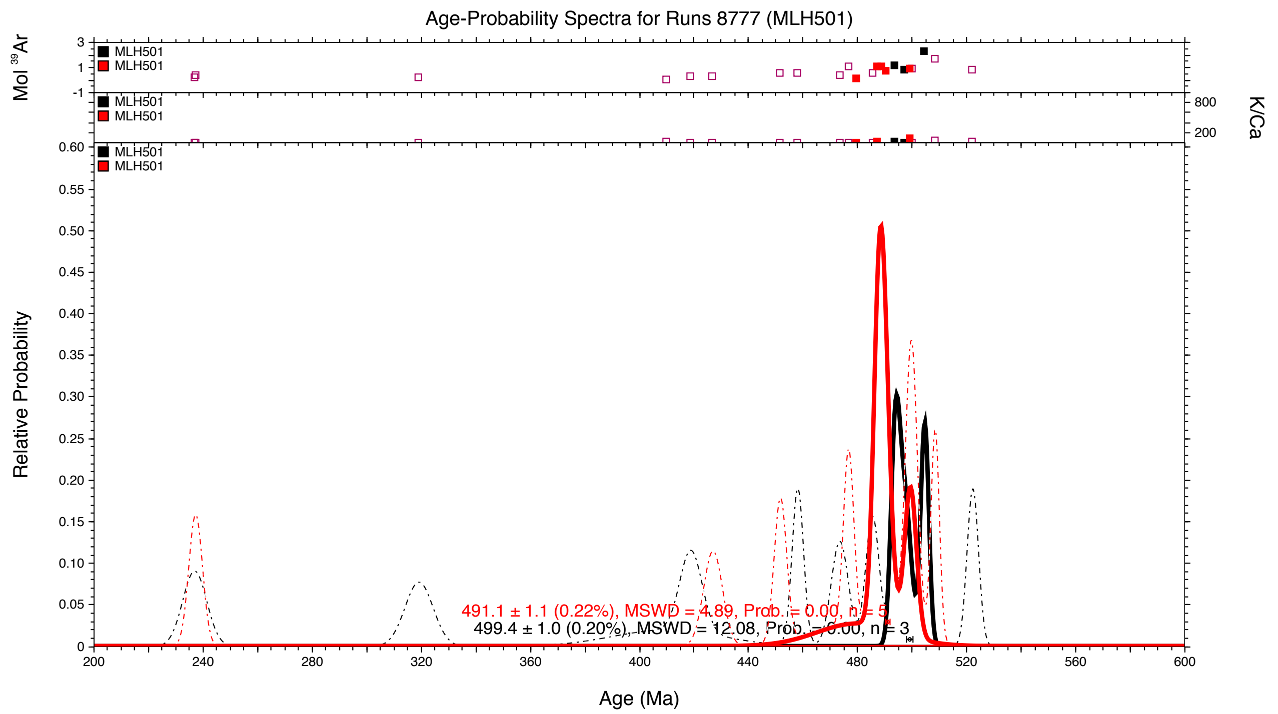

Anakie Metamorphic Group (MLH502 - WR)

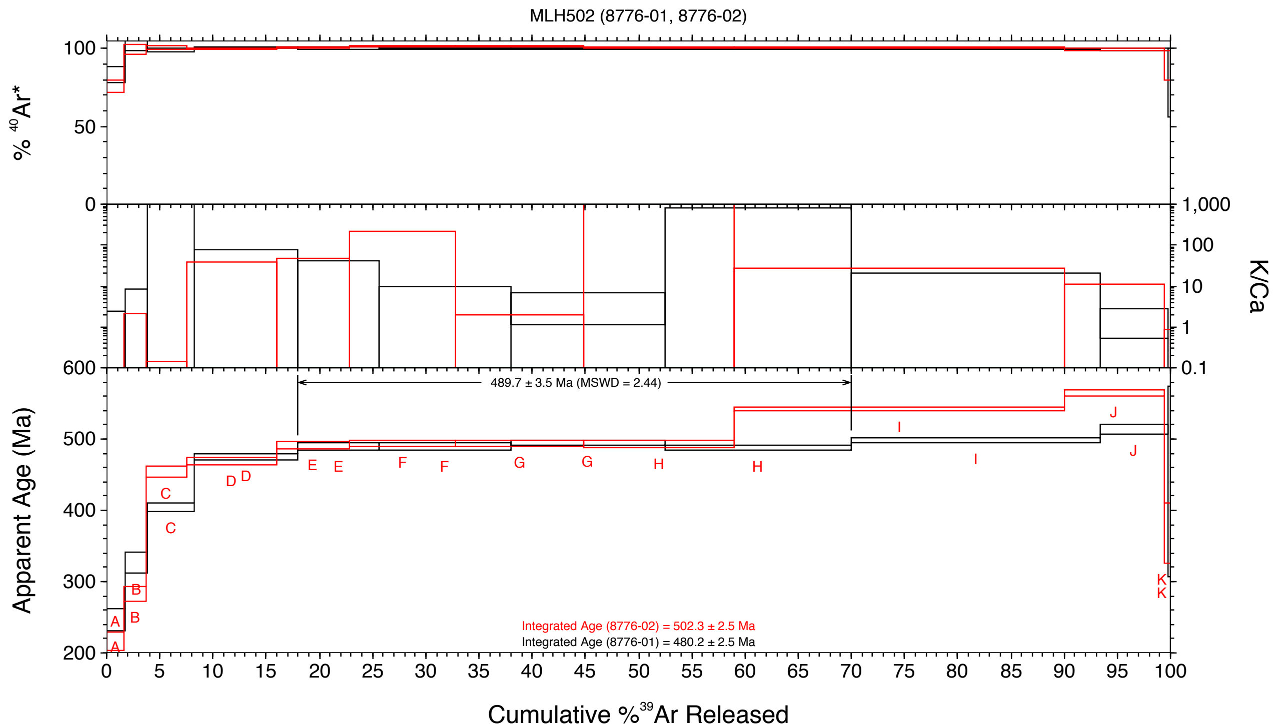

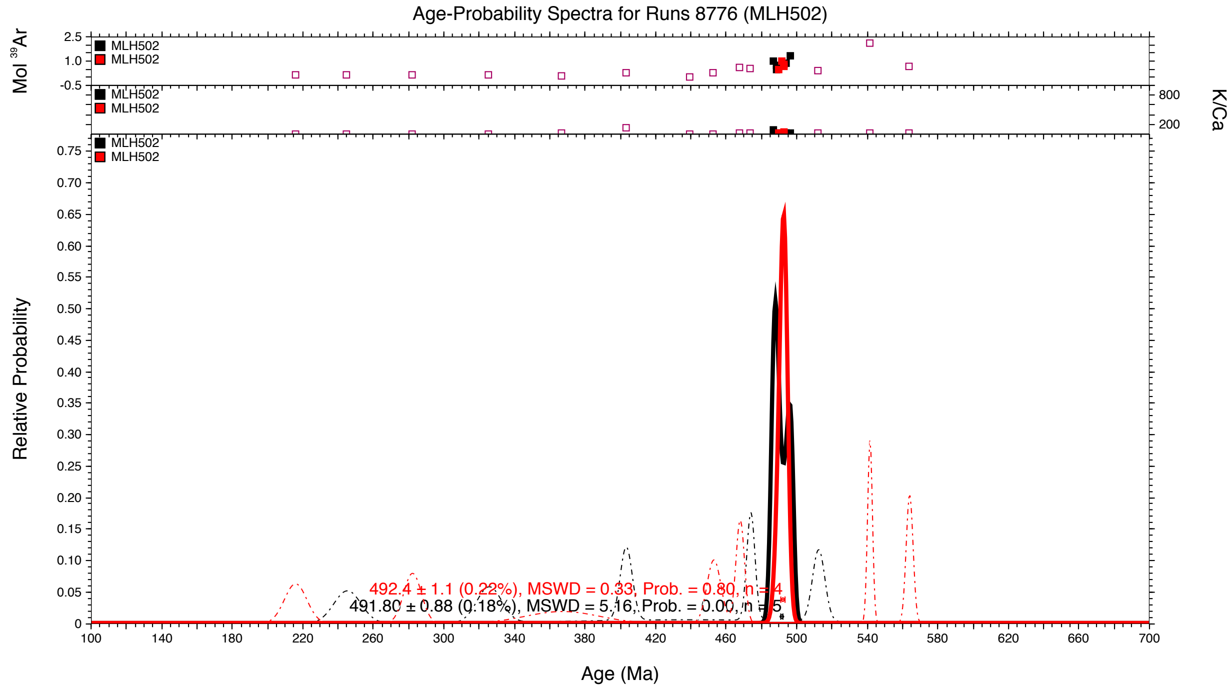

Anakie Metamorphic Group (MLH503 - WR)

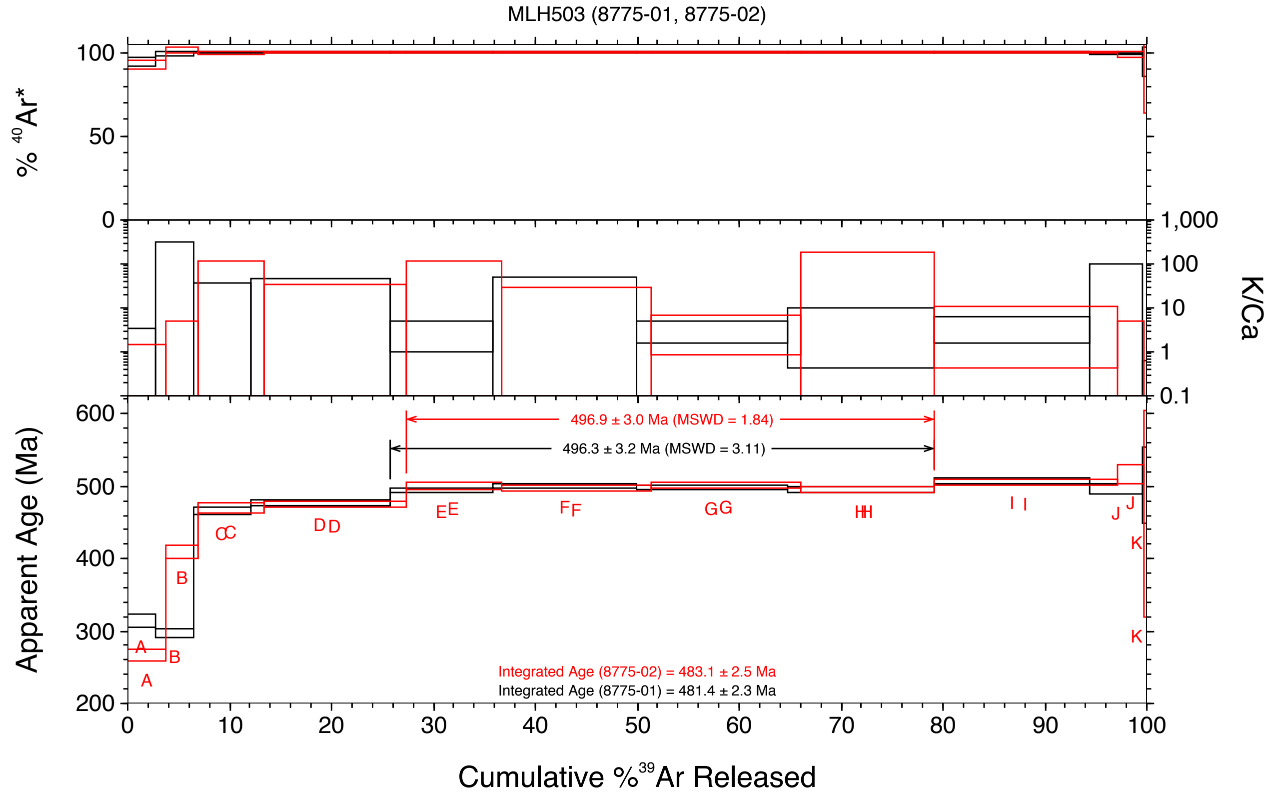

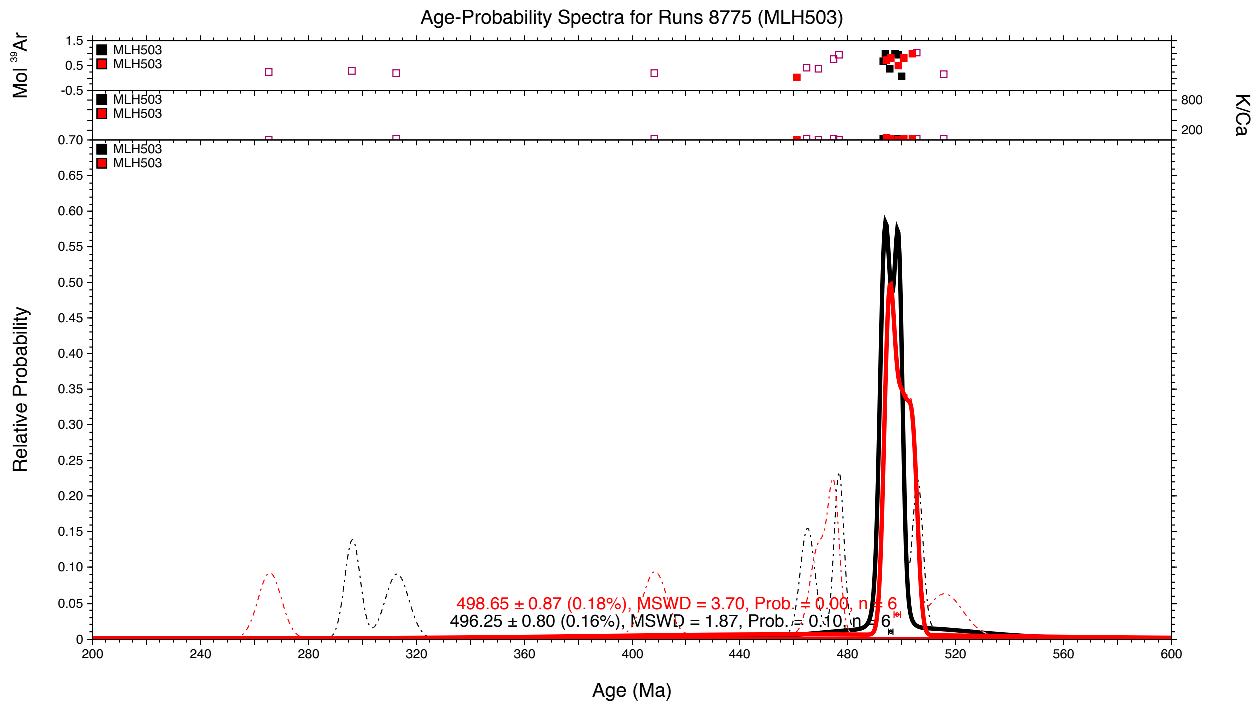

Anakie Metamorphic Group (MLH505 - WR)

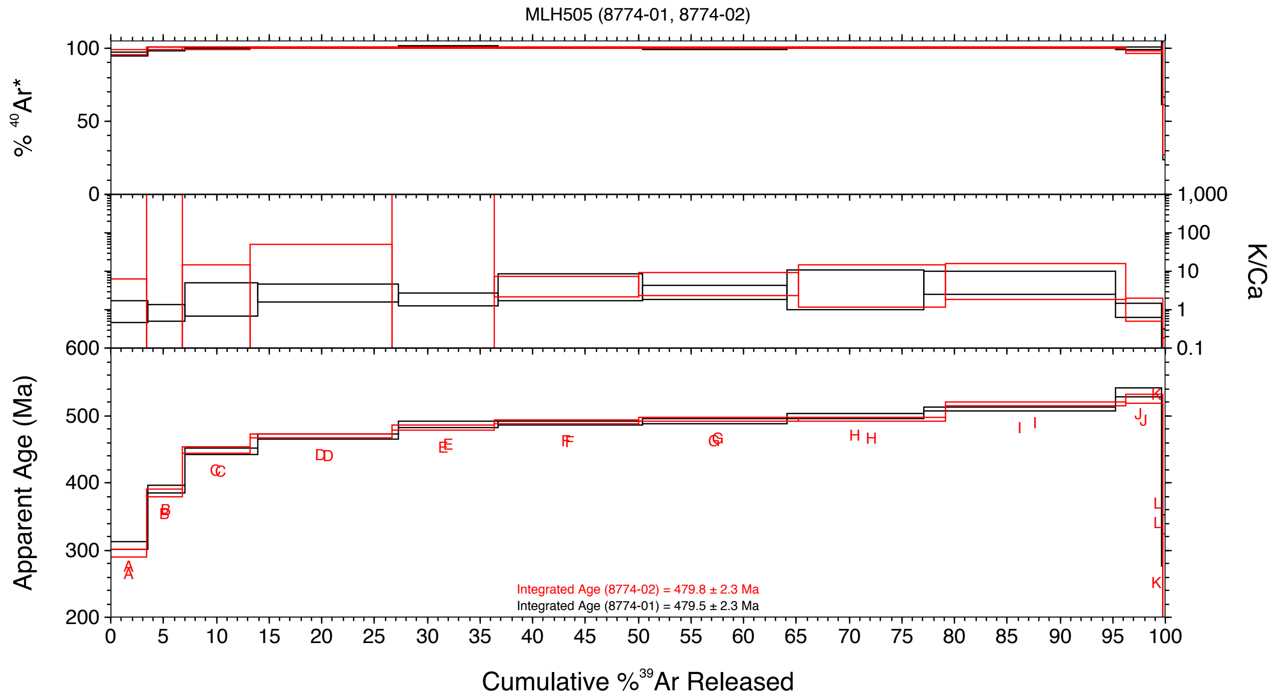

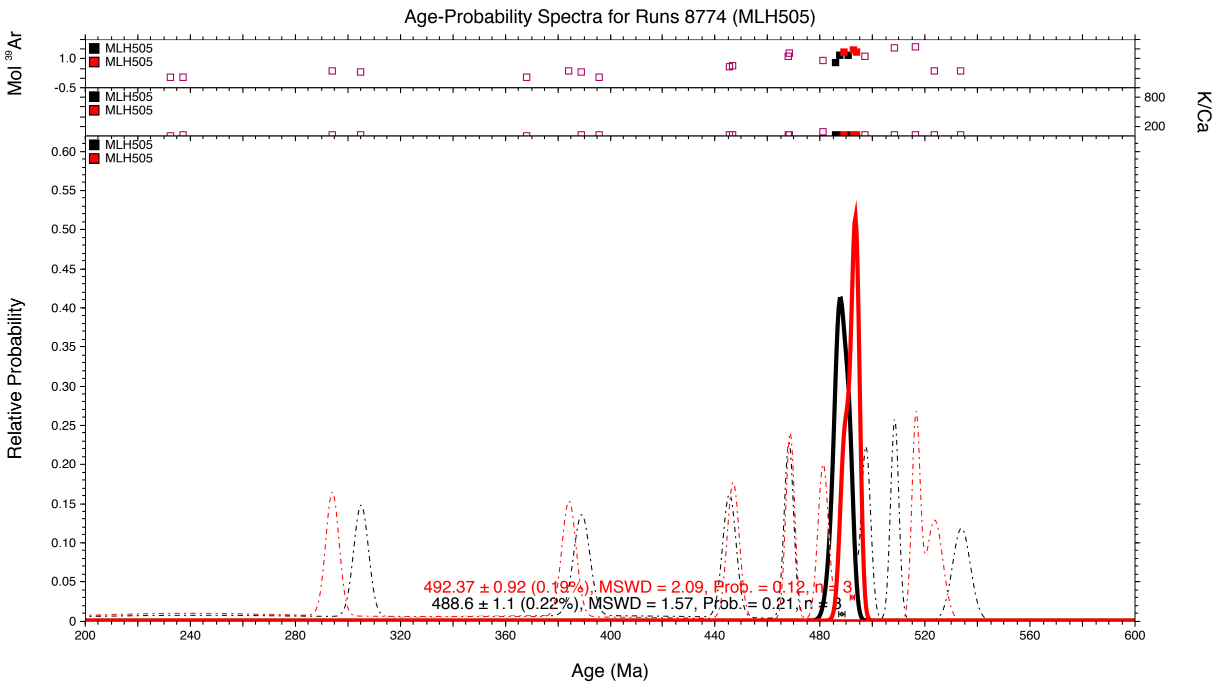

Anakie Metamorphic Group (MLH505 - WR)

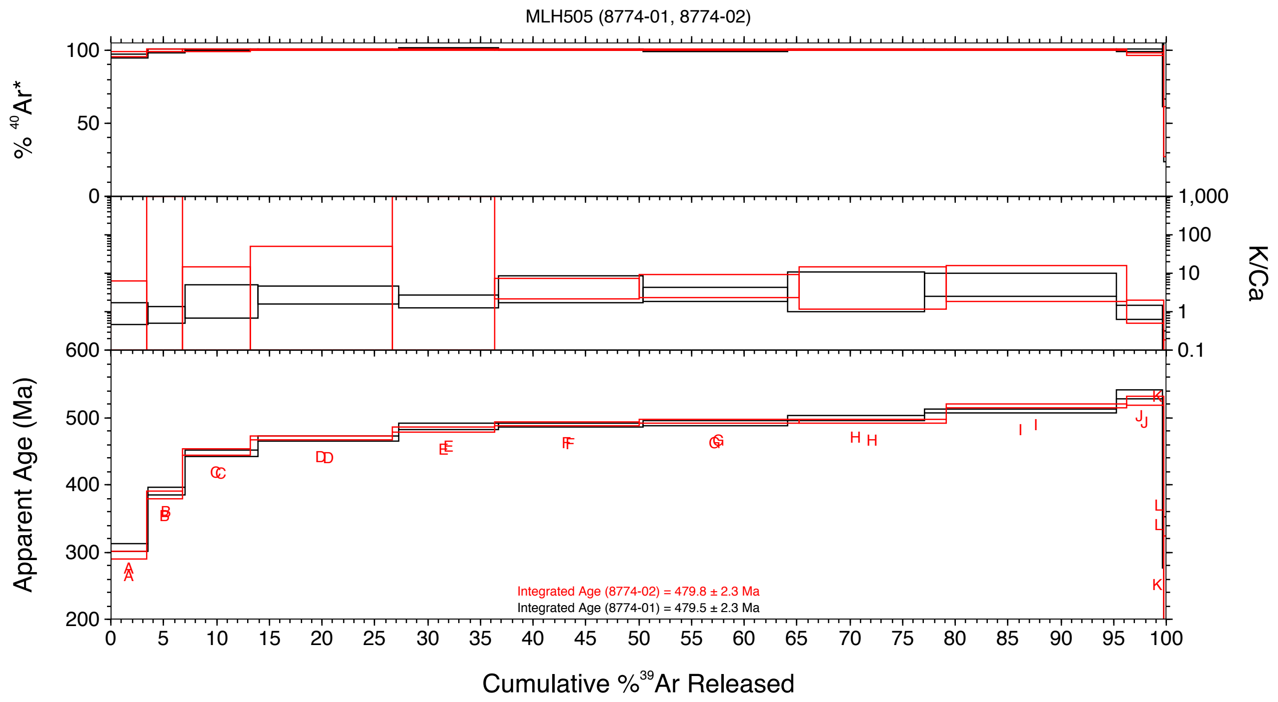

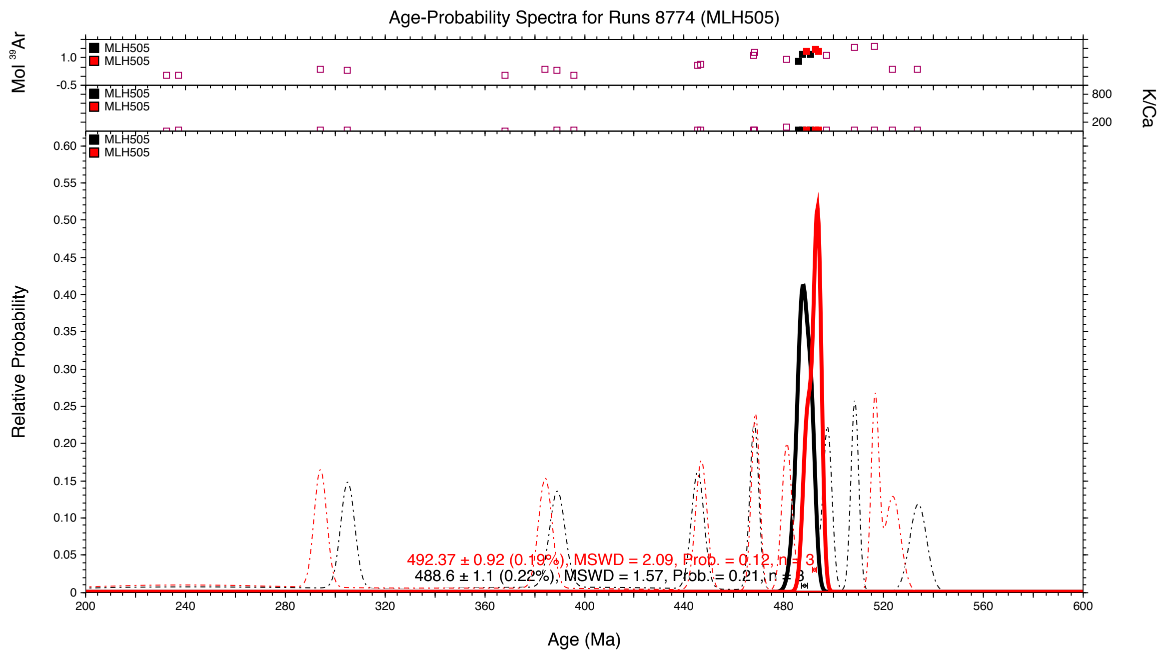

Anakie Metamorphic Group (MLPD01 - WR)

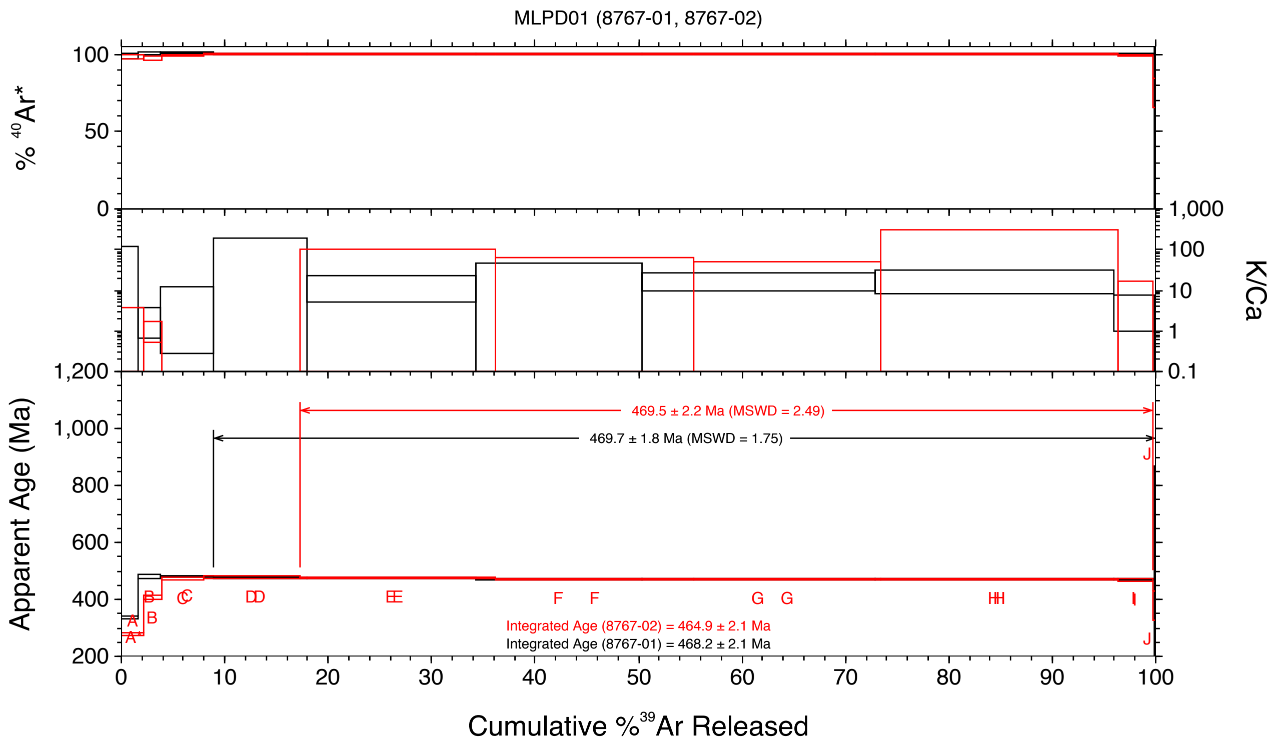

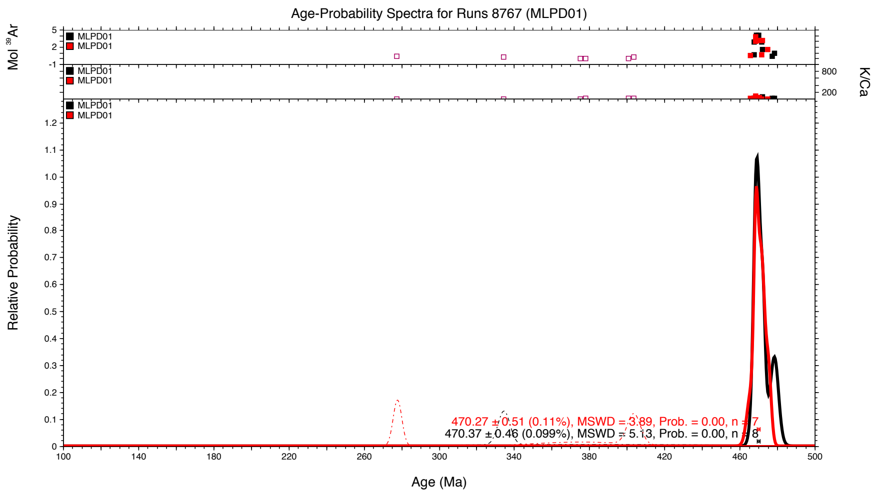

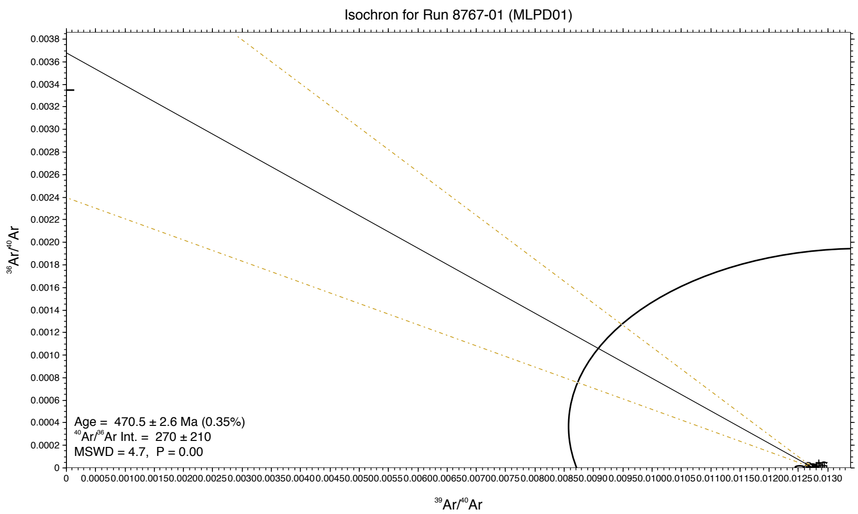

Anakie Metamorphic Group (MLPD02 - WR)